# THE REACTION OF OZONE WITH PHENOL, THIOPHENOL, CATECHOL AND RESORCINOL: A COMPUTATIONAL STUDY OF THE THERMODYNAMIC STABILITY OF THE PRIMARY OZONIDES AND REACTION BARRIERS IN THE GAS PHASE AND IN WATER

A THESIS SUBMITTED IN FULFILMENT

OF THEREQUIREMENTS FOR THE DEGREE OF

MASTER OF SCIENCE (CHEMISTRY)

OF

THE UNIVERSITY OF NAMIBIA

BY

Owen Gerrit Puley

200923579

October 2019

Supervisor**:** Prof. Edet F. Archibong
(Department of Pharmaceutical Chemistry, University of Namibia)

Co-Supervisor**:** Dr. Kathithileni M. Kalili
(Department of Chemistry and Biochemistry, University of Namibia)

**ABSTRACT**

Ozone is a highly reactive substance that can react with a vast number of chemical species. In the reaction of ozone with molecules containing carbon-carbon multiple bonds, the initial intermediate is a primary ozonide (POZ) which rearranges to a more stable secondary ozonide. The primary ozonides are transient species and very difficult to isolate experimentally. Thus, computational chemistry provides an alternative route to study the POZs. This study used quantum chemical techniques to investigate the effects of solvent (water) on the structures and thermodynamic stability of POZs derived from phenol, thiophenol, catechol and resorcinol. The reaction barriers leading to the formation of the elusive POZs were also studied.

Geometry optimization of the POZs was done at the B3LYP/6-31G(d,p) level in the gas phase and in water using the polarized continuum model. After optimizing the structures in the gas phase and in water, single point CCSD(T)/6-31G(d,p) calculations were performed to obtain more accurate energies. The effect of the solvent was determined by comparing the geometry, thermodynamic stability and reaction barriers of the POZs in water with those obtained in the gas phase.

The results of this study show that all the POZs are thermodynamically stable relative to the reactants, both in gas phase and in water. Specifically, the B3LYP/6-31G(d,p) model predicts that POZs of phenol, thiophenol, catechol and resorcinol are 24.9, 22.5, 28.7 and 26.5 kcal/mol, respectively, below the corresponding reactants in the gas phase. At the CCSD(T)/6-31G(d,p) level, the stability of the POZs increases to 28.6, 24.2, 34.4 and 30.7 kcal/mol for phenol, thiophenol, catechol and resorcinol, respectively. The most favorable pathways for the formation of the POZs go through energy barriers of 5.1, 7.4, 3.1 and

2.6 kcal/mol, for phenol, thiophenol, catechol and resorcinol, respectively, using the B3LYP/6-31G(d,p) model. Corresponding values at the CCSD(T)/6-31G(d,p) level are 9.5, 11.2, 7.6 and 8.0 kcal/mol.

The B3LYP/6-31G(d,p) results indicate that planarity is retained for some POZs of phenol, thiophenol, catechol and resorcinol in the gas phase and in water. The POZs also appear to be thermodynamically more stable in water than in the gas phase. B3LYP/6-31G(d,p) reaction barriers of 4.1, 5.7, 2.7 and 2.0 kcal/mol were computed for phenol, thiophenol, catechol and resorcinol respectively, in water. The latter results suggest that the formation of the POZs would be faster in an aqueous medium relative to the gas phase.

## TABLE OF CONTENTS

# LIST OF TABLES

**LIST OF FIGURES**

## LIST OF ABBREVIATIONS

CI Creigee Intermediates

DFT Density Functional Theory

POZ Primary Ozonide

SOZ Secondary Ozonide

## LIST OF SCHEMES

**Acknowledgements**

Firstly, I would like to thank the almighty living God for giving me the fortunate opportunity to make a worthy contribution to science.

Secondly, I want to thank Prof. Edet F. Archibong my supervisor and Dr. Kathithileni Kalili my co-supervisor for affording me the opportunity to further my studies under their guidance and leadership. I would like to acknowledge and thank the Centre for High Performance Computing (CHPC) for availing their facilities to the University of Namibia and subsequently enabling me to carrying out part of my research. To my parents who have always supported and motivated me to achieve greater things in life no matter what the challenge. I would like to thank my wife Annelize, my son Kyle and my daughter McKayla for always being supportive and patient when I had to be away working on my research and thesis.

**Declaration**

I, Owen Gerrit Puley, declare that the research is a true reflection of my own dedicated work, and that part thereof has not been submitted for a degree in any other institution of higher education.

No part of this thesis may be reproduced, stored in any retrieval system or transmitted in any form or by means (e.g. electronic, mechanical, photocopying, recording or otherwise) without the prior permission of the author, or the University of Namibia.

I, Owen Gerrit Puley student number 200923579, grant the University of Namibia the right to reproduce this thesis in whole or in part, in any manner or format, which the University of Namibia may deem fit, for any person or institution requiring it for study and research; providing that the University of Namibia shall waive this right if the whole thesis has been or is being published in a manner satisfactory to the University.

01/09/2021

…….  ……

Owen Gerrit Puley  Date

# Chapter 1

## Introduction

### 1.1 Background of the study

The first step in ozonolysis is 1,3-dipolar cycloaddition of ozone ($O_3$) to the multiple bonds of an unsaturated molecule to produce a primary ozonide (POZ), which is a compound containing an O–O–O group. The POZs produced by ozonolysis decompose to produce a carbonyl oxide—called Criegee intermediate (CI)—and an aldehyde or ketone, which rearranges to a more stable secondary ozonide (SOZ). Primary ozonides are short lived intermediates, both in the gas phase ozonolysis of unsaturated hydrocarbons in the troposphere and in solution phase organic synthesis (Osborn & Taatjes, 2015).

The stability of many organic compounds is challenged by oxidation reactions with molecular ozone from the air or in aqueous solution, in accordance with the kinetic and thermodynamic properties of the primary ozonide. Ozone has oxidation, antibacterial and antiviral properties that make it widely used in the treatment of natural, industrial and polluted water, for medical uses, etc. The advantage of treating water with ozone is that it is fast and non-selective towards micro-organisms and pollutants. Oxidation reactions initiated by ozone in water and in the atmosphere are generally complex. Despite numerous compilations of experimental thermochemical data for many molecules, those of POZs derived from phenolic compounds are very scarce in the literature because of their transient nature.

Computational techniques afford the means of determining the properties of short-lived unstable species. Due to the scarcity of kinetic and thermochemical data on the POZs of

phenolic compounds, this project was geared towards direct ozonation of phenol, thiophenol, catechol and resorcinol in the gas phase and in water using computational approach. The data presented in this study will complement previous research carried out in the gas phase and provide new data on the solvent effect, when ozone reacts with unsaturated molecules to form the POZs.

## 1.2 Problem statement

The detailed reaction mechanisms of ozone with different compounds, either in the pre-treatment of water or in the atmosphere, are not well known because most of the reaction intermediates are transient unstable species, which are extremely difficult to characterize experimentally. Furthermore, the relative stability of the intermediates and the reaction barriers leading to their formation could be affected by solvents. In order to have a deeper understanding of the mechanism of ozone reaction with unsaturated aromatic compounds, thermodynamic and kinetic data of the transient intermediates, including solvent effects are needed. Benzene and phenols may serve as representatives of aromatic unsaturated compounds. The kinetic and thermodynamic data of the primary ozonides (POZs) of thiophenol, catechol and resorcinol are very scarce in the literature, hence the motivation for this research.

## 1.3 Objectives of the study

- To computationally synthesise the POZs of phenol, thiophenol, catechol and resorcinol in the gas phase and in water.
- To compute the thermodynamic stability and reaction barriers of phenol, thiophenol, catechol and resorcinol POZs in the gas phase and in water.

- To determine the effect(s) of water on the thermodynamic stability and the reaction barriers of POZs derived from phenol, thiophenol, catechol and resorcinol.

## 1.4 Significance of the study

Kinetic and thermodynamic data are imperative for understanding the behavior of ozone when it reacts with phenolic compounds in water or in the atmosphere. This research will facilitate a better understanding of the reaction of ozone with aromatic compounds which are present either in wastewater or in the atmosphere. It will show how solvents, such as water may affect the stability, kinetics and structure of the products formed when ozone reacts with certain phenolic compounds. The information derived from this research will avail kinetic and thermodynamic parameters which can be used to compliment experimental work on the reaction of ozone with phenolic compounds.

## 1.5 Limitation of the study

Some of the results obtained in this study cannot be compared with experimental results because the latter are not available.

# Chapter 2

## Literature review

### 2.1 Ozone

#### 2.1.1 Ozone molecule

Ozone is a triatomic molecule ($O_3$) and an allotrope of elemental oxygen which exists primarily as a diatomic molecule ($O_2$) (Shakhashiri, 2017).Over the years, the electronic structure and the geometry of ozone have been subject of intense discussions in the literature. Acceptable representation of the molecule is now based on two equal weighting structures developed by Pauling (Figure 1a); the coexisting structures proposed by Weinhold (Figure 1b) and the three-electron bonding structure as proposed by Linnett (Figure 1c) (Youmin, Xiaohua, & Zhaojie, 2012).

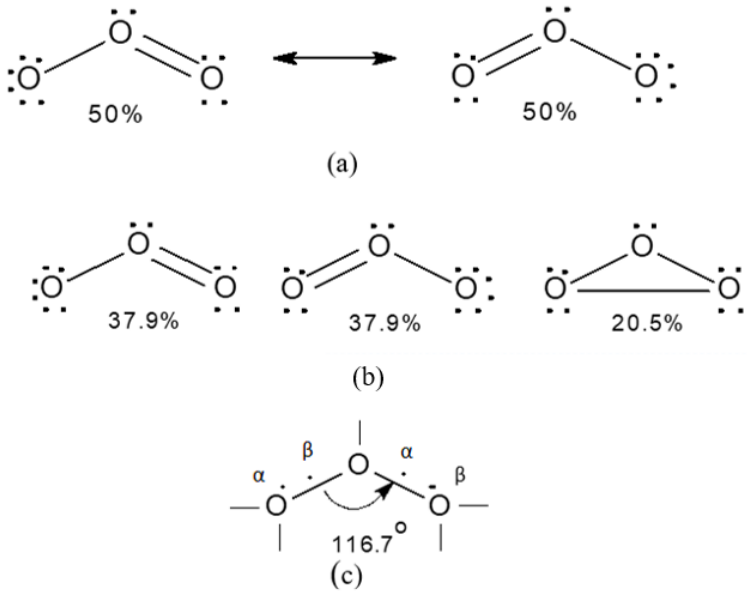


*Figure 1: The ozone structure (a) by Pauling's resonance theory, (b) Weinhold's resonance theory (NRT), and (c) Linnett's double quartet theory*

### 2.1.2 Properties of Ozone

Ozone is found naturally in the earth's atmosphere and has a bond length of 1.272Å, with an obtuse bond angle of 116.75$^{o}$ and a small dipole moment of 0.533 Debye (Schwartz, 2010). Some of the physical constants of ozone are listed in table 1.

*Table 1: Physical constants of ozone.*

| | |
|---|---|
| Molecular weight, g/mol | 48 |
| Boiling point, °C | -111.9 |
| Melting point, °C | -193 |
| Gas density, °C g/L | 2.144 |
| Critical temperature, °C | -12.1 |
| Critical pressure, atm | 54.6 |
| Critical volume, cc/mol | 147.1 |

At low concentrations ozone is a colorless gas. It develops a characteristic unpleasant odor at concentrations above 0.01ppm and turns pale blue at concentrations exceeding 5 ppm. Ozone has the ability to coexist in all three states of matter. At 161 K, it condenses into a liquid of indigo-light blue color and in the solid state, forms needle like crystals of $O_3$ and molecular oxygen, $O_2$. Pure ozone in all these states is explosive in nature and also very dangerous to prepare (Ortenberg, 2002).

The strong oxidation strength of ozone allows it to easily oxidize organic and inorganic compounds. As shown in Table 2, ozone has a reduction potential of 2.07 V compared to chlorine (1.36 V) and oxygen (1.23 V). Ozone (*Table 2*) has the second most reductive potential only to fluorine, thereby making it a powerful oxidant. The molecule has also

been found to be a very effective antiseptic and more efficient than sterilizing agents such as hydrogen peroxide ($H_2O_2$) and chlorine ($Cl_2$) (Eriksson, 2005).

*Table 2: Comparative oxidizing properties of ozone and other compounds.*

| **Reagents** | **Redox Potential (Volts)** |
|---|---|
| Fluorine ($F_2$) | 2.87 |
| Ozone ($O_3$) | 2.07 |
| Hydrogen peroxide($H_2O_2$) | 1.78 |
| Potassium permanganate($K_2MnO_4$) | 1.70 |
| Hypobromous acid (HOBr) | 1.59 |
| Hypochlorous acid (HOCl) | 1.49 |
| Chlorine ($Cl_2$) | 1.36 |
| Chlorine dioxide ($ClO_2$) | 1.27 |
| Oxygen ($O_2$) | 1.23 |
| Chromic acid ($H_2Cr0_4$) | 1.21 |
| Nitric acid ($HN0_3$) | 0.94 |
| Iodine ($I_2$) | 0.54 |

## 2.2 Phenol in waste water and in the atmosphere

Phenol is mainly released to the environment from domestic manufacturing and processing facilities. During manufacturing, phenol is released primarily to the atmosphere from storage tank vents and during transport loading. Other major sources through which phenol is released to the atmosphere, are residential wood burning and automobile exhaust. Volatilization from environmental waters and soils has been shown to be a slow process and is not expected to be a significant source of atmospheric phenol (Central pollution control board, 2016). Phenol is released into the atmosphere mainly

from industrial combustion processes such as coal burning it is also found in cigarette smoke and in plastics.

The most common anthropogenic sources of phenol in natural water include coal tar and waste water from manufacturing industries such as resins, plastics, fibers, adhesives, iron, steel, aluminum, leather, rubber and effluents from synthetic fuel manufacturing (Central pollution control board, 2016). Phenol is also released from paper pulp mills and wood treatment facilities. Other releases of phenol result from commercial use of phenol and phenol-containing products, including slimicides, general disinfectants and medicinal preparations such as mouthwashes, gargles, and antiseptic lotions.

Natural sources of phenol in aquatic media are animal wastes and decomposition of organic wastes. As a benzene moiety, phenol may also be released from publicly owned treatment works and sewage overflows. Phenols may occur in domestic and industrial wastewaters, natural waters and potable water supplies. Phenol is a quite common pollutant and has been detected in surface waters, rainwater, sediments, drinking water, groundwater, industrial effluents, urban runoffs and hazardous waste sites.

### 2.3 Reaction of ozone with compounds containing multiple bonds

Ozonation occurs via the Creigee mechanism which is the general route for the reaction of ozone with olefins. During the process of ozonation, organic micro-pollutants are oxidized with ozone selectively. Ozone reacts mainly with double bonds of activated aromatics systems and non-protonated amines. In general electron donating groups enhance oxidation by ozone whereas electron withdrawing groups reduce the reaction rate (von Gunten, 2009).

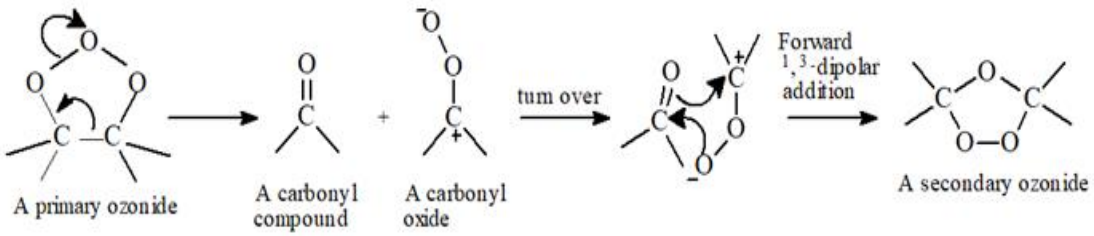


*Scheme 1: Rearrangement of POZ to SOZ*

Ozonolysis is initiated with 1,3- cycloaddition of ozone across the double bond to form a primary ozonide (POZ) which consists of a five-membered ring and is very unstable. The POZ rearranges by a concerted cyclo-reversion to produce a carbonyl compound called Criegee Intermediate (CI). Based on structural calculations, the CI is believed to adopt the carbonyl oxide structure. The two fragments produced in the reaction may recombine to form a secondary ozonide (SOZ). The POZ is less stable than the SOZ because it has two weak oxygen-oxygen bonds. On the other hand, the SOZ has only one weak oxygen-oxygen bond in its structure.

When the reaction of ozone takes place in a protic solvent such as water, the primary ozonide decomposes into a carbonyl compound (ketone or aldehyde) and a zwitterion **(I)** that quickly leads to a hydroxy-hydroperoxide **(II)** which in turn decomposes into a carbonyl compound and hydrogen peroxide.

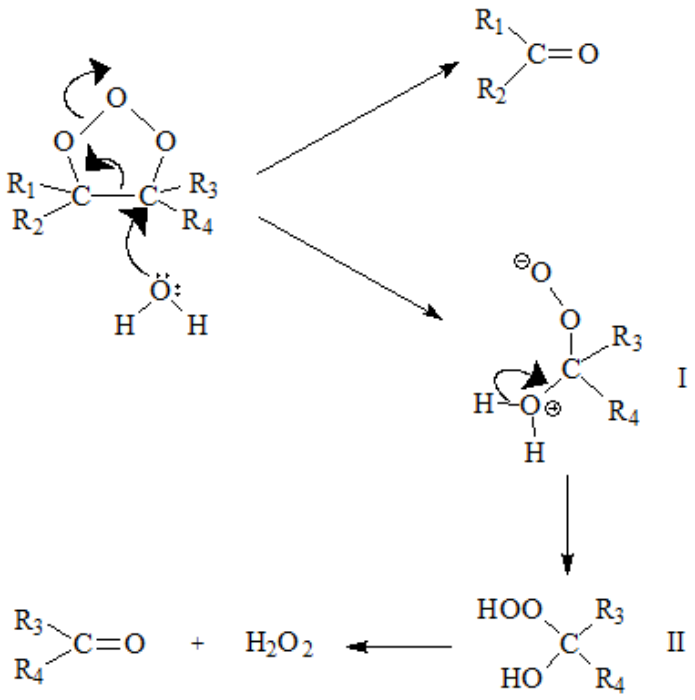


*Scheme 2: Decomposition of ozone in a protic solvent*

### 2.4 Computational study of the reaction of ozone with benzene and phenols

Previous computational studies done for the addition of ozone on benzene by Hendrickx and Vinckier (2003) deduced that the reaction between ozone and benzene proceeds in a concerted fashion. The addition can occur on two carbons in the α, β or γ position to each other. The α addition was found to produce POZ structures that were the most stable (Scheme 3). The reason for this could most probably be attributed to a 1,3-butadiene-like moiety, which is only present in the product of the α addition. Optimization of the γ structure yielded a local minimum on the potential energy surface, which at the CCSD(T) level is 15 kcal/mol higher than the α-POZ. A detailed search did not yield a stable structure in which the ozone molecule is bound to two carbon atoms that are in β position with respect to each other. Even if the study was confined to the α type addition, still two

mechanistically different approaches should be considered: the middle oxygen atom of ozone is either directed toward the benzene ring (*endo*-type) or directed away from the ring structure (*exo*-type). Hendrickx and Vinckier arrived at the conclusion that at the B3LYP and CCSD(T) levels, the energetic positions of the two conformers (i.e. *endo*- and *exo*-type) of the POZ are nearly identical, the difference being less than 0.5 kcal/mol.

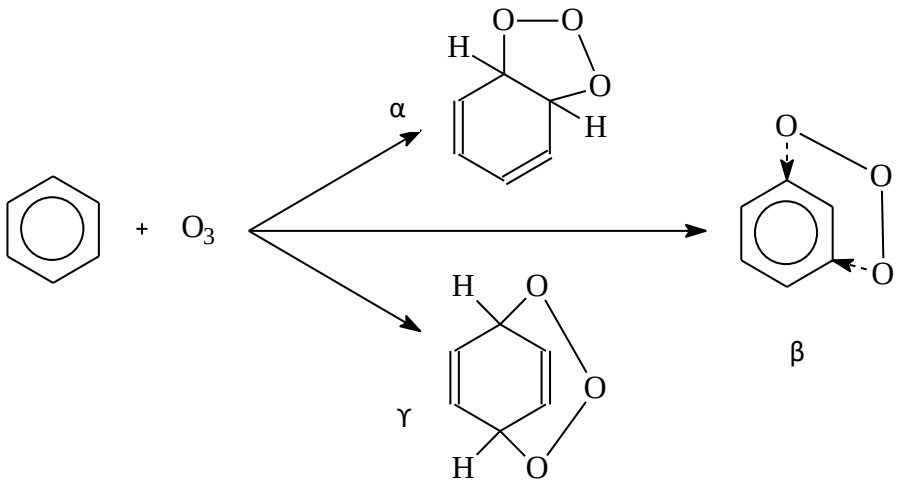


Scheme 3: Mechanism of the reaction of ozone with benzene

Hendrickx and Vinckier (2003) reported the only computational study for the reaction of ozone with phenol in the gas phase. However, the report was only concerned with the electronic energy differences, $\Delta E_e$, and also includes correction for the zero-point vibrational energies (ZPE), at the B3LYP level of theory. More recent work done by Gariseb (2013) went further by computing the thermochemical properties including enthalpies ($\Delta H$) and Gibbs free energies ($\Delta G$) for the POZs derived from substituted phenol and thiophenol. Gariseb's work provided for the first-time the thermochemical data for the POZs derived from substituted thiophenol for which no study was done previously. Specifically, Gariseb studied the potential energy surfaces of phenol,

thiophenol, chlorophenol, dihydroxybenzene and hydroxythiophenol primary ozonides (POZs) using density functional theory (DFT) in the gas phase. The focus was on processes involving the formation of POZs as intermediates in the ozonolysis of substituted phenol and thiophenol. Consequently, the structures, stability and thermochemical properties of the POZ were computed in the gas phase.

Work done by Embula etal. covered computational research done on primary ozonides formed from the ozonolysis of thiophenol in the gas phase using B3LYP density functional theory and the CCSD(T) approach (Embula, Archibong, Gariseb, Hishimone, & Ramasami, 2013).The work was primarily on the stability of thiophenol POZs in the gas phase.

# Chapter 3

## Materials and Methods

### 3.1 Computational methods

The geometries of the POZs in the gas phase and in water were fully optimized using the hybrid B3LYP Density Functional Theory (DFT) in conjunction with the 6-31G(d,p) basis set. Output files were scrutinized after each iteration of the geometry optimization for fulfillment of the convergence criteria. The first and second convergence criteria contained the maximum force on an atom in the system and the average (root mean square, RMS) force on all atoms, respectively. The maximum force and the RMS of the force were gauged against threshold values that must not be exceeded. The third and fourth convergence criteria were the maximum displacement, that is, the maximum structural change of the coordinates as well as the average (RMS) change over all structural parameters in the last two iterations. Once the current values of all four criteria fall below the thresholds, the optimization is considered completed. If these parameters were not fulfilled, tighter convergence criteria would be chosen to improve the current value and would therefore require more computer time (Electronic Structure calculations in Gaussian, 2017).

After geometry optimization, the stationary points were characterized by frequency calculations as either a minimum or a saddle point. A minimum stationary point would have Hessian index of zero (0), that is all frequencies would have positive values, and a saddle point would possess a Hessian index of one (1), that is one imaginary frequency. Transition state geometry and frequency calculations allow determination of energy barriers which could provide insight into the kinetics of the reactions. In order to improve

the energetics, the effects of electron correlation were taken into account by performing CCSD(T) calculations using the geometry obtained at the B3LYP level in the same one-particle basis set.

The Polarizable Continuum Model (PCM) (Quan, Stamm, & Maday, 2017) was used to investigate the role of solvent (water) on the thermodynamic stability of the POZs and also on the reaction barriers leading to their formation. The PCM calculations were done at the B3LYP/6-31G(d) level. In the PCM approach, the molecular free energy in solution $G_{sol}$ is computed as the sum of three terms:

$$G_{sol} = G_{es} + G_{dis} + G_{cav}$$

where

$$G_{es} = electrostatic\ contribution\ to\ the\ free\ energy$$

$$G_{dis} = dispersion - repulsion\ contribution\ to\ the\ free\ energy$$

$$G_{cav} = cavitation\ energy\ contribution\ to\ the\ free\ energy$$

The three terms above are computed via a cavity defined through interlocking van der Waals spheres centered at atomic position (Ludwig-Maximilians-University Munich, 2020). In practice, the free energy of solvation is the difference in energy of a species in the gas phase and in solution. Consequently, in this study, it was computed by subtracting the total energy of a species in the gas phase from the total energy of the species in solution, using Gaussian 16.

The relative energies in the gas phase and in water were calculated as the difference between the total energies of the product (POZ) and the reactants, i.e

$$\Delta \mathrm{E} = \mathrm{E}(\text{primary ozonide}) - \mathrm{E}(\text{reactants})$$

# Chapter 4

## Results and Discussions

### 4.1 The naming of Phenol and Thiophenol Primary Ozonides

The naming of the primary ozonides (POZs) derived from the addition of ozone to phenol and thiophenol in gas phase and water was done in the following way: the incoming ozone can attach at three distinct places as shown in Figure 2: an addition at positions 1 and 2, 2 and 3, or 3 and 4. In the following sections, we describe these three possibilities as modes I, II and III (Hendrickx & Vinckier, 2003). Moreover, the direction of the -OH or-SH hydrogen with respect to the incoming ozone results in different isomers. The hydrogen atom of these groups can be oriented either toward or away from the attached ozone. The resulting structures will therefore be denoted as endo-H (towards) or exo-H (away), respectively. Finally, the middle oxygen of the attached ozone can be oriented toward (endo-O) or away (exo-O) from the aryl ring (Hendrickx & Vinckier, 2003).

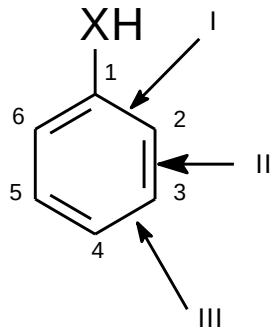


*Figure 2: Schematic representation of the three modes of 1,3-cycloaddition of ozone to phenol and thiophenol.*

Figure 3, illustrates how the atoms are labeled for the phenol and thiophenol molecule, respectively. The oxygen atom on the phenolic moiety is labeled $O_1$ and the oxygen atoms of the ozone molecule labeled $O_2$, $O_3$ and $O_4$, respectively. The carbon atoms of the aromatic ring labeled as $C_1$, $C_2$, $C_3$, $C_4$, $C_5$ and $C_6$ in the clockwise direction. The sulphur atom of the thiophenol ring are labeled S and the oxygen atoms of the ozone molecule are labeled $O_1$, $O_2$ and $O_3$. The carbon atoms of the thiophenol ring are labeled $C_1$, $C_2$, $C_3$, $C_4$, $C_5$ and $C_6$ in the clockwise direction.

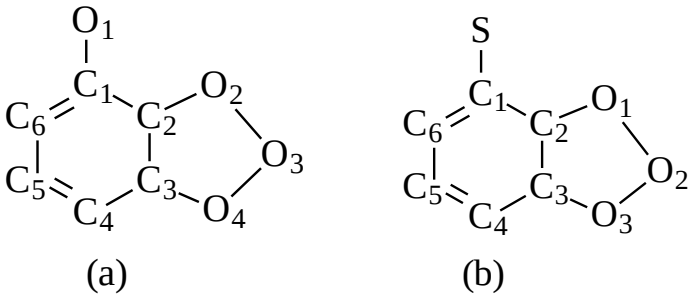


*Figure 3: Illustration of how the atoms are labeled for (a) phenol and (b) thiophenol molecules.*

Figure 4, shows the geometric parameters that were considered when comparing structures of POZs formed in the gas phase and in water. The character X represents oxygen or sulphur atom. The C-X (i.e C-O and C-S) bond length is represented by $R_1$ for both phenol and thiophenol POZs. $R_2$ and $R_5$ are respective bond distances of the ozone terminal O atoms to the carbon atoms on the ring. Finally, $R_3$ is the O-O bond distance nearer to –XH and $R_4$ the one farther away from –XH. The O-O-O bond angle is represented by $\theta$.

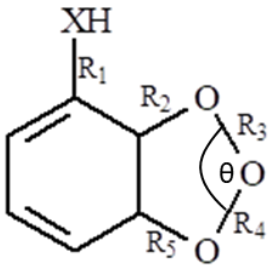


*Figure 4: The figure shows a diagram of the bonds which were considered in the study and how they were identified for both phenol and thiophenol POZs.*

### 4.2 Primary ozonides (POZs) of phenol in the gas phase and in water

A calibration study was done at the beginning of this study to determine the appropriate level of theory that could yield accurate results at low computational cost. Based on previous studies of phenol (Hendrickx & Vinckier, 2003) and thiophenol (Embula, Archibong, Gariseb, Hishimone, & Ramasami, 2013) POZs, it was imperative to use the electron correlation method when computing the energetics of these systems. In this work, the results of the initial calibration studies on the phenol POZs, using a robust CCSD(T)/6-311++G(2df,2p)//B3LYP/6-311++G(2df,2p) model and the lower level CCSD(T)/6-31G(d)//B3LYP/6-31G(d) model, indicated that the relative energies predicted by the two models do not differ by more than 1.5 kcal/mol. Consequently, the CCSD(T)/6-31G(d)//B3LYP/6-31G(d) model was chosen to study the energetics.

Table 3 lists the relative energies, including the zero-point vibrational energies ($\Delta E_e$ + ΔZPE), of phenol POZs in the gas phase (G) and in water (W). The table also includes the relative energies of the corresponding transition state structures. The computations were carried out at the B3LYP/6-31G(d,p) and CCSD(T)/6-31G(d,p)//B3LYP/6-31G(d,p) levels.

*Table 3: Relative energies of the POZ isomers and the transition state structures leading to the formation of the POZs in the 1,3-cycloaddition of Ozone to Phenol*

| | | | Zero-point vibrational energies ($\Delta E_e + \Delta$ZP (kcal/mol) | | | | | |
|---|---|---|---|---|---|---|---|---|
| | | | Primary Ozonide | | | Transition State | | |
| | | | CCSD(T) (Gas phase) | B3LYP (Gas phase) | B3LYP (Water) | CCSD(T) (Gas phase) | B3LYP (Gas phase) | B3LYP (Water) |
| Mode I | | | | | | | | |
| 1,2-addition | endo-O | endo-H | -26.6 | -23.5 | -23.8 | 9.5 | 5.1 | 4.5 |
| | endo-O | exo-H | -24.6 | -21.7 | -23.0 | 11.2 | 6.8 | 4.6 |
| | exo-O | endo-H | -28.5 | -24.9 | -25.4 | 12.2 | 8.5 | 6.8 |
| | exo-O | exo-H | -28.6 | -24.8 | -26.1 | 12.2 | 8.7 | 6.2 |
| | | | | | | | | |
| Mode II | | | | | | | | |
| 2,3-addition | endo-O | endo-H | -23.3 | -22.3 | -22.9 | 12.5 | 7.9 | 6.8 |
| | endo-O | exo-H | -22.6 | -21.7 | -23.7 | 12.5 | 8.1 | 6.1 |
| | exo-O | endo-H | -23.8 | -22.9 | -23.0 | 14.4 | 9.9 | 8.3 |
| | exo-O | exo-H | -22.6 | -21.7 | -23.7 | 14.4 | 8.1 | 7.8 |
| | | | | | | | | |
| Mode III | | | | | | | | |
| 3,4-addition | endo-O | endo-H | -23.3 | -22.2 | -24.0 | 11.3 | 6.2 | 4.1 |
| | endo-O | exo-H | -21.2 | -20.3 | -22.8 | 12.4 | 7.1 | 4.5 |
| | exo-O | endo-H | -23.8 | -23.5 | -24.3 | 13.4 | 8.5 | 6.0 |
| | exo-O | exo-H | -21.8 | -21.6 | -23.1 | 14.5 | 9.6 | 6.5 |

### 4.2.1 Phenol POZs in the gas phase

The reaction of ozone with phenol in the gas phase has been studied previously by Hendrickx and Vinckier. That work (Hendrickx & Vinckier, 2003) has been used to benchmark the gas phase results of the current work. It has also been used to study the effects of solvent (water) on the stability of the POZs and the transition states leading to their formation. According to the B3LYP/6-31G(d,p) results of Hendrickx et al., all primary ozonides of phenol were found atleast 20 kcal/mol below the reactants in an exothermic reaction. The latter result has been confirmed in the current study. Furthermore, Table 3 shows that the isoenergetic exo_O_exo_H and exo_O_endo_H 1,2-

addition products, are roughly 25 kcal/mol below the reactants and appear to be the most stable POZs of phenol at the B3LYP/6-31G(d) level.

*Figure 5* shows the calculated relative energies of the five most stable isomers produced from the addition of ozone to phenol in the gas phase at the B3LYP/6-31G(d,p) and CCSD(T)/6-31G(d,p)/B3LYP/6-31G(d,p) levels of theory. Using the CCSD(T)/6-31G(d,p)/B3LYP/6-31G(d,p) approximation, the relative energies of the POZs increases from roughly 0.2 – 3.8 kcal/mol, with the 1,2-addition products (mode I) at the higher end in the range 2.9-3.8 kcal/mol. This suggests greater stability of the POZs and the importance of electron correlation in calculating the energies of these species.

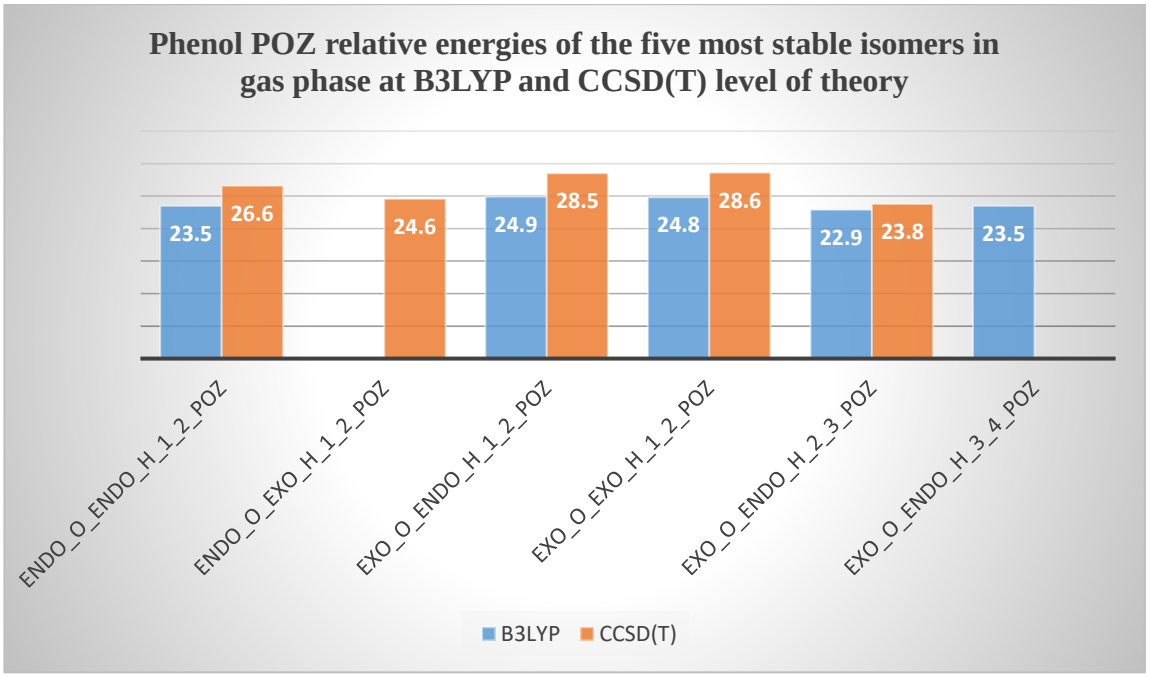


*Figure 5: Relative energies of the five most stable phenol POZ isomers in gas phase at the B3LYP and CCSD(T) levels.*

Figure 6 is the B3LYP/6-31G(d,p) reaction profile for the most and least favored pathway, respectively, in 1,3-cycloaddition of ozone to phenol in the gas phase. From the results

presented in Table 3 and Figure 6, mode I seems to be energetically the most favorable pathway. At the B3LYP/6-31G(d,p) level, the 1,2-addition endo_O_endo_H isomer has the lowest energy barrier of 5.1 kcal/mol and the corresponding CCSD(T)/6-31G(d,p)//B3LYP/6-31G(d,p) value is 9.5 kcal/mol, representing the lowest energy barrier predicted by the correlated method. On the other hand, the energy barrier for the formation of the isoenergetic exo_O_exo_H and exo_O_endo_H 1,2-addition is predicted to be 12.2 kcal/mol, using the CCSD(T)/6-31G(d,p)//B3LYP/6-31G(d,p) model. Based on these results, formation of the most stable isomers of phenol POZ in the gas phase will likely go through the 1,2-addition channel (mode I). The highest energy barrier, based on the CCSD(T) calculations, was found to be 14.5 kcal/mol for the path leading to the formation of the exo_O_exo_H 3,4-addition product. In contrast, the highest energy barrier predicted by the B3LYP model is 9.9 kcal/mol for the formation of the exo_O_endo_H 2,3-addition product.

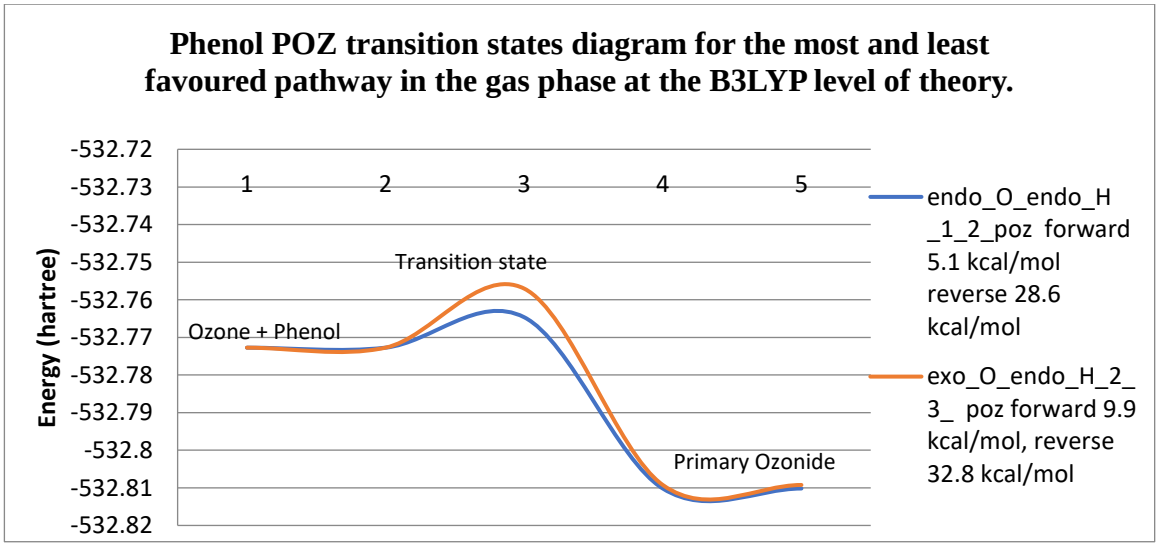


*Figure 6: Phenol POZ reaction profile for the most and least favored pathway in the gas phase at the B3LYP level.*

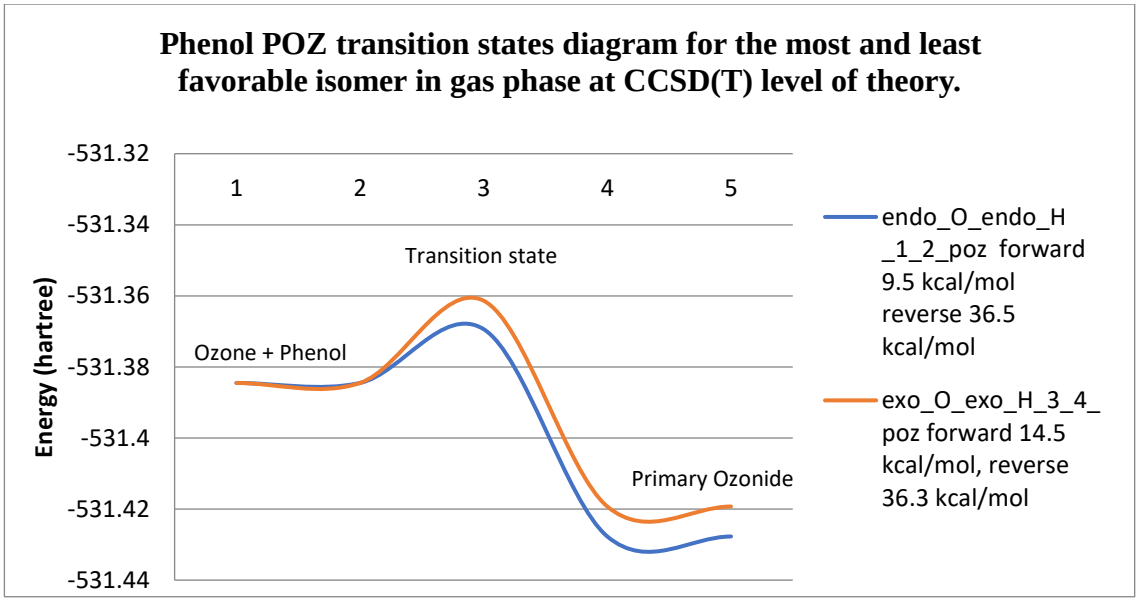


*Figure 7: Phenol POZ reaction profile for the most and least favored pathway in the gas phase at the CCSD(T) level.*

The reaction profile computed with the CCSD(T)/6-31G(d,p) is found in Figure 7.

It is noted that the CCSD(T) energy barriers are consistently higher than those predicted by B3LYP in accord with the results presented in the study done by Hendrickx and Vinckier.

According to Hendrickx and Vinckier the reason for mode I in the gas phase being the most favorable is because of the electron-withdrawing ability of the hydroxyl group of phenol that causes the carbon ($C_1$) atom attached to the -OH to have a positive Mulliken charge in gas phase by as much as ~+32 $e^-$, whereas the rest of the carbon atoms in the ring have a negative charge (~-0.10 $e^-$) in the gas phase at B3LYP level. The increased reactivity of ozone towards phenol has been attributed to the attractive electrostatic forces between $C_1$ and the terminal oxygen atoms of ozone, thereby making mode I most favored at room temperature.

*Table 4: The most stable isomers formed from the 1,3-cycloaddition of ozone to phenol in the gas phase and the most favored transition state structures, computed at the B3LYP and CCSD(T) levels.*

| **B3LYP/6-31G(d,p)** | **CCSD(T)/6-31G(d,p)** |
|---|---|
| **The most stable isomers** | |
| exo_O_endo_H_1_2_poz | exo_O_exo_H_1_2_poz |
| 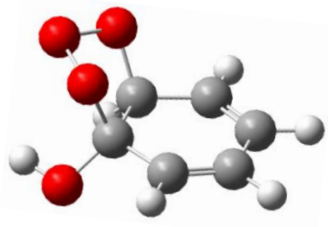 | 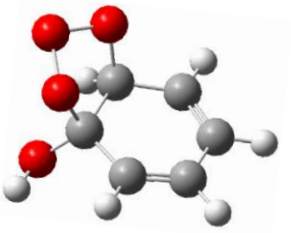 |
| **The lowest energy transition state structures** | |
| endo_O_endo_H_1_2_poz | endo_O_endo_H_1_2_poz |
| 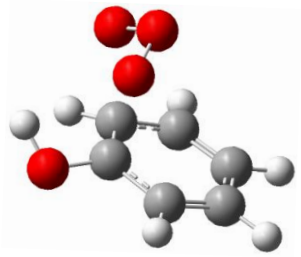 | 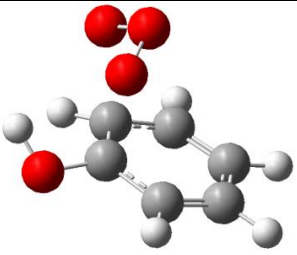 |

Table  shows the most stable and most favored isomers in gas phase at the B3LYP and CCSD(T) levels. The planarity of most POZs formed from the reaction of ozone with phenol in the gas phase was found to be lost. It seems only two isomers formed through mode I retained their planarity. First, when the central oxygen of the ozone is in the endo position and the hydroxyl hydrogen is in the exo position. Second, when the central oxygen of ozone is in the exo position and the hydroxyl hydrogen is in the endo position.

A relative increase in bond length is noticed for $R_1$ from 1.368 Å to ~1.4 Å when the ozone molecule attaches to the phenol molecule via modes I and II. According to Hendrickx, this elongation reflects the fact that the conjugation effect of the hydroxyl group with the $\pi$ system of the phenyl ring is no longer active in the POZs. Mode III shows

a slight reduction in $R_1$ when compared to that of the isolated phenol molecule in gas phase. The angle θ ranges from 101-102$^0$ for most POZs formed through modes I, II and III. The bond angle of 104.4$^0$ formed by 2,3-addition is due to the severe twisting of the aryl ring.

### 4.2.2 HOMO-LUMO gap and hydrogen bonding analysis of the most stable phenol POZs in the gas phase at the B3LYP level.

Gas phase calculations at the B3LYP/6-31G(d,p) level of theory indicated that the most stable phenol POZ formed via mode I appeared to be the exo_O_endo_H 1,2-addition product. The latter lies at 24.9 kcal/mol below the reactants. In Table 5, the HOMO-LUMO gap for this isomer was 0.188 a.u and the largest when compared to HOMO-LUMO gap of other isomers formed via this mode. The most stable isomer generated via mode II was exo_O_endo_H 2,3-addition with a relative energy at 22.9 kcal/mol below the reactants. Table 5 shows that the HOMO-LUMO gap for this isomers was 0.171 a.u and appears to be the smallest when compared to other isomers structures in this mode. The most stable isomer generated via mode III was exo_O_endo_H 3,4-addition with a relative energy at 23.5 kcal/mol below the reactants. The HOMO-LUMO gap for this isomer was 0.182 a.u and the largest when compared to other structures in this mode.

*Table 5: HOMO- LUMO gap, energy barriers and relative energy (including zero-point energy correction) for phenol POZs in the gas phase at the B3LYP/6-31G(d,p) level.*

| | | | HOMO-LUMO Gap | Transition state | POZ |
|---|---|---|---|---|---|
| | | | (a.u) | B3LYP (Gas phase) $\Delta E_e + \Delta ZPE$ kcal/mol | B3LYP (Gas phase) $\Delta E_e + \Delta ZPE$ kcal/mol |
| Mode I | | | | | |
| 1,2-addition | endo-O | endo-H | 0.183 | 5.1 | -23.5 |
| | endo-O | exo-H | 0.185 | 6.8 | -21.7 |
| | exo-O | endo-H | 0.188 | 8.5 | -24.9 |
| | exo-O | exo-H | 0.187 | 8.7 | -24.8 |
| | | | | | |
| Mode II | | | | | |
| 2,3-addition | endo-O | endo-H | 0.171 | 7.9 | -22.3 |
| | endo-O | exo-H | 0.175 | 8.1 | -21.7 |
| | exo-O | endo-H | 0.171 | 9.9 | -22.9 |
| | exo-O | exo-H | 0.176 | 8.1* | -21.7 |
| | | | | | |
| Mode III | | | | | |
| 3,4-addition | endo-O | endo-H | 0.179 | 6.2 | -22.2 |
| | endo-O | exo-H | 0.172 | 7.1 | -20.3 |
| | exo-O | endo-H | 0.182 | 8.5 | -23.5 |
| | exo-O | exo-H | 0.176 | 9.6 | -21.6 |

Overall, the most stable POZs (exo_O_endo_H and exo_O_exo_H) from the reaction of ozone with phenol in the gas phase were generated via mode I. At the B3LYP level, the HOMO-LUMO gaps of the phenol POZs formed via mode I are the largest, indicating the kinetic stability of these isomers. The loss of both planarity and delocalization of $\pi$ electron system of the phenyl ring in most of the POZs (modes I-III) might result in lower stability. On the other hand, the observed stability of the mode I isomers could be attributed to hydrogen bonding between the hydroxyl hydrogen and the attached oxygen atoms of the ozone. This is evident in Table 6 below where the results appear to indicate that mode I has the shortest hydrogen bond distance of 2.01 Å.

*Table 6: Bond distance between the hydroxyl hydrogen and the surrounding oxygen atoms for the most stable phenol POZ isomers at each mode of addition in the gas phase at the B3LYP level.*

| | Mode | $O_2$-H (Å) | $O_3$-H(Å) | $O_4$-H(Å) |
|---|---|---|---|---|
| The most stable POZ for each mode | I | 2.46 | 2.58 | 2.01 |
| | II | 2.17 | 3.43 | 3.82 |
| | III | 5.12 | 6.17 | 5.68 |

Table 7 shows the molecular orbitals for the HOMO and LUMO of the most stable POZs formed via each mode of addition. The HOMO of the POZ generated via mode I is bonding with contributions from atomic orbitals on $C_2$-$C_3$-$C_4$ and $C_5$-$C_6$-$C_1$ respectively, however it is anti-bonding on $C_1$-$C_2$ and $C_4$-$C_5$, respectively. The LUMO exhibits bonding character on $C_6$-$C_1$-$C_2$-$C_3$ and $C_4$-$C_5$, respectively, but anti-bonding on $C_3$-$C_4$ and $C_5$-$C_6$, respectively. The HOMO for primary ozonide generated via mode II is bonding on $C_6$-$C_1$-$C_2$ and $C_4$-$C_5$, respectively, but anti-bonding on OH-$C_1$, $C_3$-$C_4$ and $C_5$-$C_6$. The LUMO shows bonding character on $C_1$-$C_2$-$C_3$-$C_4$ and $C_5$-$C_6$, respectively, but anti-bonding on OH-$C_1$, $C_4$-$C_5$ and $C_6$-$C_1$, respectively. The HOMO for the primary ozonide generated via mode III is bonding on $C_6$-$C_1$ and $C_2$-$C_3$, however anti-bonding on OH-$C_1$, $C_1$-$C_2$ and $C_5$-$C_6$, respectively. The LUMO is bonding on $C_1$-$C_6$, $C_5$-$C_6$ and $C_4$-$C_5$ and anti-bonding on OH-$C_1$, $C_1$-$C_2$ and $C_5$-$C_6$, respectively.

*Table 7: HOMO-LUMO of the most stable phenol POZs in gas phase at the B3LYP level for each mode.*

| | HOMO | LUMO |
|---|---|---|
| Mode I | 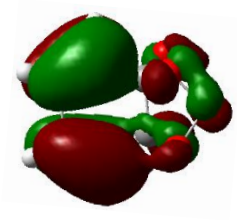 | 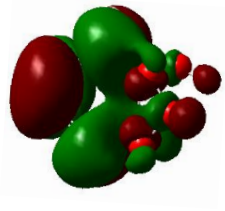 |
| Mode II | 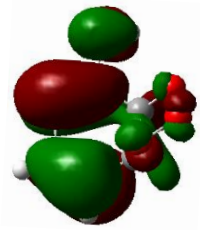 | 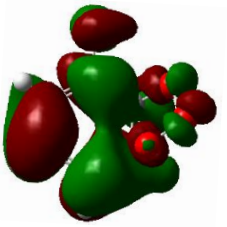 |
| Mode III | 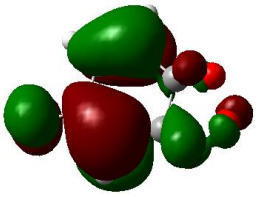 | 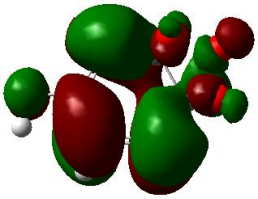 |

### 4.2.3 Phenol POZs in water

Using the B3LYP/6-31G(d,p) model, the most stable POZ formed in the 1,3-cycloaddition of ozone to phenol in water at 298.15 K, appeared to be the exo_O_exo_H 1,2-addition product. The latter isomer was computed to be at 26.1 kcal/mol below the reactants. The least stable POZ was the exo_O_exo_H 3,4-addition isomer generated via mode III. It was calculated to be at 22.8 kcal/mol below the reactants. All POZs computed via modes II and III appeared to be more stable by 22.9-24.3 kcal/mol than the reactants. Figure 8 shows the calculated relative energies of the five most stable phenol POZs that were formed in water at 298.15 K.

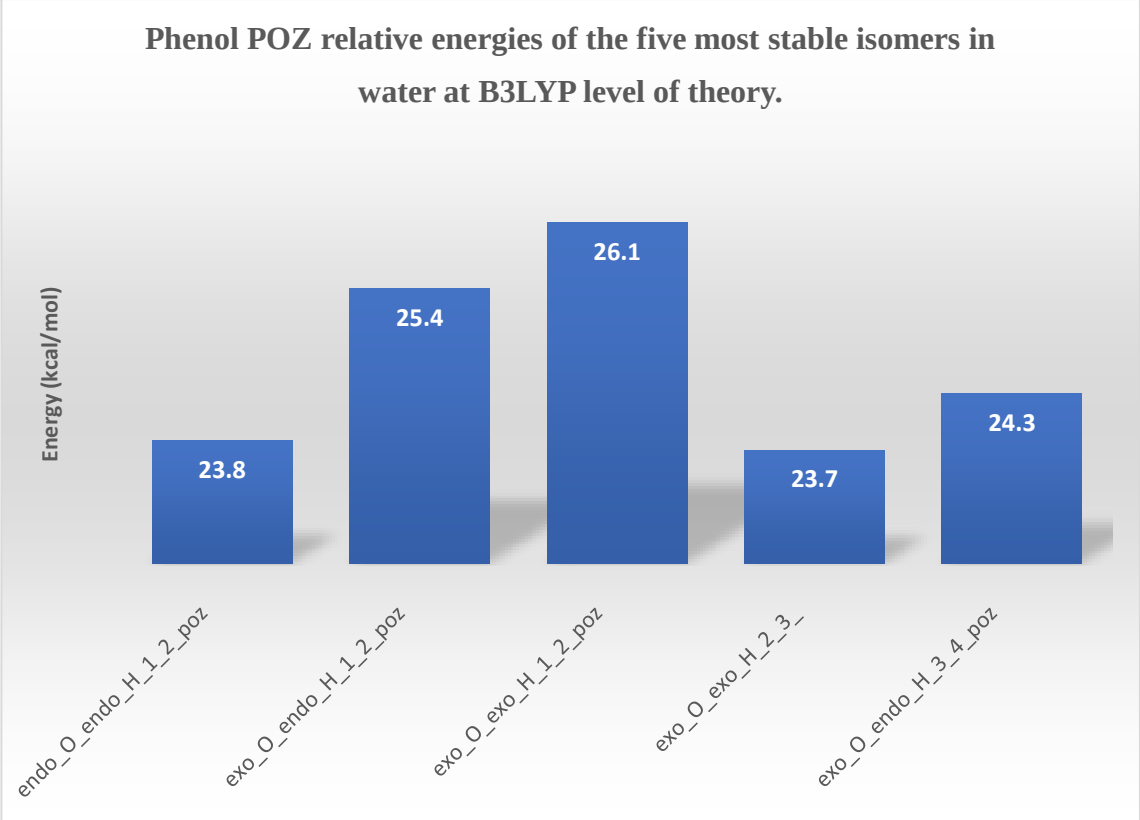


*Figure 8: Relative energies of the five most stable phenol POZs in water at 298.15 K computed at the B3LYP/6-31G(d,p) level.*

Transition state structure calculations in water at the B3LYP/6-31G(d,p) level suggested mode III to be energetically the most favorable pathway. The endo_O_endo_H 3,4-addition POZ structure has the lowest relative energy barrier of 4.1 kcal/mol. The highest energy barrier in water was 8.3 kcal/mol associated with mode II exo_O_endo_H 2,3-addition structure. This POZ would be least favored to form because of the high-energy barrier. Figure 9 is the potential energy diagram for the most and the least favored paths for the addition of ozone to phenol in water at the B3LYP/6-31G(d,p) level of theory.

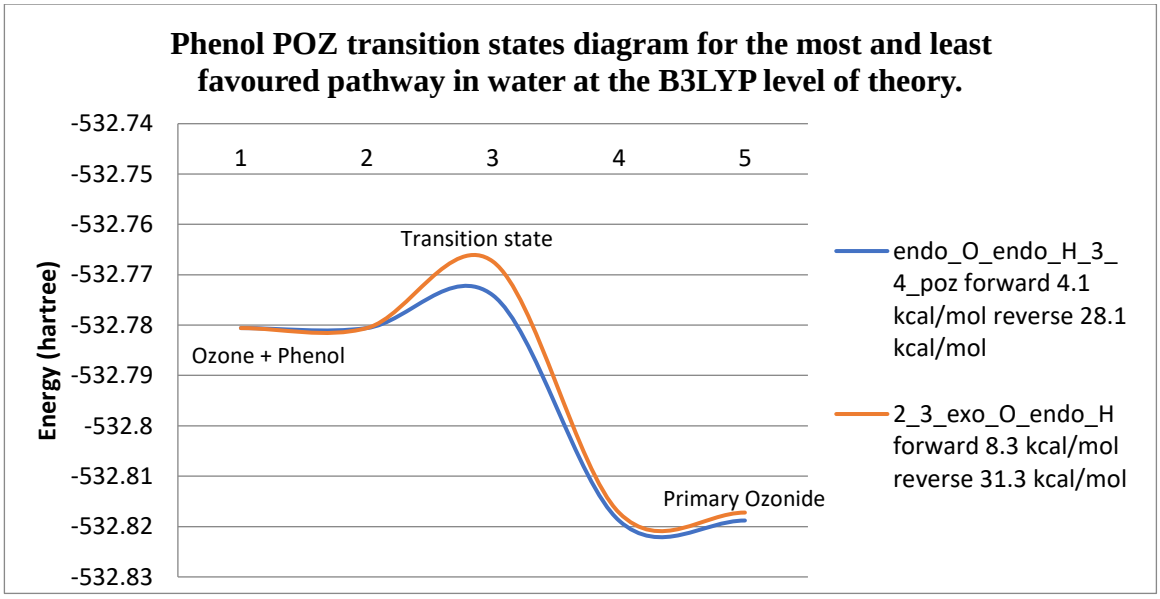


*Figure 9: Phenol POZ reaction profile for the most and least favored pathway in the water at the B3LYP level.*

The planarity of most POZs formed in water is lost and this is pronounced for the exo_O POZs. Only mode III retains planarity for the endo_O POZs. Table 8 shows the most stable isomer and the structure corresponding to the lowest energy barrier at the B3LYP/6-31G(d,p) level.

*Table 8: The most stable isomer and the structure with the lowest energy barrier for the 1,3-cycloaddition of ozone to phenol in water at the B3LYP/6-31G(d,p) level.*

| **B3LYP/6-31G(d,p)** | |
|---|---|
| **The most stable isomers** | **The lowest energy transition state structure** |
| exo_O_exo_H_1_2_poz | exo_O_exo_H_3_4_poz |
| 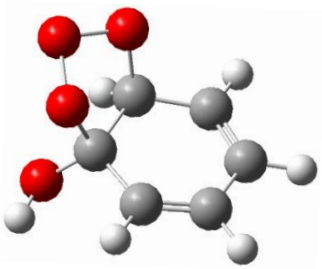 | 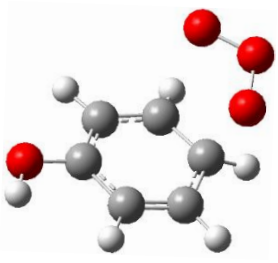 |

In water, the bond length $R_1$ was computed to be 1.37 Å for the phenol molecule and this parameter changed little (not more than $\pm$0.02 Å) in the POZs. The bond angle of $118^0$ computed for the ozone molecule in water was reduced to between 101-$102^0$ in the ozone moiety of the POZs. The only exemption was in exo_O_endo_H POZ of mode II where $104^0$ was computed.

### 4.2.4 Phenol POZs in gas phase vs Phenol POZs in water

All primary ozonides in the gas phase and in water were much more stable than the reactants. The most stable POZ both in the gas phase and in water appeared to be the exo_O_exo_H 1,2-addition isomer. This isomer was more stable in water by just 1.2 kcal/mol. The lowest energy transition state structures in the gas phase and in water were different. In the gas phase, the lowest relative transition state energy barrier of 5.1 kcal/mol was computed for the endo_O_endo_H 1,2-addition structure. In water, the lowest relative transition state energy barrier of 4.1 kcal/mol was computed for the endo_O_endo_H 3,4-addition structure. A comparison of the lowest energy barriers (kcal/mol) computed in the 1,3-cycloaddition of ozone to phenol in the gas phase and in water at the B3LYP/6-31G(d,p) level are depicted in Figure 10 below.

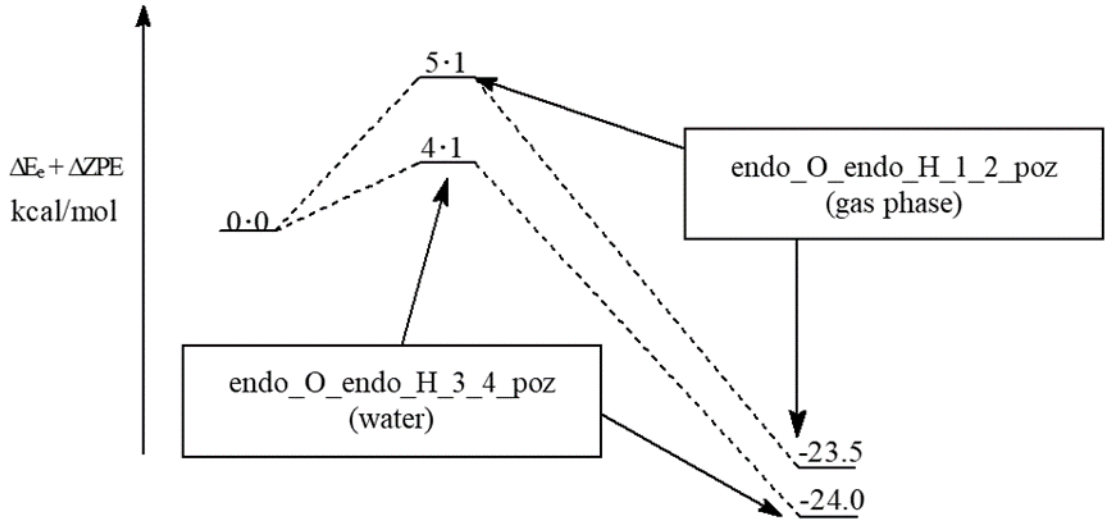


*Figure 10: A comparison of the lowest energy barriers (kcal/mol) computed in the 1,3-cycloaddition of ozone to phenol in the gas phase and in water at the B3LYP/6-31G(d,p) level.*

In the gas phase, the computed bond length $R_1$ increases by roughly 0.03Å in going from the phenol molecule to the phenol moiety in the POZs (exo_O mode I). The opposite effect was observed in water where the bond length $R_1$ in the POZs was shorter by approximately 0.01Å when compared to that calculated for the phenol molecule. The bonds $R_2$, $R_3$, $R_4$, and $R_5$ are slightly shorter for the POZs formed in the gas phase when compared to the POZs formed in water for all modes. The bond angle θ for the attached ozone is in the range of 101-102$^o$ for most POZs formed in the gas phase and in water.

### 4.3 Primary ozonides (POZs) of thiophenol in gas phase and in water

Table 9 shows the relative energies including the zero-point vibrational energies ($\Delta E_e$ +ΔZPE) for the POZ products of 1,3-cycloaddition of ozone to thiophenol in the gas phase (G) and in water (W).

*Table 9: Relative energies of the POZ isomers and the transition state structures leading to the formation of the POZs in the1,3-cycloaddition of ozone to thiophenol*

| | | | Zero-point vibrational energies ($\Delta E_e$ + ΔZPE) (kcal/mol) | | | | | |
|---|---|---|---|---|---|---|---|---|
| | | | Primary Ozonide (kcal/mol) | | | Transition Sate (kcal/mol) | | |
| | | | CCSD(T) (G) ΔEe + ΔZPE | B3LYP (G) ΔEe + ΔZPE | B3LYP (W) $\Delta E_e$ + ΔZPE | CCSD(T) (G) ΔEe + ΔZPE | B3LYP (G) $\Delta E_e$ + ΔZPE | B3LYP (W) $\Delta E_e$ + ΔZPE |
| Mode I | | | | | | | | |
| 1,2-addition | endo-O | endo-H | -22.9 | -19.7 | -20.5 | 12.0 | 8.9 | 7.9 |
| | endo-O | exo-H | -22.2 | -19.2 | -20.6 | 13.1 | 9.7 | 7.8 |
| | exo-O | endo-H | -24.2 | -21.0 | -21.9 | 14.7 | 12.1 | 10.2 |
| | exo-O | exo-H | -24.1 | -21.3 | -22.6 | 14.6 | 11.8 | 9.7 |
| | | | | | | | | |
| Mode II | | | | | | | | |
| 2,3-addition | endo-O | endo-H | -24.0 | -22.5 | -23.4 | 11.2 | 7.6 | 7.2 |
| | endo-O | exo-H | -22.2 | -21.1 | -23.0 | 12.8 | 8.6 | 7.1 |
| | exo-O | endo-H | -23.8 | -22.2 | -22.9 | 13.5 | 9.9 | 8.7 |
| | exo-O | exo-H | -22.3 | -21.1 | -22.9 | 14.6 | 10.6 | 8.7 |
| | | | | | | | | |
| Mode III | | | | | | | | |
| 3,4-addition | endo-O | endo-H | -22.1 | -21.1 | -23.0 | 12.4 | 7.4 | 5.7 |
| | endo-O | exo-H | -22.0 | -20.7 | -22.7 | 12.6 | 7.6 | 5.8 |
| | exo-O | endo-H | -22.3 | -21.1 | -22.8 | 14.5 | 9.8 | 7.7 |
| | exo-O | exo-H | -22.0 | -20.5 | -22.4 | 14.8 | 10.2 | 7.9 |

#### 4.3.1 Thiophenol POZs in gas phase

The calculations for the reaction of ozone with thiophenol in the gas phase were carried out at the B3LYP/6-31G(d,p) and CCSD(T)/6-31G(d,p)//B3LYP/6-31G(d,p) levels of theory. At both levels of theory, the results in Table 9 show that the POZs are more stable relative to the reactants. The energies of the isomers are within 3.3 and 2.2 kcal/mol of each other at the B3LYP/6-31G(d,p) and CCSD(T)/6-31G(d,p)//B3LYP/6-31G(d,p)

levels, respectively. The B3LYP functional predicted the endo_O_endo_H 2,3-addition isomer as the most stable POZ of thiophenol. On the other hand, the more accurate CCSD(T) approximation predicted the exo_O_endo_H 1,2-addition as the lowest energy isomer. The results listed in Table 9 also indicate that electron correlation stabilizes the POZs from about 1.0-3.3 kcal/mol. Figure 11 depicts the calculated relative energies of the five most stable isomers produced from the addition of ozone to thiophenol in the gas phase at the B3LYP/6-31G(d,p) and CCSD(T)/6-31G(d,p) levels of theory.

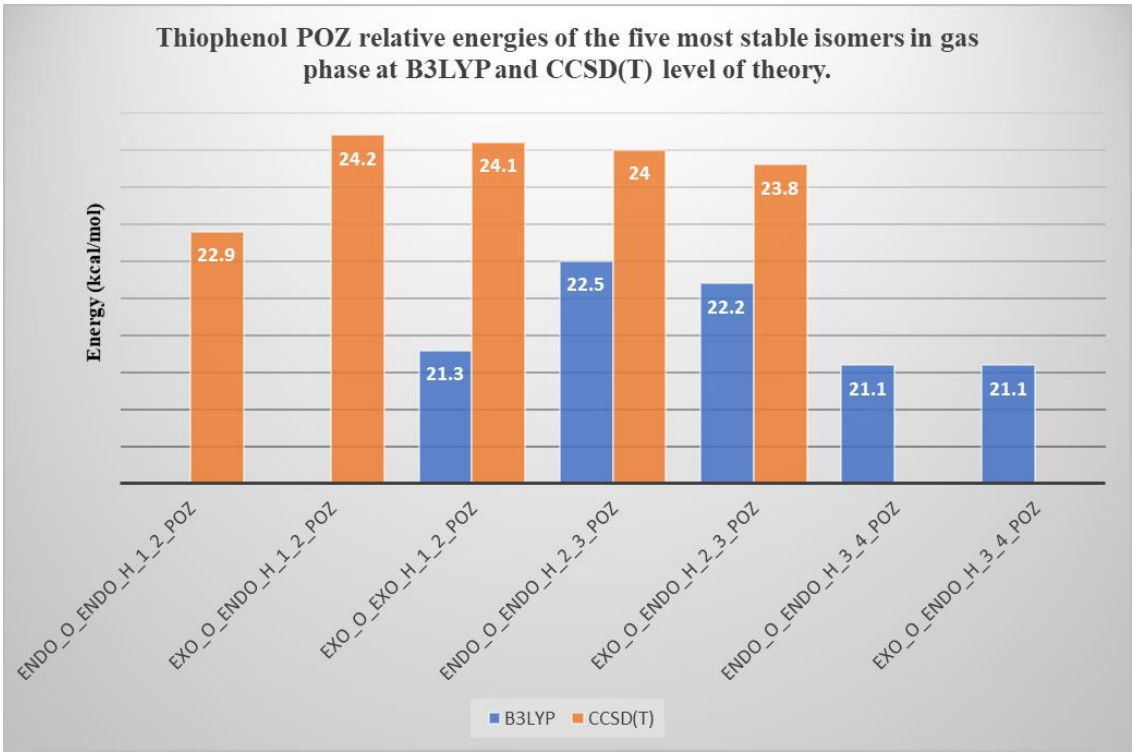


*Figure 11: Relative energies for the five most stable POZ isomers in the gas phase at the B3LYP and CCSD(T) levels*

The calculations of the energy barrier at the B3LYP/6-31G(d,p) level suggested that mode III appeared to be energetically the most favorable pathway. At this level of theory, the endo_O_endo_H 3,4-addition structure was found with the lowest energy barrier of 7.4 kcal/mol. The structure with the highest energy barrier (12.1 kcal/mol) appeared to be

exo_O_endo_H 1,2-addition. This POZ would be the least favorable isomer to form because of the high-energy barrier. Figure 12 depicts the lowest and highest energy paths for the addition of ozone to thiophenol in the gas phase at the B3LYP/6-31G(d,p) level of theory.

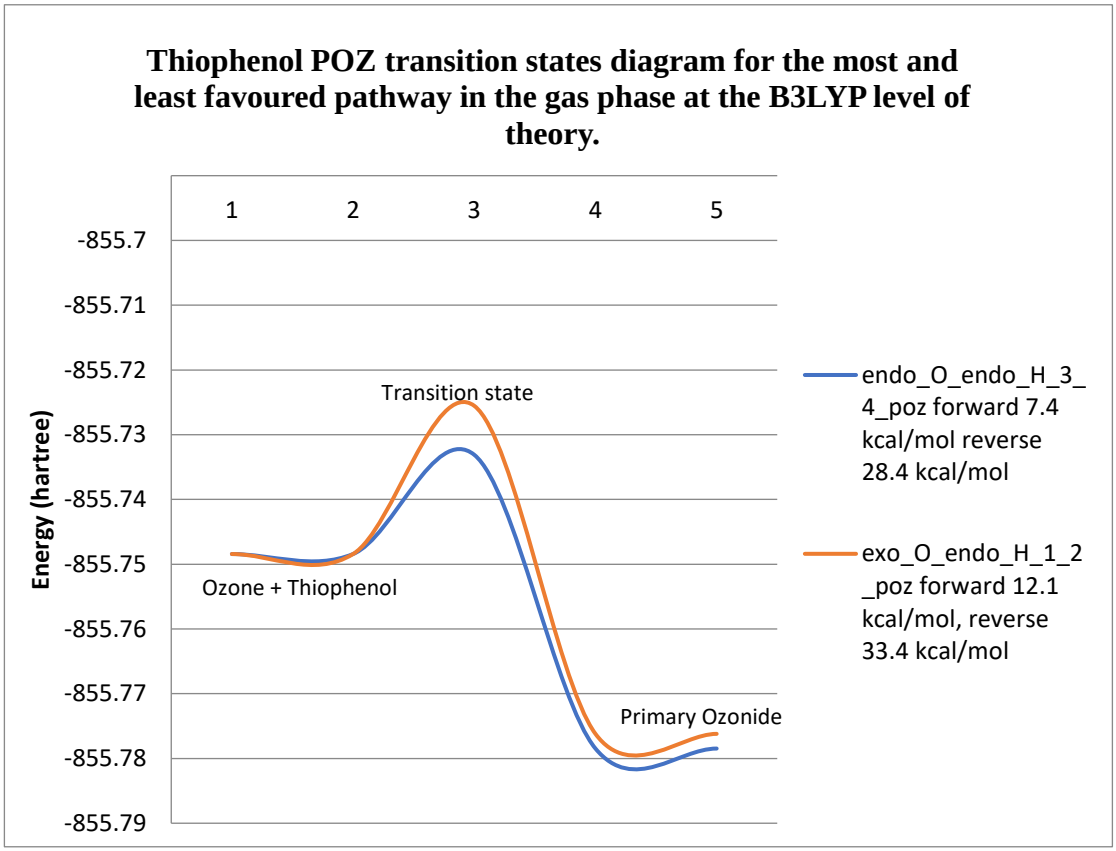


*Figure 12: Thiophenol POZ reaction profile for the most and least favored pathway in the gas phase at the B3LYP level.*

At the CCSD(T)/6-31G(d,p) level of theory, the computed energy barriers were higher than those obtained at the B3LYP/6-31G(d,p) level and mode II appeared to be energetically the most favorable pathway. The CCSD(T)/6-31G(d,p) calculations predicted lowest energy barrier of 11.2 kcal/mol associated with the endo_O_endo_H 2,3-addition transition state structure. The difference between the CCSD(T) and B3LYP

prediction for the lowest energy barrier, corresponding to different transition state structures, is 3.8 kcal/mol in the gas phase. Figure 13 shows the lowest energy paths for the addition of ozone to thiophenol in the gas phase at the CCSD/6-31G(d,p) level.

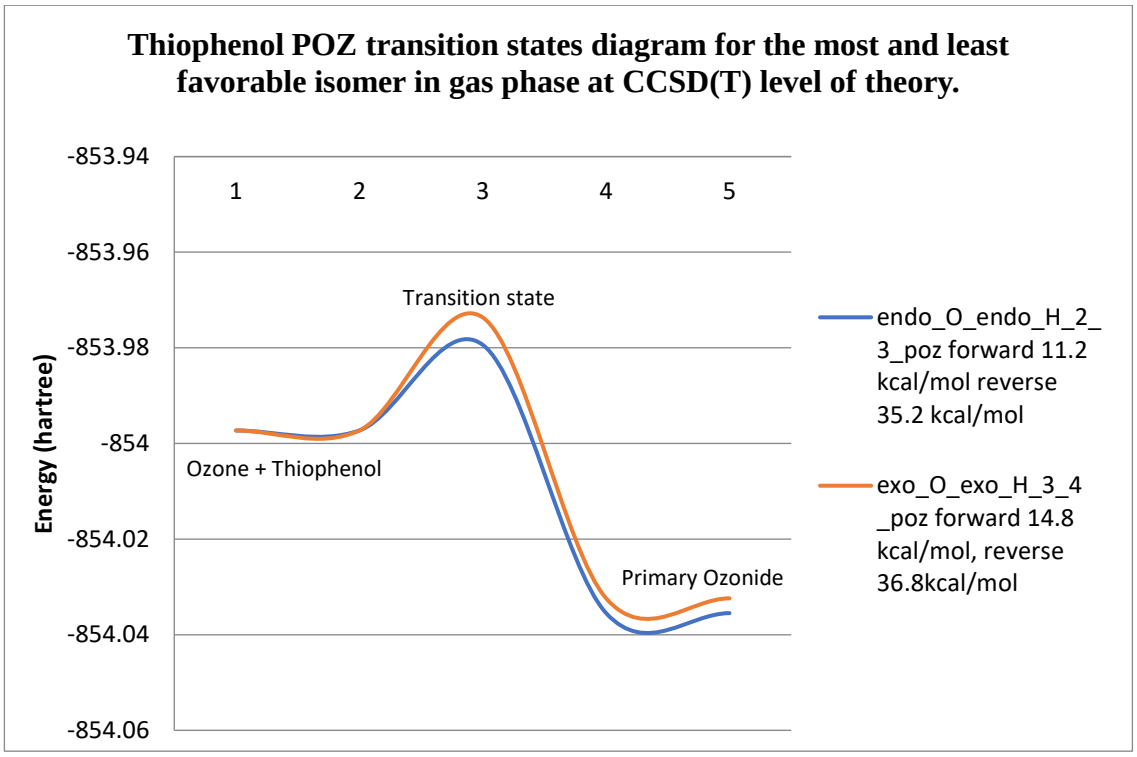


*Figure 13: Thiophenol POZ reaction profile for the most and least favored pathway in the gas phase at the CCSD(T) level.*

In the gas phase, the planarity of the aryl ring was lost for most thiophenol POZs, with the exception of the endo_O isomers formed through mode III. Table 10 shows the most stable isomer and the lowest energy transition state structure at the B3LYP and CCSD(T) levels.

*Table 10: The most stable isomer from the 1,3-cycloaddition of ozone to thiophenol in the gas phase and the most favored transition state structures computed at the B3LYP and CCSD(T) levels.*

| **B3LYP/6-31G(d,p)** | **CCSD(T)/6-31G(d,p)** |
|---|---|
| **The most stable isomers** | |
| exo_O_endo_H_2_3_poz | exo_O_endo_H_1_2_poz |
| 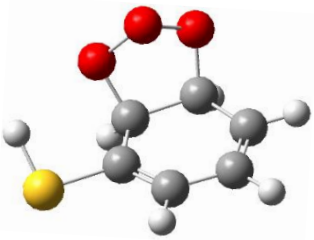 | 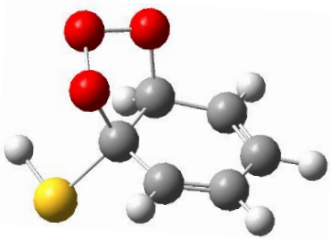 |
| **The lowest energy transition state structures** | |
| endo_O_endo_H_3_4_poz | endo_O_endo_H_2_3_poz |
| 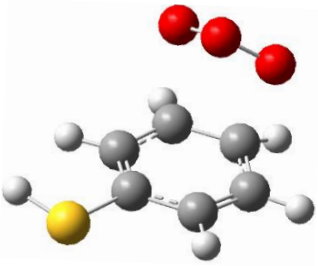 | 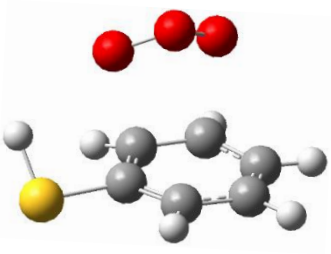 |

An increase was observed for the $R_1$ bond length, from 1.79 Å in the isolated thiophenol molecule to~1.85 Å in the corresponding POZs. A smaller increase of roughly 0.01 Å was observed for POZs formed through modes II and III. Generally, the bond angle θ of 118º in ozone decreased by roughly 7º for all POZs formed through modes I-III.

### 4.4.1 HOMO-LUMO gap and hydrogen bonding analysis of the most stable thiophenol POZs in the gas phase at the B3LYP level.

*Table 11 HOMO- LUMO gap, energy barriers and relative energy (including zero-point energy correction) for thiophenol POZs in the gas phase at the B3LYP/6-31G(d,p) level..*

| | | | HOMO-LUMO Gap | Transition state | POZ |
|---|---|---|---|---|---|
| | | | (a.u) | B3LYP (G) $\Delta E_e + \Delta ZPE$ (kcal/mol) | B3LYP (G) $\Delta E_e + \Delta ZPE$ (kcal/mol) |
| Mode I | | | | | |
| 1,2-addition | endo-O | endo-H | 0.182 | 8.9 | -19.7 |
| | endo-O | exo-H | 0.178 | 9.7 | -19.2 |
| | exo-O | endo-H | 0.180 | 12.1 | -21.0 |
| | exo-O | exo-H | 0.179 | 11.8 | -21.3 |
| | | | | | |
| Mode II | | | | | |
| 2,3-addition | endo-O | endo-H | 0.164 | 7.6 | -22.5 |
| | endo-O | exo-H | 0.162 | 8.6 | -21.1 |
| | exo-O | endo-H | 0.164 | 9.9 | -22.2 |
| | exo-O | exo-H | 0.163 | 10.6 | -21.1 |
| | | | | | |
| Mode III | | | | | |
| 3,4-addition | endo-O | endo-H | 0.171 | 7.4 | -21.1 |
| | endo-O | exo-H | 0.173 | 7.6 | -20.7 |
| | exo-O | endo-H | 0.173 | 9.8 | -21.1 |
| | exo-O | exo-H | 0.172 | 10.2 | -20.5 |

At the B3LYP/6-31G(d,p) level the HOMO-LUMO gap of the thiophenol POZs ranged from 0.162-0.182 a.u. The smallest gap was associated with endo_O_exo_H 2,3-addition and the largest with 1,2-addition endo_O_endo_H.

The B3LYP results in Table 9 and Table 11 suggest that the most stable thiophenol POZ in the gas phase was the 2,3-addition endo_O_endo_H product. Planarity and delocalization of the $\pi$ electron system of the phenyl ring was lost in this isomer and this might suggest loss of stability. However, the observed relative stability of this isomer might be explained by the presence of hydrogen bonding between the thiol hydrogen and

the terminal oxygen atom of the ozone moiety. This can be supported by the results in Table 12 which indicates that mode II has the shortest hydrogen bond distance of 2.53 Å.

*Table 12: Bond distance between the thiol hydrogen and the surrounding oxygen atoms for the most stable thiophenol POZ isomers at each mode of addition in the gas phase at the B3LYP level.*

| | Mode | $O_1$-H (Å) | $O_2$-H (Å) | $O_3$-H (Å) |
|---|---|---|---|---|
| The most stable POZ for each mode | I | 2.81 | 2.96 | 3.60 |
| | II | 2.53 | 3.58 | 4.60 |
| | III | 4.93 | 5.42 | 6.05 |

Table 13, shows the HOMO and LUMO of the most stable POZs formed via each mode of addition. The HOMO for mode I POZ is bonding on $C_5$-$C_6$-$C_1$-S-$O_2$ and $C_3$-$C_4$, respectively, however anti-bonding on $C_2$-$C_3$ and $C_4$-$C_5$, respectively. The LUMO is bonding on $C_6$-$C_1$-$C_2$-$C_3$ and $C_4$-$C_5$, respectively, however anti-bonding on $C_3$-$C_4$ and $C_5$-$C_6$, respectively. The HOMO of mode II POZ is bonding between $C_6$-$C_1$-S and $C_4$-$C_5$, respectively, but antibonding on $C_1$-$C_2$, $C_3$-$C_4$ and $C_5$-$C_6$, respectively. The LUMO is bonding on $C_1$-$C_2$-$C_3$-$C_4$ and $C_5$-$C_6$, respectively, however anti-bonding on $C_4$-$C_5$ and $C_6$-$C_1$, respectively. The HOMO for mode III POZ is bonding on $C_1$-$C_2$ and $C_5$-$C_6$, respectively, however anti-bonding on S-$C_1$, $C_2$-$C_3$, $C_4$-$C_5$ and $C_6$-$C_1$. The LUMO shows $\pi$ bonding on $C_1$-$C_6$ and $C_2$-$C_3$-$C_4$-$C_5$, respectively, however anti-bonding on S-$C_1$, $C_1$-$C_2$ and $C_5$-$C_6$, respectively.

*Table 13: HOMO-LUMO of the most stable thiophenol POZs in gas phase at the B3LYP level for each mode.*

| | HOMO | LUMO |
|---|---|---|
| Mode I | 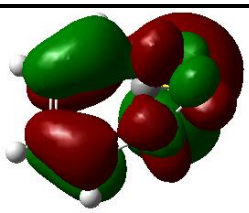 | 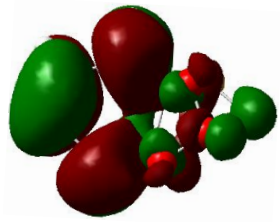 |
| Mode II | 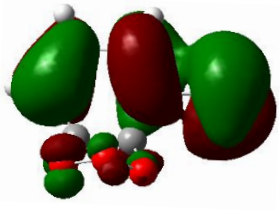 | 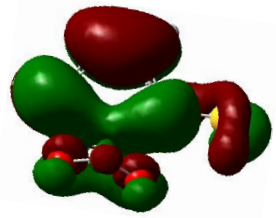 |
| Mode III | 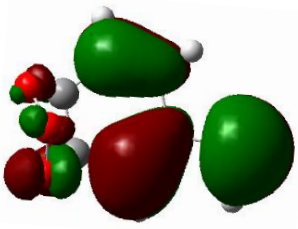 | 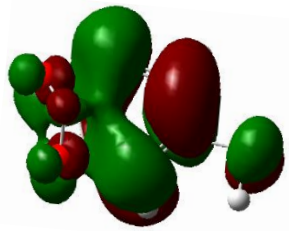 |

### 4.3.3. Thiophenol POZs in water

At the B3LYP/6-31G(d,p) level, the POZs formed in water appeared to be more stable than those in gas phase. Results in Table 9 indicate that the slightly lower stability in water ranges from 0.7 kcal/mol in the n exo_O_endo_H 2,3-additio isomer to 2.0 kcal/mol in endo_O_exo_H 3,4-addition. The most stable POZ in water at 298.15 K appeared to be the endo_O_endo_H 2,3-addition isomer computed at 23.4 kcal/mol below the reactants. The least stable isomer in water was found to be the endo_O_endo_H 1,2-addition isomer with energy of 20.5 kcal/mol below the reactants. Figure 14 shows the calculated relative energies of the five most stable POZ isomers of thiophenol in water at the B3LYP/6-31G(d,p) level of theory.

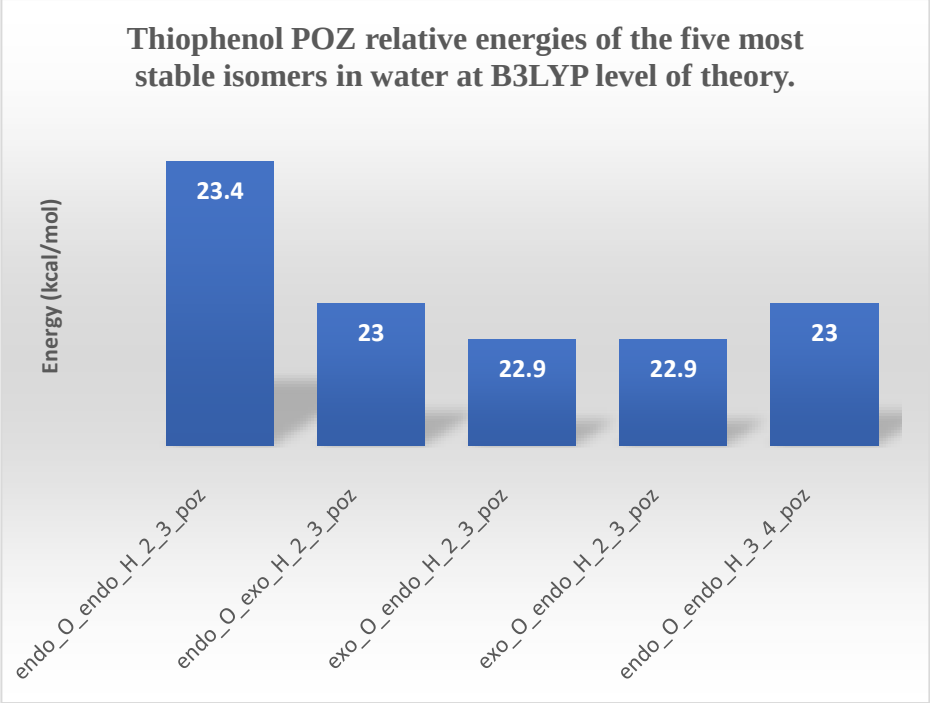


*Figure 14: Relative energies for the five most stable thiophenol POZs in water computed at B3LYP level.*

The energy barrier calculations for the formation of thiophenol POZs at the B3LYP/6-31G(d,p) level suggested mode III to be energetically the most favorable pathway. The lowest energy barrier of 5.7 kcal/mol was associated with the endo_O_endo_H 3,4-addition transition state structure. The highest energy barrier of 10.2 kcal/mol was generated through mode I and associated with the exo_O_endo_H 1,2-addition structure. Figure 15 illustrates the energy difference between the most and the least favored energy paths for the formation of thiophenol POZs at the B3LYP/6-31G(d,p) level of theory.

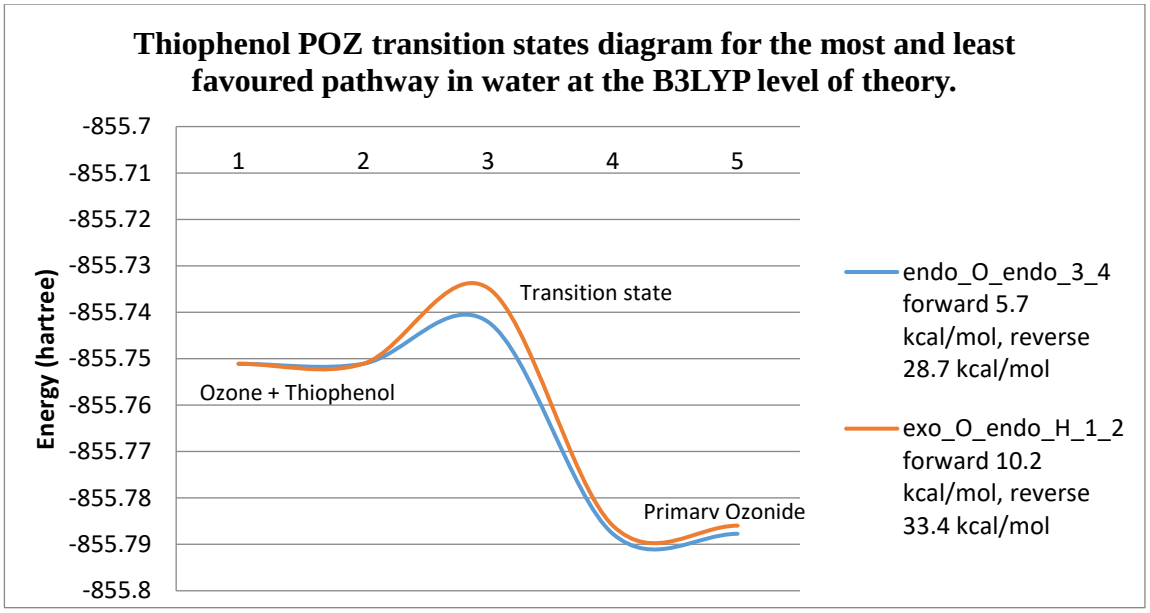


*Figure 15: The potential energy diagram for the most and least favored energy paths for the addition of ozone to thiophenol in water at the B3LYP level.*

The planarity of most thiophenol POZs in water was lost. This was notable for the exo_O POZs. Only mode III retains planarity for the endo_O POZs. Table 14 shows thiophenol POZ, most stable isomer and the structure with the lowest energy barrier for the addition of ozone to thiophenol in water at the B3LYP level.

*Table 14: The most stable isomer and the structure with the lowest energy barrier for the 1,3-cycloaddition of ozone to thiophenol in water at the B3LYP/6-31G(d,p) level.*

| **B3LYP/6-31G(d,p)** | |
|---|---|
| **The most stable isomer** | **The lowest energy transition state structure** |
| endo_O_endo_H_2_3_poz | endo_O_endo_H_3_4_poz |
| 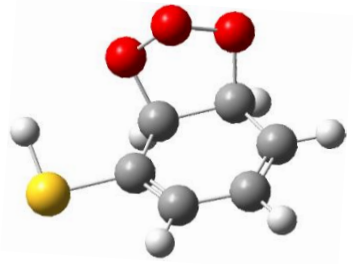 | 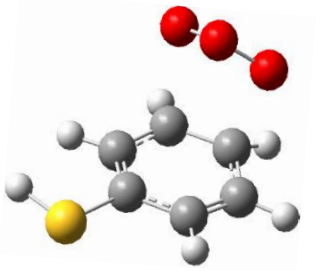 |

The bond length $R_1$ increases from 1.79 Å in the isolated thiophenol molecule in water to ~1.85Å when the POZs are formed through mode I. For modes II and III the bond length $R_1$ decreases by merely 0.01 Å once the POZs are formed. The bond angle θ decreases from 118$^o$ in the isolated ozone molecule in water to 101$^o$ for all POZs formed through modes I, II and III.

### 4.3.4 Thiophenol POZs in gas phase vs Thiophenol POZs in water

The results listed in Table 9 indicate that in the gas phase and in water, all thiophenol POZs were much more stable than the reactants at the B3LYP/6-31G(d,p) and CCSD(T)/6-31G(d,p)//B3LYP/6-31G(d,p) theoretical levels. Based on the B3LYP results in Table 9, the most stable POZ in the gas phase is the exo_O_endo_H 1,2-addition isomer at 24.2 kcal/mol below the reactants. On the other hand, in water, the most stable isomer appeared to be the endo_O_endo_H 2,3-addition lying approximately at 23.4 kcal/mol below the reactants. Furthermore, Table 9 also shows that all the POZ isomers were

slightly more stabilized in water by roughly 0.7 – 2.0 kcal/mol, when compared to the corresponding gas phase products. The energy barriers computed at the B3LYP/6-31G(d,p) level indicated that the pathways for the formation of the POZs were of lower energy in water by 0.40 to 2.30 kcal/mol, compared to corresponding pathways in the gas phase.

The $R_1$ bond length increased in the gas phase and in water from 1.79 Å for the isolated thiophenol to roughly 1.85 Å in the POZs formed through mode I. The bonds $R_2$, $R_3$, $R_4$, and $R_5$ were slightly shorter for POZs formed in the gas phase compared to POZs formed in water for all modes. The bond angle θ for the attached ozone was in the range of 101-102$^o$ for most POZs formed in the gas phase and in water. The planarity of the aryl ring was retained for more POZ structures in water compared to POZ structures in the gas phase.

The Mulliken charge on the terminal oxygen atoms of the ozone molecule in water was more negative with a charge of -0.128 $e^-$ compared to -0.116 $e^-$ in the gas phase at the B3LYP level. The Mulliken charge on the sulphur atom in the thiol group increased from -0.012 $e^-$ in the gas phase to -0.038 $e^-$ in water. A similar observation was made for the carbon atom attached to the thiol group which carried a charge of -0.086 $e^-$ in the gas phase but -0.099 $e^-$ in water.

Figure 16 compares the energy barriers for the most favored pathways in the gas phase and in water, respectively.

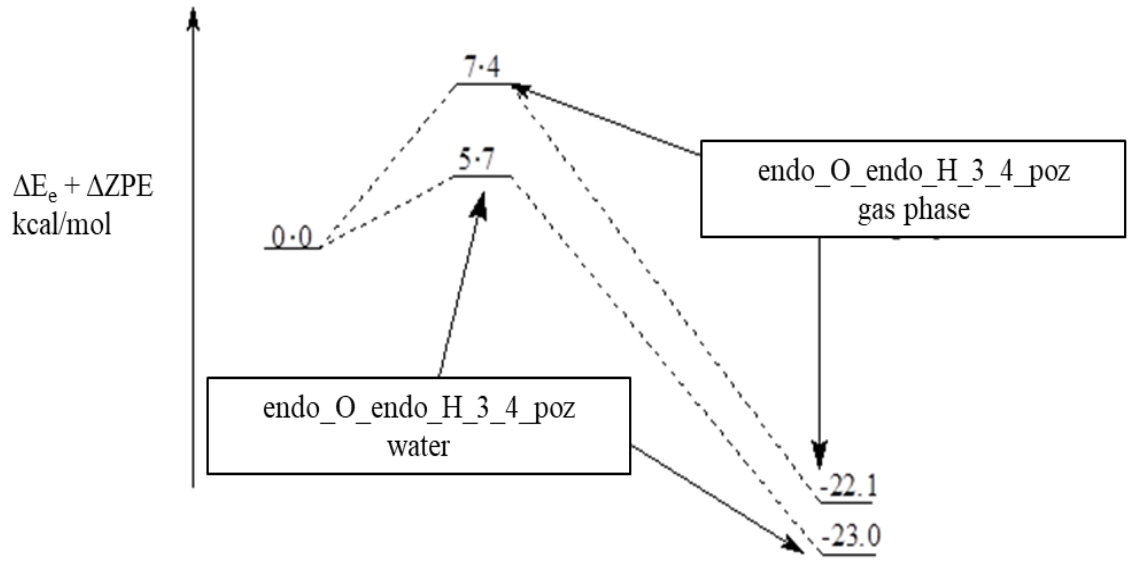


*Figure 16: Comparison of the activation barriers (kcal/mol) for the most favored pathways in the gas phase and in water at the B3LYP/6-31G(d,p) level.*

### 4.4 Naming Catechol and Resorcinol Primary Ozonides

The naming of the two di-hydroxybenzenes POZs were done in the following way:

The carbon atom of the parent phenolic group is labelled $C_1$. The first digit in the names refers to the position of the second phenolic group. The first hydrogen (-H) refers to the hydrogen atom attached to the parent phenolic group. This hydrogen atom can be oriented either towards (endo) or away (exo) from the attached ozone. If the H atom lies nearly or in the same plane as the aromatic ring, then it will be classified as either pointing in a clockwise (c) or anti-clockwise (a) direction. Consequently, in terms of their orientation, the hydrogen of the parent phenolic group can be endo_H, exo_H, c_H or a_H, respectively. The middle oxygen (O) of the attached ozone can be oriented toward (endo-O) or away (exo-O) from the phenyl ring. The hydrogen on the second phenolic group was classified using the same criteria as that used for the parent phenolic hydrogen. The last two numbers before POZ would refer to the carbon atoms to which the terminal

oxygen atoms of ozone are attached. For purposes of simplifying the identification of the compounds, they will be labelled as “structure 1, 2, 3, etc.” according to their ranking on the table of relative energies.

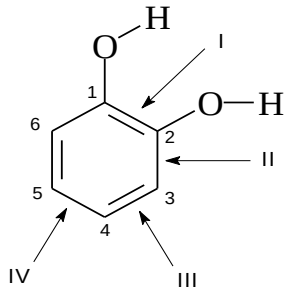


*Figure 17: Schematic representation of the four modes of addition in catechol.*

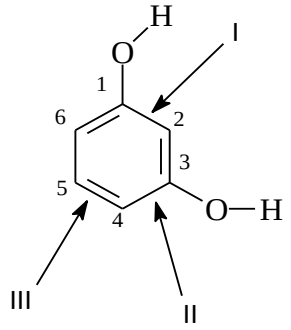


*Figure 18: Schematic representation of the three modes of addition in resorcinol.*

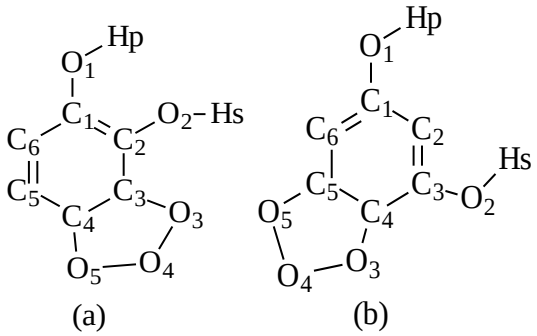


*Figure 19: Illustration of how the atoms are labeled in (a) Catechol and (b) Resorcinol.*

Figures 17 and 18 illustrated the modes of addition of ozone to catechol and resorcinol and Figure 19 shows how the atoms are labeled in the molecules. As depicted in Figure 19, the oxygen atom of the parent phenolic group is labeled $O_1$ and the oxygen atom of the second phenolic group is labelled $O_2$. The oxygen atoms of the ozone molecule are labelled $O_3$, $O_4$ and $O_5$. The hydrogen atom attached to the parent oxygen atom is labelled as $H_p$ and the hydrogen atom of the second phenolic group is labelled as $H_s$. The carbon atoms of the phenyl ring are labelled as $C_1$, $C_2$, $C_3$, $C_4$, $C_5$ and $C_6$ in the direction of counting. The same format will be used for labeling the atoms of the resorcinol and the ozone molecule.

Figure 20 shows the geometric parameters that will be considered when comparing the bonds of POZs formed in the gas phase and in water for both catechol and resorcinol.

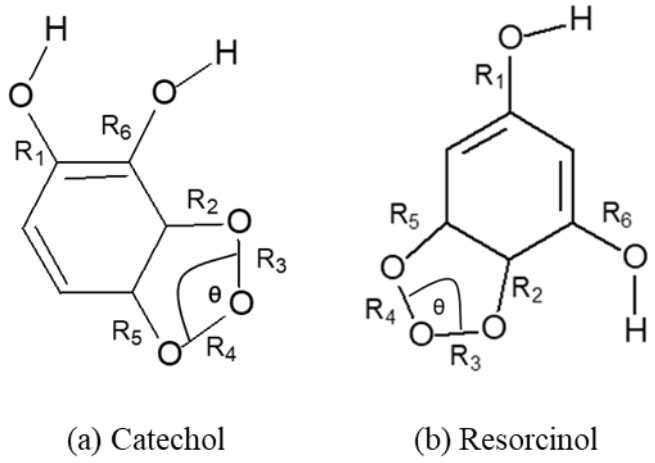


*Figure 20: Geometrical parameters that were considered for (a) catechol and (b) resorcinol POZs*

### 4.4.2 Primary Ozonides (POZ) of catechol in the gas phase and in water

Table 15 lists the relative energies including correction for zero-point vibrational energies ($\Delta E_e+\Delta ZPE$) for catechol POZs in the gas phase (G) and also in water (W).

*Table 15: Relative energies of catechol POZs and the transition state structures leading to the formation of the POZs.*

| | | Primary Ozonide Isomers (kcal/mol) | | | Transition States (kcal/mol) | | |
|---|---|---|---|---|---|---|---|
| | | CCSD(T) (G) $\Delta E_e + \Delta ZPE$ | B3LYP (G) $\Delta E_e + \Delta ZPE$ | B3LYP (W) $\Delta E_e + \Delta ZPE$ | CCSD(T) (G) $\Delta E_e + \Delta ZPE$ | B3LYP (G) $\Delta E_e + \Delta ZPE$ | B3LYP (W) $\Delta E_e + \Delta ZPE$ |
| Structures | Mode I | | | | | | |
| | 1_2_POZs | | | | | | |
| 1 | 2_OH_endo_H_endo_O_a_H_1_2_poz | -31.9 | -26.2 | -25.7 | 7.6 | 3.6 | 3.7 |
| 2 | 2_OH_c_H_endo_O_exo_H_1_2_poz | -29.3 | -24.5 | -25.9 | 7.6 | 3.6 | 3.7 |
| 3 | 2_OH_exo_H_endo_O_exo_H_1_2 | -22.9 | -18.3 | -22.1 | 13.7 | 9.4 | 5.0 |
| 4 | 2_OH_exo_H_exo_O_a_H_1_2_poz | -33.0 | -27.4 | -29.2 | 11.8 | 9.1 | 7.2 |
| 5 | 2_OH_c_H_exo_O_endo_H_1_2_poz | -34.4 | -28.7 | -29.4 | 11.8 | 9.1 | 7.2 |
| 6 | 2_OH_exo_H_exo_O_exo_H_1_2_poz | -28.2 | -22.4 | -25.6 | 16.9 | 13.7 | 9.4 |
| | Mode II | | | | | | |
| | 2_3_POZs | | | | | | |
| 7 | 2_OH_c_H_endo_O_endo_H_2_3_poz | -29.2 | -26.0 | -25.7 | 7.6 | 3.1 | 3.0 |
| 8 | 2_OH_a_H_endo_O_exo_H_2_3_poz | -26.5 | -23.4 | -25.3 | 9.7 | 5.5 | 3.0 |
| 9 | 2_OH_endo_H_endo_O_exo_H_2_3_poz | -26.2 | -22.5 | -22.8 | 9.7 | 5.0 | 3.0 |
| 10 | 2_OH_a_H_endo_O_endo_H_2_3_poz | -25.0 | -21.9 | -23.9 | 12.1 | 7.5 | 4.8 |
| 11 | 2_OH_c_H_exo_O_endo_H_2_3_poz | -30.0 | -26.7 | -26.5 | 10.2 | 6.6 | 5.5 |
| 12 | 2_OH_a_H_exo_O_exo_H_2_3_poz | -29.5 | -25.9 | -27.7 | 11.1 | 7.5 | 4.7 |
| 13 | 2_OH_endo_H_exo_O_exo_H_2_3_poz | -28.7 | -24.9 | -25.2 | 11.1 | 7.5 | 4.7 |
| 14 | 2_OH_a_H_exo_O_endo_H_2_3_poz | -26.8 | -23.5 | -25.8 | 15.0 | 11.1 | 7.3 |
| | Mode III | | | | | | |
| | 3_4_POZs | | | | | | |
| 15 | 2_OH_c_H_endo_O_endo_H_3_4_poz | -23.7 | -22.1 | -22.4 | 9.5 | 5.0 | 4.2 |
| 16 | 2_OH_endo_H_endo_O_a_H_3_4_poz | -20.9 | -19.6 | -21.7 | 13.5 | 8.6 | 5.6 |
| 17 | 2_OH_a_H_endo_O_endo_H_3_4_poz | -17.6 | -16.6 | -19.5 | 15.7 | 10.8 | 7.2 |
| 18 | 2_OH_c_H_exo_O_endo_H_3_4_poz | -22.9 | -21.4 | -21.7 | 12.3 | 7.9 | 6.4 |
| 19 | 2_OH_exo_H_exo_O_a_H_3_4_poz | -21.2 | -19.5 | -21.7 | 15.3 | 10.6 | 7.5 |
| 20 | 2_OH_endo_H_exo_O_a_H_3_4_poz | -20.9 | -19.5 | -21.5 | 15.3 | 10.6 | 7.5 |
| 21 | 2_OH_endo_H_exo_O_endo_H_3_4_poz | -17.4 | -16.2 | -19.0 | 18.3 | 13.4 | 9.2 |
| | Mode IV | | | | | | |
| | 4_5_POZs | | | | | | |
| 22 | 2_OH_exo_H_endo_O_a_H_4_5_poz | -24.1 | -23.5 | -25.8 | 10.6 | 5.1 | 2.7 |
| 23 | 2_OH_exo_H_endo_O_exo_H_4_5_poz | -20.9 | -20.1 | -23.7 | 14.3 | 8.7 | 4.8 |
| 24 | 2_OH_c_H_exo_O_exo_H_4_5_poz | -24.6 | -23.7 | -25.9 | 12.5 | 7.2 | 4.3 |
| 25 | 2_OH_exo_H_exo_O_exo_H_4_5 | -21.2 | -20.3 | -23.8 | 16.1 | 10.6 | 6.3 |

### 4.4.3 Catechol POZs in the gas phase

At the B3LYP/6-31G(d,p) and CCSD(T)/6-31G(d,p)//B3LYP/6-31G(d,p) levels of theory, the results in Table 15 show that the POZ isomers are lower in energy relative to the reactants. The most stable catechol POZ at the B3LYP/6-31G(d,p) level in the gas phase appeared to be structure 5 (2_OH_c_H_exo_O_endo_H_1_2_poz), formed via mode I. The isomer was found at 28.7 kcal/mol below the reactants. The CCSD(T)/6-31G(d,p)//B3LYP/6-31G(d,p) model equally predicted structure 5 as the most stable POZ isomer of catechol at 34.4 kcal/mol below the reactants. The relative energies of catechol POZ isomers produced through modes II, III and IV ranged from 17.4-30.0 kcal/mol at the B3LYP/6-31G(d,p) level and 16.2-26.7 kcal/mol at the CCSD(T)/6-31G(d,p)//B3LYP/6-31G(d,p) level. Figure 21 depicts the computed relative energies of the five most stable POZ isomers of catechol in the gas phase at the B3LYP/6-31G(d,p) and CCSD(T)/6-31G(d,p)//B3LYP/6-31G(d,p) levels.

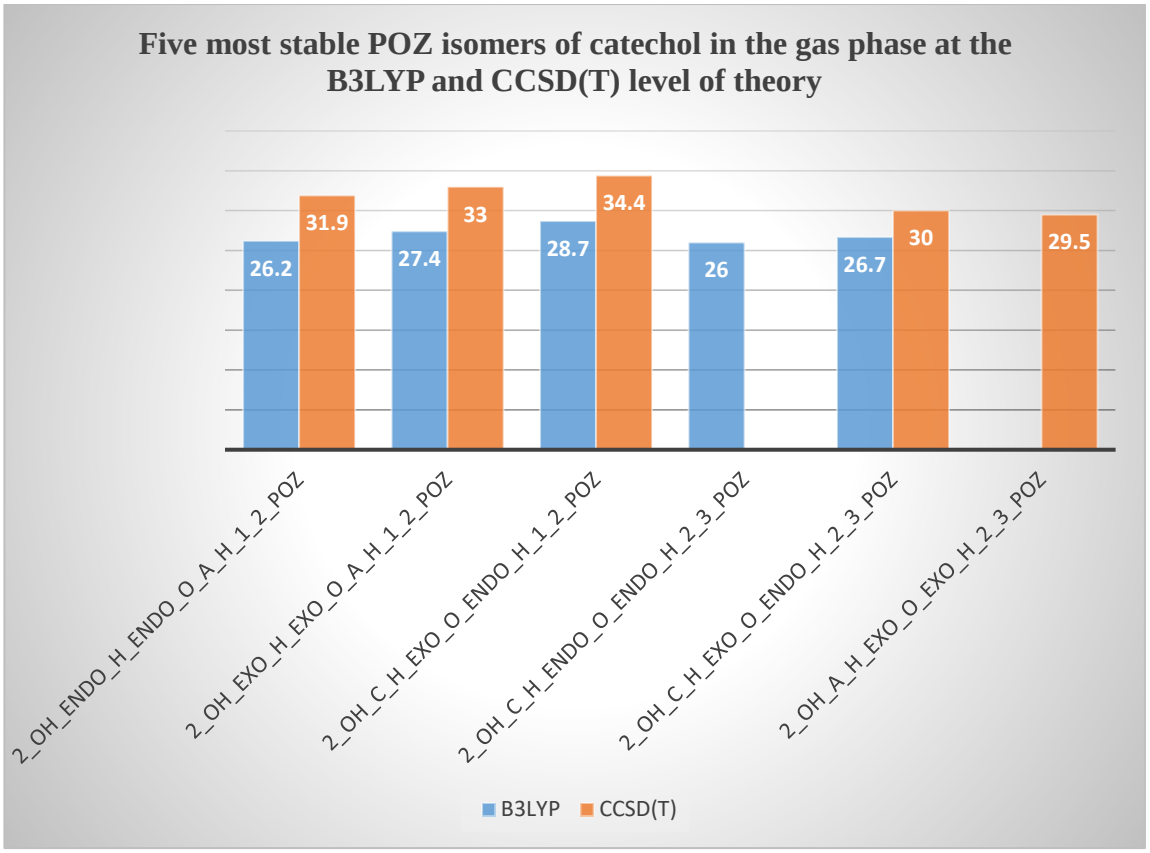


*Figure 21: Relative energies of the five most stable POZ isomers of catechol in the gas phase at the B3LYP/6-31G(d,p) and CCSD(T)/6-31G(d,p)//B3LYP/6-31G(d,p) levels.*

Transition state calculations at the B3LYP/6-31G(d,p) level favored mode II to be energetically the most favorable pathway. The lowest energy barrier of 3.1 kcal/mol was associated with structure 7 (2_OH_c_H_endo_O_endo_H_2_3_poz). The highest energy barrier was 13.7 kcal/mol via structure 6 (2_OH_exo_H_exo_O_exo_H_1_2_poz) of mode I. Figure 22 illustrates the most and the least favored pathways for primary ozonides formed from the addition of ozone to catechol in the gas phase at the B3LYP/6-31G(d,p) level of theory.

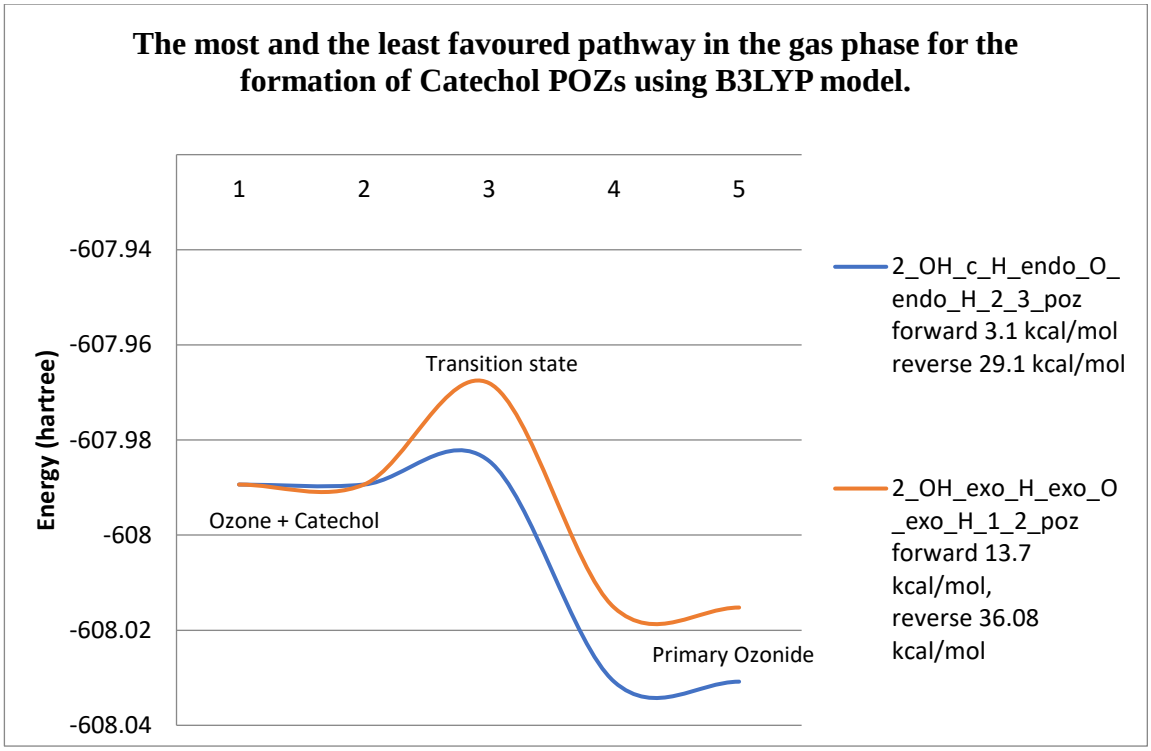


*Figure 22: The reaction profile for the most and least favored pathways for the formation of catechol POZs in the gas phase at the B3LYP/6-31G(d) level.*

The more accurate CCSD(T)//B3LYP energy barriers were higher by roughly 3 kcal/mol when compared to corresponding ones computed at the B3LYP level. The lowest energy barrier computed at the CCSD(T)/6-31G(d,p) level was 7.6 kcal/mol for the path leading to the formation of structures 1, 2 and 7. Kinetically, these structures are more favored to be formed. The highest energy path computed at the CCSD(T)/6-31G(d) level has a barrier of 18.3 kcal/mol associated with the formation of structure 6 (2_OH_exo_H_exo_O_exo_H_1_2_poz) of mode I. Figure 23 illustrates the most and the least favored energy paths for the formation of catechol POZs as computed in the gas phase at the CCSD(T)/6-31G(d,p) level.

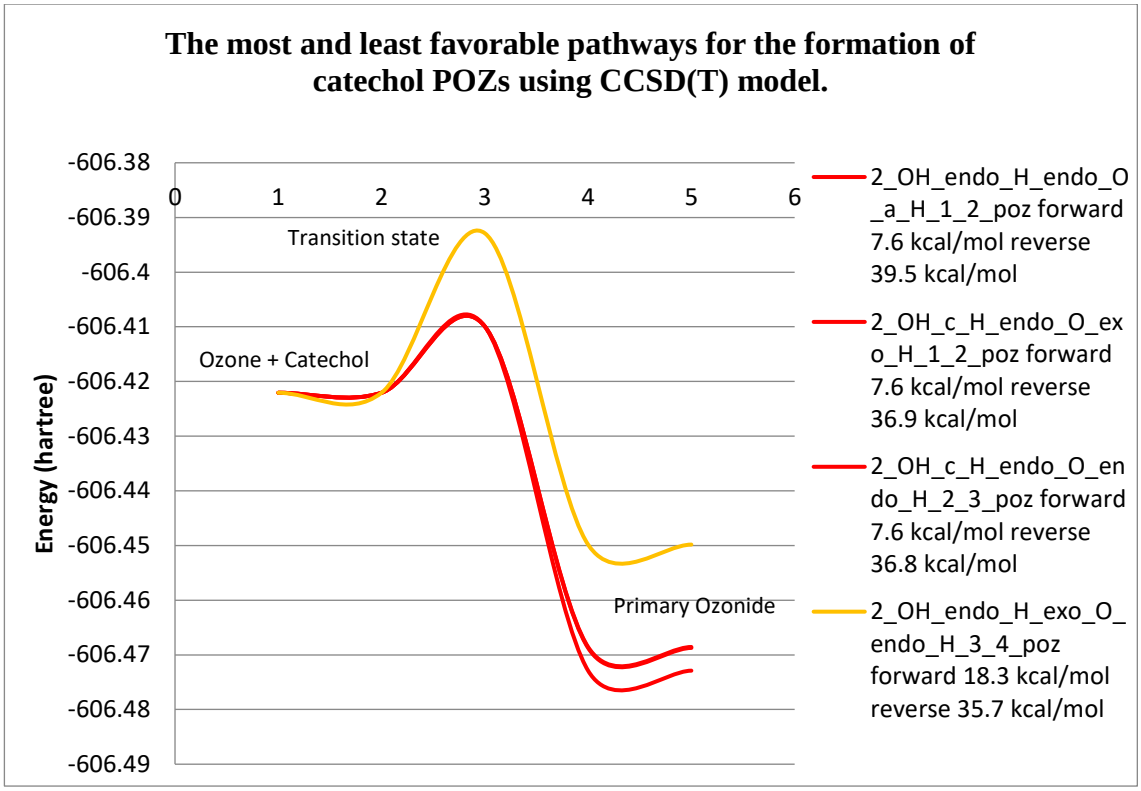


*Figure 23: The reaction profile showing the most and least favored pathways for the formation of catechol POZs in the gas phase at the CCSD(T)/6-31G(d,p) level.*

A relative increase was observed for $R_1$ and $R_6$ for all POZs produced through mode I. The increase ranged from 1.38 and 1.36 Å in isolated catechol to roughly 1.4 and 1.39Å, respectively in the POZs. Mode II showed a decrease from 1.38 Å to approximately 1.36 Å for $R_1$ and an increase in $R_6$ from 1.36 Å to roughly 1.39 Å when going from isolated catechol to the POZs. This elongation reflects the fact that the conjugation effect of the lone pairs on the oxygen atom of the hydroxyl group with the $\pi$ system of the aromatic ring is no longer active in the POZ. Mode III did not show any major change for $R_1$ and $R_6$, with the average bond length maintained at roughly 1.37 Å and 1.36 Å, respectively. However, Mode IV showed a decrease in bond length, with the average bond length at roughly 1.36 Å for both $R_1$ and $R_6$. The average bond length for ozone terminal oxygen

atoms attached to the phenyl ring ranged from 1.44 to 1.45 Å for all modes. The bond angle θ for ozone decreased from 118$^{o}$ in the isolated molecule to between 100$^{o}$-103$^{o}$ in all POZs. Table 16 shows the most stable isomer and the most favored transition state structure in the gas phase at the B3LYP level.

*Table 16: The most stable POZ isomers for catechol and the most favored transition state structures computed at the B3LYP level.*

| **B3LYP/6-31G(d,p)** | |
|---|---|
| **The most stable isomer** | **The lowest energy transition state structure** |
| 2_OH_c_H_exo_O_endo_H_1_2_poz | 2_OH_c_H_endo_O_endo_H_2_3_poz |
| 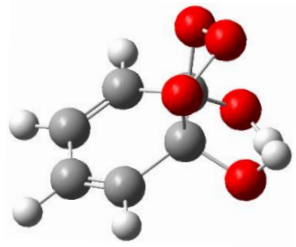 | 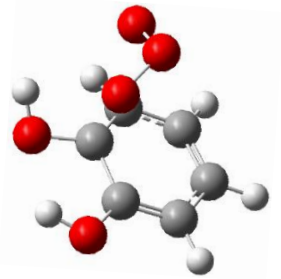 |

### 4.4.4 HOMO-LUMO gap and hydrogen bonding analysis of the most stable Catechol POZs in the gas phase at the B3LYP level

Table 17 includes the HOMO-LUMO gap computed at the B3LYP/6-31G(d,p) level for the catechol POZ isomers. The HOMO-LUMO gap ranges from 0.154 au in structure 21 of mode III to 0.188 au in structures 4 and 6 of mode I. It is worth noting that the HOMO-LUMO gap of thermodynamically most stable catechol POZ (structure 5) is 0.186 au. This suggests that structure 5 is also kinetically stable similar to structures 4 and 6 with the largest HOMO-LUMO gap.

*Table 17: HOMO- LUMO gap, energy barriers and relative energy (including zero-point energy correction) for catechol POZs in the gas phase at the B3LYP/6-31G(d,p) level.*

| | | HOMO-LUMO Gap | Transition state | POZ |
|---|---|---|---|---|
| | | (a.u) | B3LYP (G) $\Delta E_e$ +$\Delta$ZPE (kcal/mol) | B3LYP (G) $\Delta E_e$ +$\Delta$ZPE (kcal/mol) |
| **Structure** | Mode I | | | |
| | 1_2_POZs | | | |
| 1 | 2_OH_endo_H_endo_O_a_H | 0.181 | 7.6 | -26.2 |
| 2 | 2_OH_c_H_endo_O_exo_H_ | 0.182 | 7.6 | -24.5 |
| 3 | 2_OH_exo_H_endo_O_exo_H | 0.183 | 13.7 | -18.3 |
| 4 | 2_OH_exo_H_exo_O_a_H | 0.188 | 11.8 | -27.4 |
| 5 | 2_OH_c_H_exo_O_endo_H | 0.186 | 11.8 | -28.7 |
| 6 | 2_OH_exo_H_exo_O_exo_H | 0.188 | 16.9 | -22.4 |
| | Mode II | | | |
| | 2_3_POZs | | | |
| 7 | 2_OH_c_H_endo_O_endo_H | 0.169 | 7.6 | -26.0 |
| 8 | 2_OH_a_H_endo_O_exo_H | 0.179 | 9.7 | -23.4 |
| 9 | 2_OH_endo_H_endo_O_exo_H | 0.178 | 9.7 | -22.5 |
| 10 | 2_OH_a_H_endo_O_endo_H | 0.175 | 12.1 | -21.9 |
| 11 | 2_OH_c_H_exo_O_endo_H | 0.173 | 10.2 | -26.7 |
| 12 | 2_OH_a_H_exo_O_exo_H | 0.180 | 11.1 | -25.9 |
| 13 | 2_OH_endo_H_exo_O_exo_H | 0.180 | 11.1 | -24.9 |
| 14 | 2_OH_a_H_exo_O_endo_H | 0.178 | 15.0 | -23.5 |
| | Mode III | | | |
| | 3_4_POZs | | | |
| 15 | 2_OH_c_H_endo_O_endo_H | 0.164 | 9.5 | -22.1 |
| 16 | 2_OH_endo_H_endo_O_a_H | 0.163 | 13.5 | -19.6 |
| 17 | 2_OH_a_H_endo_O_endo_H | 0.156 | 15.7 | -16.6 |
| 18 | 2_OH_c_H_exo_O_endo_H | 0.164 | 12.3 | -21.4 |
| 19 | 2_OH_exo_H_exo_O_a_H | 0.163 | 15.3 | -19.5 |

| | | | | |
|---|---|---|---|---|
| 20 | 2_OH_endo_H_exo_O_a_H | 0.165 | 15.3 | -19.5 |
| 21 | 2_OH_endo_H_exo_O_endo_H | 0.154 | 18.3 | -16.2 |
| | Mode IV | | | |
| | 4_5_POZs | | | |
| 22 | 2_OH_exo_H_endo_O_a_H | 0.179 | 10.6 | -23.5 |
| 23 | 2_OH_exo_H_endo_O_exo_H | 0.181 | 14.3 | -20.1 |
| 24 | 2_OH_c_H_exo_O_exo_H_ | 0.181 | 12.5 | -23.7 |
| 25 | 2_OH_exo_H_exo_O_exo_H_4_5 | 0.183 | 16.1 | -20.3 |

Structure 5 of catechol POZs retained its planarity and delocalization of $\pi$ electron system in the ring, thereby contributing to its stability. Additionally, the stability is significantly supported by hydrogen bonding between the parent hydroxyl hydrogen atom and the substituent hydroxyl oxygen atom. This can be observed in Table 18 which indicates that mode I has the shortest hydrogen bond distance of 1.9 Å.

*Table 18: Bond distance between the hydroxyl hydrogens and the surrounding oxygen atoms for the most stable catechol POZs of each mode of addition in the gas phase at the B3LYP level.*

| | Group | Mode | $O_3$ (Å) | $O_4$ (Å) | $O_5$ (Å) | $O_1$(Å) | $O_2$ (Å) |
|---|---|---|---|---|---|---|---|
| The most stable POZ for each mode | $H_p$ | I | 2.86 | 3.12 | 3.33 | | 1.9 |
| | $H_s$ | I | 3.27 | 2.48 | 2.25 | 2.98 | |
| | $H_p$ | II | 2.83 | 4.08 | 4.66 | | 2.14 |
| | $H_s$ | II | 2.42 | 2.46 | 3.144 | 3.52 | |
| | $H_p$ | III | 4.62 | 4.98 | 5.56 | | 2.24 |
| | $H_s$ | III | 2.53 | 3.53 | 4.47 | 3.53 | |
| | $H_p$ | IV | 5.522 | 6.12 | 5.14 | | 2.01 |
| | $H_s$ | IV | 4.65 | 5.83 | 5.51 | 3.56 | |

$O_1$-Oxygen of the parent OH group; $O_2$-Oxygen of the substituent OH group; $H_p$- Hydrogen of the parent group and $H_s$- Hydrogen of the substituent group.

The stability of the isomers generated via mode I is additionally supported by the Mulliken population which clearly showed that the terminal oxygen atoms of the ozone molecule carried a negative charge. The Mulliken population analysis also showed that the carbon atoms to which the parent and the substituent hydroxyl groups of the catechol molecule were attached carried a positive charge, thus making them the most attractive sites for the attachment of the ozone molecule.

Table 19, shows the molecular orbitals for the HOMO and LUMO of the most stable POZs formed via each mode of addition. The HOMO of the POZ generated via mode I was bonding between $C_5$-$C_6$-$C_1$ and $C_3$-$C_4$, and anti-bonding between $C_1$-$C_2$, $C_2$-$C_3$ and $C_4$-$C_5$, respectively. The LUMO, on the other hand was bonding between $C_6$-$C_1$-$C_2$-$C_3$ and $C_4$-$C_5$ but antibonding between $C_3$-$C_4$ and $C_5$-$C_6$.

*Table 19: HOMO- LUMO of the most stable catechol POZs at the B3LYP level for each mode of addition.*

| | HOMO | LUMO |
|---|---|---|
| Mode I | 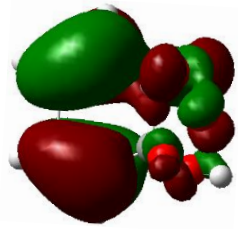 | 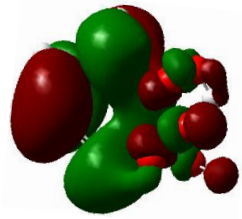 |
| Mode II | 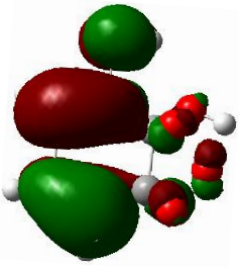 | 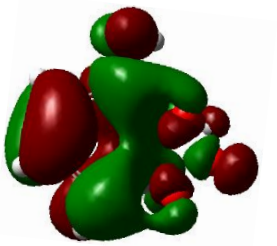 |
| Mode III | 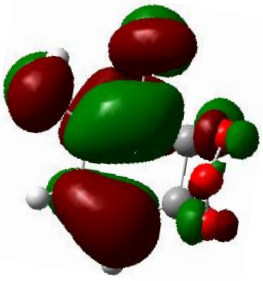 | 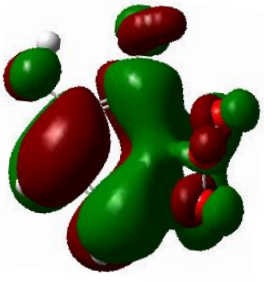 |

| | | |
|---|---|---|
| Mode IV | 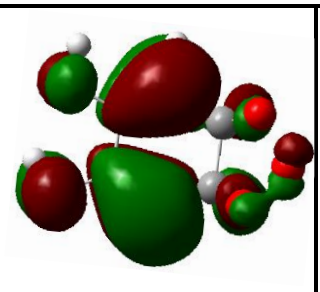 | 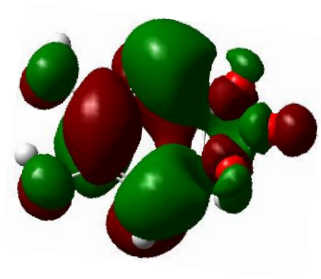 |

The HOMO of POZ generated via mode II was bonding between $C_6$-$C_1$-$C_2$ and $C_3$-$C_4$-$C_5$ but anti-bonding between $C_2$-$C_3$ and $C_5$-$C_6$. The LUMO was bonding between $C_1$-$C_2$-$C_3$-$C_4$ and $C_5$-$C_6$ however anti-bonding between $C_4$-$C_5$ and $C_6$-$C_1$. For POZ generated via mode III, the HOMO was bonding with respect to $C_1$-$C_2$-$C_3$ and $C_5$-$C_6$, but anti-bonding between $C_1$-$C_6$, $C_3$-$C_4$ and $C_4$-$C_5$. The LUMO was bonding in $C_1$-$C_6$ and $C_2$-$C_3$-$C_4$-$C_5$, however anti-bonding between $C_1$-$C_2$ and $C_5$-$C_6$. The HOMO of POZ generated via mode IV was bonding with respect to $C_1$-$C_6$-$C_5$ and $C_2$-$C_3$-$C_4$ , however anti-bonding between $C_1$-$C_2$ and $C_3$-$C_4$. The LUMO showed bonding property between $C_1$-$C_2$ and $C_3$-$C_4$-$C_5$-$C_6$ but anti-bonding between $C_1$-$C_6$ and $C_2$-$C_3$.

### 4.4.5 Catechol POZs in water

The most stable structure of catechol POZ in water at 298.15 K appeared to be mode I structure 5 (2_OH_c_H_exo_O_endo_H_1_2_poz), computed at 29.4 kcal/mol below the reactants using the B3LYP/6-31G(d,p) model. The least stable isomer in water was mode III structure 21 (2_OH_endo_H_exo_O_endo_H_3_4_poz) computationally found at 19.0 kcal/mol below the reactants. Calculations done on the POZ structures obtained via modes II, III and IV provided relative energies which ranged between 19.0-25.9 kcal/mol at the B3LYP/6-31G(d,p) level. Figure 24 shows the calculated relative energies of the five most stable catechol POZs in water computed at the B3LYP/6-31G(d,p) level.

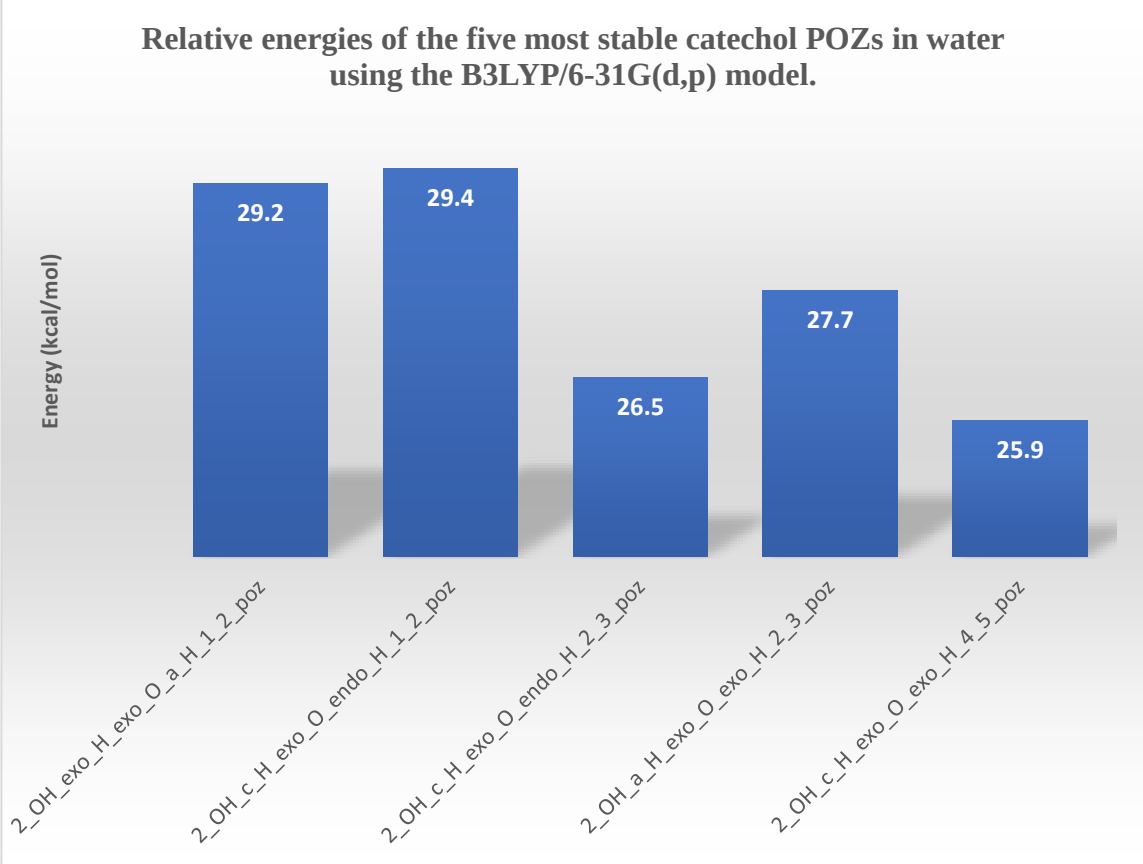


*Figure 24: Relative energies of the five most stable catechol POZ in water at 298.15 K computed at the B3LYP/6-31G(d,p) level.*

At the B3LYP/6-31G(d,p) level, the lowest energy barrier computed in water at 298.15 K was 2.7 kcal/mol. The latter was associated with structure 22 (2_OH_exo_H_endo_O_a_H_4_5_poz). The highest relative energy barrier of 9.4 kcal/mol was linked to mode I structure 6 (2_OH_exo_H_exo_O_exo_H_1_2_poz). Figure 25 illustrates the energy difference between the most and the least favored pathways for the formation of catechol POZs in water as predicted by the B3LYP/6-31G(d,p) model.

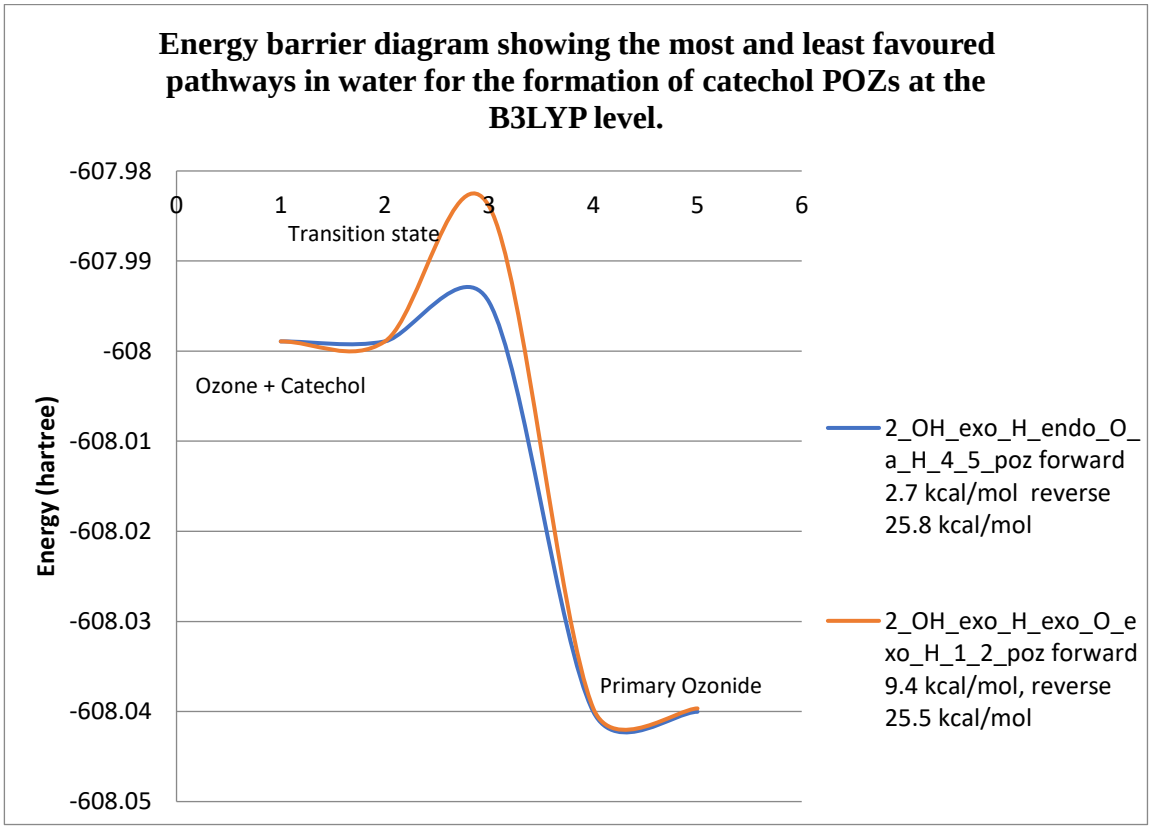


*Figure 25: The Potential energy diagram for the most and least favored energy paths for the addition of ozone to catechol in water at the B3LY/6-31G(d,p) level.*

Not all aryl rings maintained their planarity upon the formation of the catechol POZs. The planarity was retained only for some isomers formed through modes I and III. For mode

IV, all the isomers retained their planarity. On the other hand, none of the POZ isomers generated via mode II retained their planarity. Table 20 shows the most stable isomer and the structure with the lowest energy barrier in water at the B3LYP/6-31G(d,p) level.

*Table 20: The most stable isomer and the structure with the lowest energy barrier for the 1,3-cycloaddition of ozone to catechol in water at the B3LYP/6-31G(d,p) level.*

| **B3LYP/6-31G(d,p)** | |
|---|---|
| **The most stable isomer** | **The lowest energy transition state structure** |
| 2_OH_c_H_exo_O_endo_H_1_2_poz | 2_OH_exo_H_endo_O_a_H_4_5_poz |
| 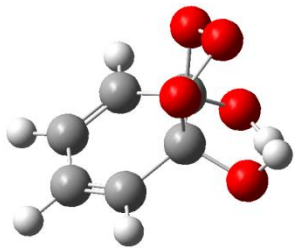 | 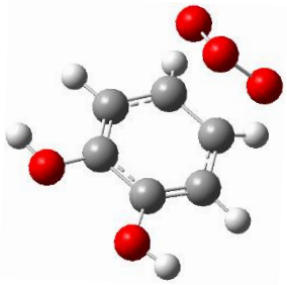 |

In water, the $R_1$ and $R_6$ bond distance never changed by more than 0.02 Å, in going from isolated catechol to the POZs, for all attachment modes. The average bond distance for the attachment of terminal oxygen atoms of ozone to the ring ranged between approximately 1.44 to 1.45 Å for all modes. The bond angle θ of ozone decreased form 118$^o$ in the isolated molecule to between 100-103$^o$ for all POZs.

### 4.4.6 Catechol POZs in the gas phase vs POZs in water

The B3LYP and CCSD(T) calculations in this study predicted that all POZs formed in the gas phase and in water were much more stable than the reactants. The most stable POZ predicted by the B3LYP and CCSD(T) approximations in the gas phase was mode I structure 5 (2_OH_c_H_exo_O_endo_H_1_2_poz). The latter was also predicted to be the most stable POZ isomer in water using the B3LYP method. Structure 5 POZ was about

0.7 kcal/mol more stabilized in water than in the gas phase. The B3LYP/6-31G(d,p) results indicated that the structures corresponding to the lowest energy barrier were different in the gas phase and in water. Figure 26 compares the lowest activation barriers in the gas phase and in water. The lowest energy barrier computed in the gas phase was 3.1 kcal/mol associated with Structure 7 (2_OH_c_H_endo_O_endo_H_2_3_poz) while the lowest barrier in water was 2.7 kcal/mol associated with structure 22 (2_OH_exo_H_endo_O_a_H_4_5_poz). Apart from structures 1 and 2, the energy barriers for the formation of the POZs were consistently lower in water than in the gas phase, suggesting that the POZs would be formed at a faster rate in water.

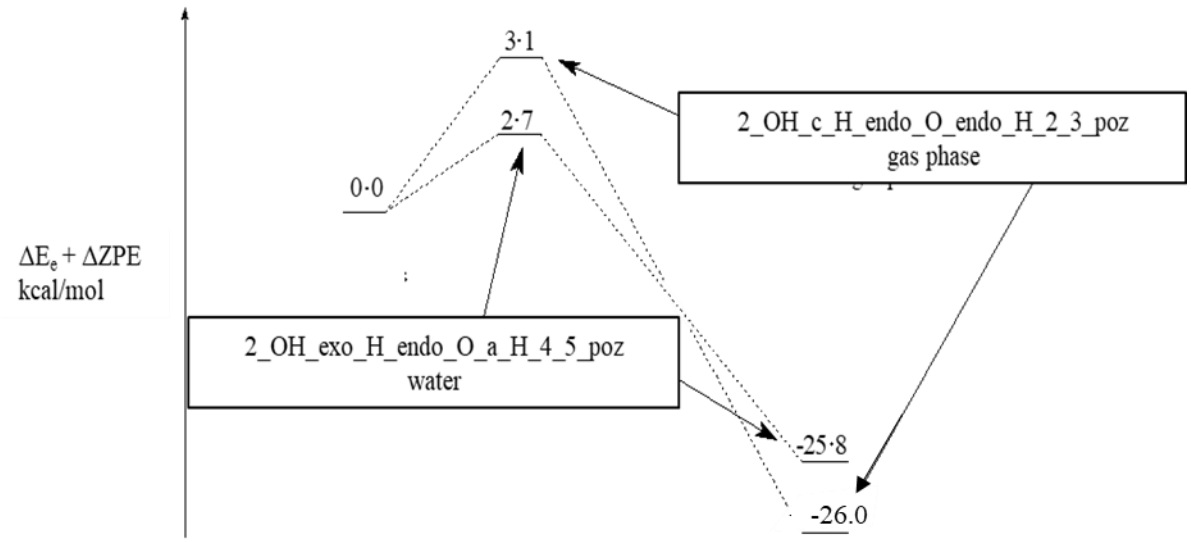


*Figure 26: A comparison of the lowest energy barriers (kcal/mol) computed for catechol transition state structures in the gas phase and in water at the B3LYP/6-31G(d,p) level.*

### 4.5 Primary ozonides (POZ) of resorcinol in the gas phase and in water

Table 21 lists the relative energies including correction for zero-point vibrational energies ($\Delta E_e+\Delta ZPE$) for resorcinol POZs in the gas phase (G) and also in water (W).

*Table 21: Relative energies of resorcinol POZs and the transition state structures leading to the formation of the POZs*

| | | Primary Ozonide (kcal/mol) | | | Transition State (kcal/mol) | | |
|---|---|---|---|---|---|---|---|
| | | CCSD(T) (G) $\Delta E_e + \Delta ZPE$ | B3LYP (G) $\Delta E_e + \Delta ZPE$ | B3LYP (W) $\Delta E_e + \Delta ZPE$ | CCSD(T) (G) $\Delta E_e + \Delta ZPE$ | B3LYP (G) $\Delta E_e + \Delta ZPE$ | B3LYP (W) $\Delta E_e + \Delta ZPE$ |
| | | | | | | | |
| Structure | Mode I | | | | | | |
| | 1_2_POZs | | | | | | |
| 1 | 3_OH_endo_H_endo_O_endo_H_1_2_poz | -26.1 | -25.3 | -24.5 | 8.6 | 3.8 | 4.6 |
| 2 | 3_OH_exo_H_endo_O_c_H_1_2_poz | -25.3 | -22.4 | -24.1 | 11.4 | 6.9 | 4.6 |
| 3 | 3_OH_endo_H_endo_O_c_H_1_2_poz | -27.2 | -24 | -24.6 | 9.7 | 4.9 | 4.5 |
| 4 | 3_OH_exo_H_endo_O_endo_H_1_2_poz | -26.5 | -23.4 | -23.6 | 10.6 | 6 | 4.9 |
| 5 | 3_OH_endo_H_exo_O_endo_H_1_2_poz | -30.2 | -26.3 | -24.9 | 11.5 | 7.1 | 6.5 |
| 6 | 3_OH_exo_H_exo_O_c_H_1_2_poz | -28.9 | -25.4 | -26.9 | 11.9 | 7.8 | 5.3 |
| 7 | 3_OH_endo_H_exo_O_c_H_1_2_poz | -29.3 | -25.6 | -26.3 | 11.9 | 7.7 | 5.9 |
| 8 | 3_OH_exo_H_exo_O_endo_H_1_2_poz | -28.7 | -25.4 | -25.6 | 11.4 | 7.1 | 5.8 |
| | Mode II | | | | | | |
| | 3_4_POZs | | | | | | |
| 9 | 3_OH_c_H_endo_O_endo_H_3_4_poz | -28.7 | -25 | -25.2 | 8 | 2.6 | 2.3 |
| 10 | 3_OH_a_H_endo_O_exo_H_3_4_poz | -24.3 | -21.3 | -23.5 | 10.9 | 5.9 | 2.8 |
| 11 | 3_OH_c_H_endo_O_exo_H_3_4_poz | -26.1 | -22.8 | -24.5 | 10.5 | 5.5 | 2.6 |
| 12 | 3_OH_a_H_endo_O_endo_H_3_4_poz | -26.3 | -22.9 | -24 | 9.0 | 3.7 | 9.5 |
| 13 | 3_OH_c_H_exo_O_endo_H_3_4_poz | -30.7 | -26.5 | -26.9 | 11.4 | 6.7 | 4.8 |
| 14 | 3_OH_a_H_exo_O_exo_H_3_4_poz | -28 | -24.2 | -26 | 12.4 | 7.9 | 4.8 |
| 15 | 3_OH_c_H_exo_O_exo_H_3_4_poz | -28.8 | -25.8 | -27.2 | 11.7 | 7.4 | 4.5 |
| 16 | 3_OH_a_H_exo_O_endo_H_3_4_poz | -28.3 | -24.4 | -25.6 | 12.5 | 7.8 | 5.2 |
| | Mode III | | | | | | |
| | 4_5_POZs | | | | | | |
| 17 | 3_OH_c_H_endo_O_endo_H_4_5_poz | -23.5 | -22.7 | -23.8 | 10.9 | 5.2 | 2.8 |
| 18 | 3_OH_a_H_endo_O_exo_H_4_5_poz | -24.2 | -23.3 | -25.3 | 10.4 | 4.8 | 2.0 |
| 19 | 3_OH_c_H_endo_O_exo_H_4_5_poz | -21.8 | -21.1 | -24.1 | 11.7 | 6.2 | 2.3 |
| 20 | 3_OH_a_H_endo_O_endo_H_4_5_poz | -25.1 | -24.2 | -24.8 | 10.4 | 4.6 | 2.6 |
| 21 | 3_OH_c_H_exo_O_endo_H_4_5_poz | -25.1 | -24.5 | -24.8 | 12.6 | 7.2 | 4.2 |
| 22 | 3_OH_a_H_exo_O_exo_H_4_5_poz | -24.6 | -23.7 | -25.9 | 12.4 | 7 | 3.6 |
| 23 | 3_OH_c_H_exo_O_exo_H_4_5_poz | -22.3 | -21.6 | -24.7 | 13.8 | 8.5 | 3.9 |
| 24 | 3_OH_a_H_exo_O_endo_H_4_5_poz | -26.4 | -25.7 | -25.8 | 12.2 | 6.5 | 4.1 |

### 4.5.1 Resorcinol POZs in the gas phase

The structures of resorcinol POZs were optimized at the B3LYP/6-31G(d,p) level followed by CCSD(T)/6-31G(d,p) single point calculations using the B3LYP optimized structures. The most stable resorcinol POZ in the gas phase was computed to be mode II

structure 13 (3_OH_c_H_exo_O_endo_H_3_4_poz), lying below the reactants at 26.5 kcal/mol [B3LYP] and 30.7 kcal/mol [CCSD(T)], respectively. The POZs computed through modes I and III were located between 21.1-26.3 kcal/mol below the reactants at the B3LYP/6-31G(d,p) level and between 21.8-30.2 kcal/mol at the CCSD(T)/6-31G(d,p) level. Figure 27 shows the calculated relative energies of the five most stable POZs produced from the addition of ozone to resorcinol in the gas phase at the B3LYP/6-31G(d,p) and CCSD(T)/6-31G(d,p) levels.

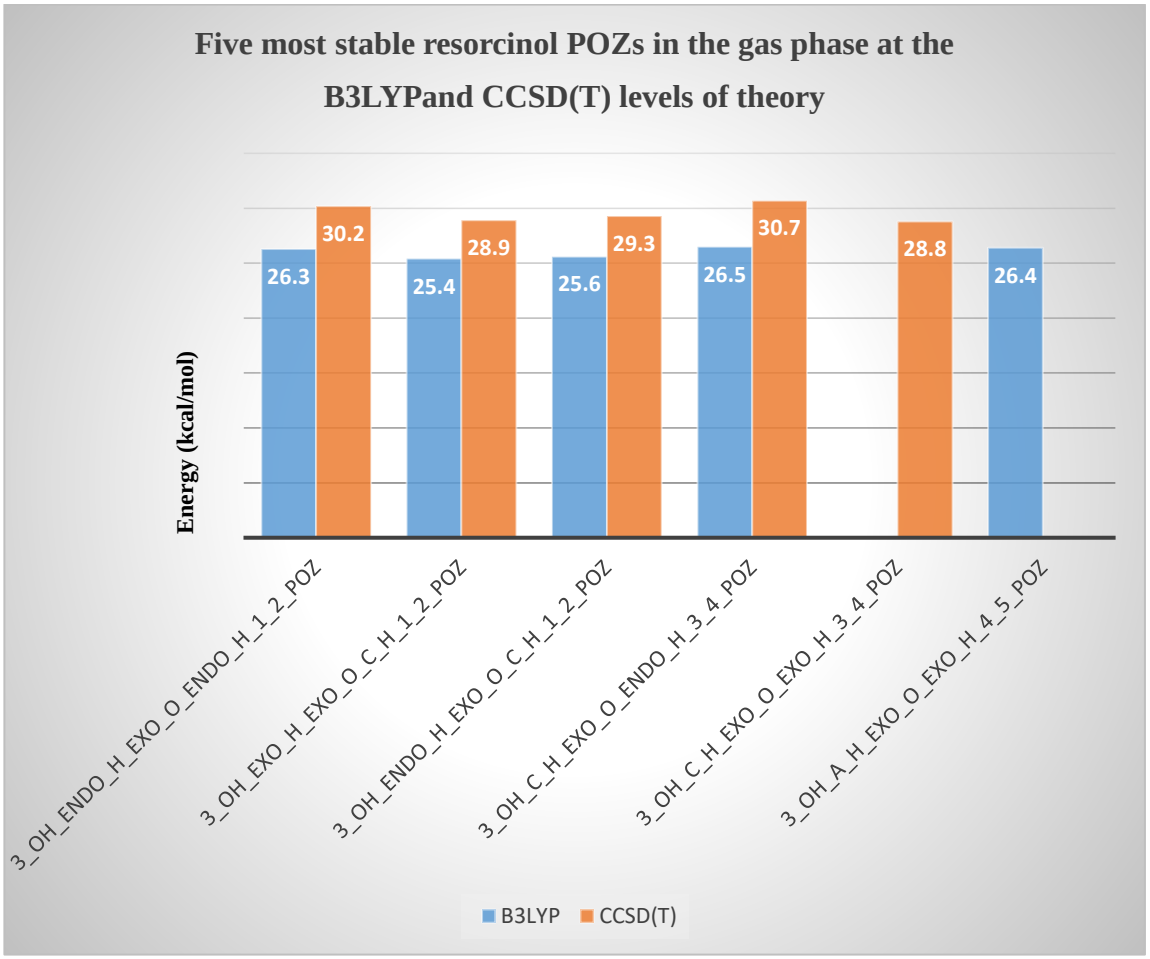


*Figure 27: Relative energies of the five most stable resorcinol POZs in the gas phase at the B3LYP and CCSD(T) levels.*

The results obtained from the calculations done at the B3LYP/6-31G(d,p) level suggested mode II to be energetically the most favorable pathway, with the lowest relative transition state energy barrier of 2.6 kcal/mol associated with structure 9 (3_OH_c_H_endo_O_endo_H_3_4_poz). Kinetically, the POZ formed via this pathway would therefore be the most favored when the reaction takes place in the gas phase at room temperature. The highest energy barrier was 8.5 kcal/mol associated with structure 23 (2_OH_c_H_exo_O_exo_H_4_5_poz) of mode III. Kinetically, this structure would be the least favored because of the high-energy barrier. Figure 28 illustrates the energy difference between the most and the least favored pathways for the formation of resorcinol POZs in the gas phase at the B3LYP/6-31G(d,p) level of theory.

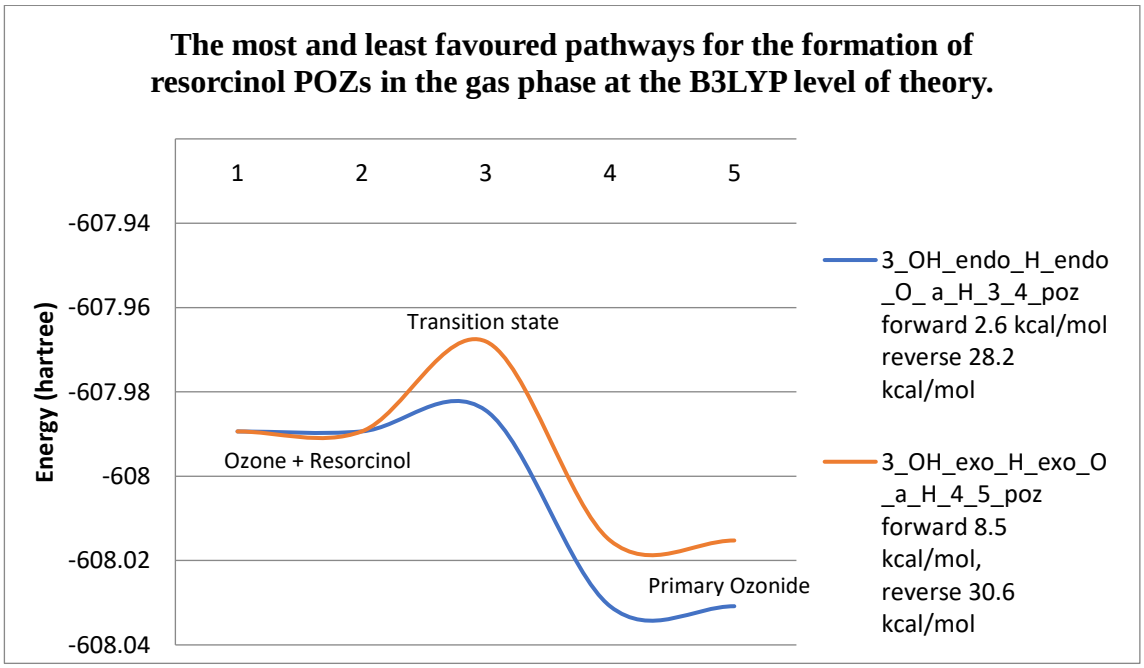


*Figure 28: Reaction profile for the most and least favored pathways for the formation of resorcinol POZs in the gas phase at the B3LYP level.*

Similar to the B3LYP/6-31G(d,p) model, calculations at the CCSD(T)/6-31G(d,p) level predicted structure 9 (3_OH_c_H_endo_O_endo_H_3_4_poz) as having the lowest

energy barrier (8.0 kcal/mol) and structure 23 (3_OH_c_H_exo_O_exo_H_4_5_poz) as having the highest energy barrier (13.8 kcal/mol). Kinetically, the POZ resulting from structure 9 will be the most favored while that resulting from structure 23 will be least favored, in accordance to the results of the highly correlated CCSD(T) method. It is noteworthy that the barriers predicted by the CCSD(T) approximation were consistently higher than corresponding barriers predicted using B3LYP. Figure 29 shows the energy difference between the most and the least favorable pathways for the formation of resorcinol POZs at the CCSD(T)/6-31G(d,p) level of theory.

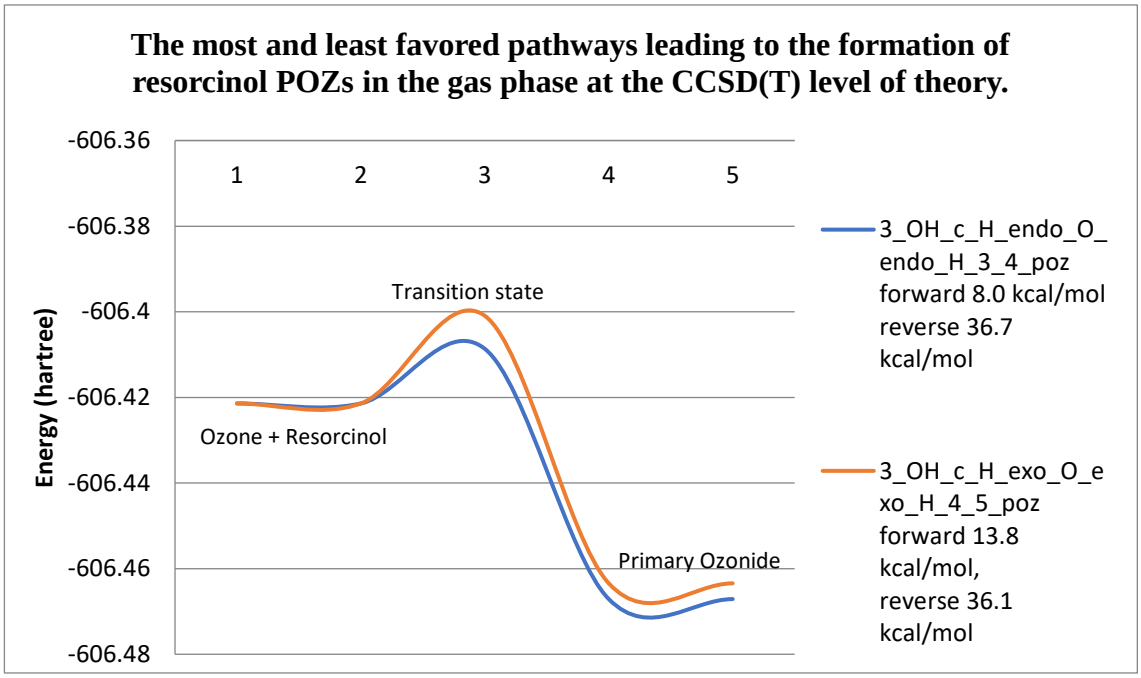


*Figure 29: The reaction profile showing the most and least favored pathways leading to the formation of resorcinol POZs in the gas phase at the CCSD(T) level.*

Table 22 shows the structure of the most stable resorcinol POZ and the structure with the lowest energy barrier. The planarity of the aryl ring in resorcinol was lost upon the formation of the POZs in the gas phase. The $R_1$ and $R_6$ bond distances in the POZs were

within 0.04 Å of the respective ones computed for the isolated molecules and the bond angle θ in the isolated ozone molecule decreased from 118$^{o}$ to roughly 100-102$^{o}$ in the POZs.

*Table 22: The most stable resorcinol POZ and the structure with the lowest energy barrier at the B3LYP level.*

| **B3LYP/6-31G(d,p)** | |
|---|---|
| **The most stable resorcinol POZ** | **Structure with the lowest energy barrier** |
| 13 (3_OH_c_H_exo_O_endo_H_3_4_poz) | 9 (3_OH_c_H_endo_O_endo_H_3_4_poz) |
| 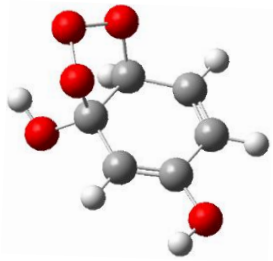 | 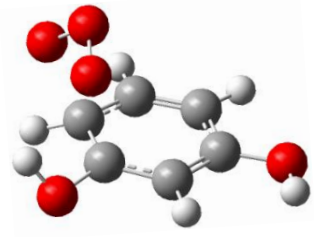 |

### 4.5.2 HOMO-LUMO gap and hydrogen bonding analysis of the most stable Resorcinol POZs in the gas phase at the B3LYP level

*Table 23: HOMO- LUMO gap, energy barriers and relative energy (including zero-point energy correction) for resorcinol POZs in the gas phase at the B3LYP/6-31G(d,p) level.*

| | | HOMO-LUMO Gap | Transition state | POZ |
|---|---|---|---|---|
| | | (a.u) | B3LYP (G) $\Delta E_e$ +ΔZPE (kcal\mol) | B3LYP (G) $\Delta E_e$ +ΔZPE (kcal\mol) |
| Structure | POZ Isomers | | | |
| | Mode I | | | |
| | 1_2_POZs | | | |
| 1 | 3_OH_endo_H_endo_O_endo_H | 0.171 | 8.6 | -25.3 |
| 2 | 3_OH_exo_H_endo_O_c_H | 0.175 | 11.4 | -22.4 |
| 3 | 3_OH_endo_H_endo_O_c_H | 0.174 | 9.7 | -24.0 |
| 4 | 3_OH_exo_H_endo_O_endo_H | 0.173 | 10.6 | -23.4 |
| 5 | 3_OH_endo_H_exo_O_endo_H | 0.172 | 11.5 | -26.3 |
| 6 | 3_OH_exo_H_exo_O_c_H | 0.178 | 11.9 | -25.4 |
| 7 | 3_OH_endo_H_exo_O_c_H | 0.178 | 11.9 | -25.6 |
| 8 | 3_OH_exo_H_exo_O_endo_ | 0.175 | 11.4 | -25.4 |

| | | | | |
|---|---|---|---|---|
| | Mode II | | | |
| | 3_4_POZs | | | |
| 9 | 3_OH_c_H_endo_O_endo_H | 0.177 | 8.0 | -25.0 |
| 10 | 3_OH_a_H_endo_O_exo_H | 0.173 | 10.9 | -21.3 |
| 11 | 3_OH_c_H_endo_O_exo_H | 0.180 | 10.5 | -22.8 |
| 12 | 3_OH_a_H_endo_O_endo_H | 0.170 | 9.0 | -22.9 |
| 13 | 3_OH_c_H_exo_O_endo_H | 0.183 | 11.4 | -26.5 |
| 14 | 3_OH_a_H_exo_O_exo_H | 0.175 | 12.4 | -24.2 |
| 15 | 3_OH_c_H_exo_O_exo_H | 0.182 | 11.7 | -25.8 |
| 16 | 3_OH_a_H_exo_O_endo_H | 0.179 | 12.5 | -24.4 |
| | Mode III | | | |
| | 4_5_POZs | | | |
| 17 | 3_OH_c_H_endo_O_endo_H | 0.170 | 10.9 | -22.7 |
| 18 | 3_OH_a_H_endo_O_exo_H | 0.177 | 10.4 | -23.3 |
| 19 | 3_OH_c_H_endo_O_exo_H | 0.172 | 11.7 | -21.1 |
| 20 | 3_OH_a_H_endo_O_endo_H | 0.175 | 10.4 | -24.2 |
| 21 | 3_OH_c_H_exo_O_endo_H | 0.174 | 12.6 | -24.5 |
| 22 | 3_OH_a_H_exo_O_exo_H | 0.181 | 12.4 | -23.7 |
| 23 | 3_OH_c_H_exo_O_exo_H | 0.176 | 13.8 | -21.6 |
| 24 | 3_OH_a_H_exo_O_endo_H | 0.177 | 12.2 | -25.7 |

At the B3LYP/6-31G(d,p) level of theory in the gas phase, HOMO-LUMO gap for the most stable POZ (structure 13) is 0.183 a.u. The latter is the largest HOMO-LUMO gap when compared to all other resorcinol POZs, thereby supporting the kinetic stability of this isomer in addition to being thermodynamically the most stable. Interestingly, when compared to the isolated resorcinol molecule, planarity of the aryl ring was lost in structure 13 and the delocalization of the $\pi$ electron system disrupted. Consequently, the stability of structure 13 might be due to a different factor such as hydrogen bonding. Table 24 lists the hydrogen bond distance computed for the most stable POZ of each mode. It could be speculated that the kinetic and thermodynamic stability of structure 13 resulted from hydrogen bonding between the hydrogen of the OH group in position 3 ($H_s$), and the terminal ($O_3$) and central ($O_4$) oxygen atoms of the ozone moiety in the POZ. While short hydrogen bond distances were also computed for most stable POZs of modes I and III, their lower stability might be due to steric-hindrance.

*Table 24: Bond distance between the hydroxyl hydrogens and the surrounding oxygen atoms for the most stable resorcinol POZs at each mode of addition in the gas phase at the B3LYP level.*

| | Group | Mode | $O_3$ (Å) | $O_4$ (Å) | $O_5$ (Å) | $O_1$ (Å) | $O_2$ (Å) |
|---|---|---|---|---|---|---|---|
| The most stable POZ for each mode | $H_p$ | I | 2.43 | 2.28 | 2.64 | | 4.97 |
| | $H_s$ | I | 3.81 | 3.42 | 2.19 | 4.77 | |
| | $H_p$ | II | 4.59 | 5.86 | 5.71 | | 4.67 |
| | $H_s$ | II | 2.42 | 2.44 | 3.09 | 5.51 | |
| | $H_p$ | III | 5.9 | 5.88 | 4.59 | | 5.52 |
| | $H_s$ | III | 2.15 | 3.39 | 3.78 | 5.43 | |

Where:$O_1$-Oxygen of the parent OH group; $O_2$-Oxygen of the substituent OH group; $H_p$- Hydrogen of the parent group and $H_s$- Hydrogen of the substituent group.

The HOMO and LUMO of the most stable POZs formed via each mode of addition are shown in Table 25. For mode I, the HOMO was bonding between $C_5$-$C_6$-$C_1$-$O_2$ and $C_3$-$C_4$, respectively, but anti-bonding between $C_2$-$C_3$ and $C_4$-$C_5$, respectively. The LUMO was bonding between $C_6$-$C_1$-$C_2$-$C_3$ and $C_4$-$C_5$, respectively, however anti-bonding between $C_3$-$C_4$ and $C_5$-$C_6$, respectively. The HOMO for primary ozonide generated via mode II was bonding between $C_6$-$C_1$ and $C_4$-$C_5$, respectively but anti-bonding between $C_1$-$C_2$, $C_3$-$C_4$ and $C_5$-$C_6$, respectively. The LUMO was bonding between $C_1$-$C_2$-$C_3$-$C_4$ and $C_5$-$C_6$, respectively, however anti-bonding between $C_4$-$C_5$ and $C_6$-$C_1$, respectively. In case of mode III, the HOMO was bonding between $C_1$-$C_2$ and $C_5$-$C_6$, respectively but anti-bonding between (Sulphur) S-$C_1$, $C_2$-$C_3$, $C_4$-$C_5$ and $C_6$-$C_1$. The LUMO was π bonding between $C_1$-$C_6$ and $C_2$-$C_3$-$C_4$-$C_5$, respectively, however anti-bonding between S-$C_1$, $C_1$-$C_2$ and $C_5$-$C_6$, respectively.

*Table 25: HOMO-LUMO of the most stable resorcinol POZs in gas phase at the B3LYP level for each mode.*

| | HOMO | LUMO |
|---|---|---|
| Mode I | 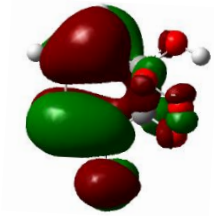 | 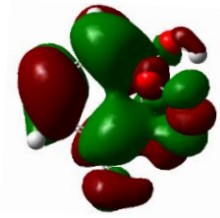 |
| Mode II | 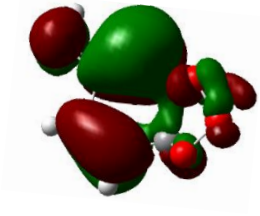 | 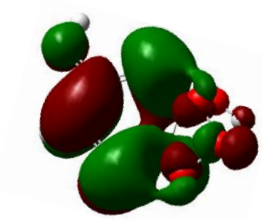 |
| Mode III | 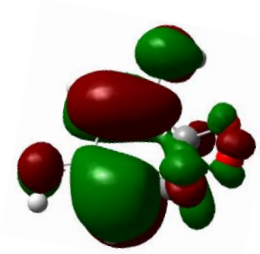 |  |

### 4.5.3 Resorcinol POZs in water

The most stable resorcinol POZ formed in water at 298.15 K appeared to be structure 15 (3_OH_c_H_exo_O_exo_H_3_4_poz) of mode II. B3LYP/6-31G(d,p) calculations found the latter at 27.2 kcal/mol below the reactants. At the same level of theory, the least stable isomer was also generated via mode II and was found to be structure 10 (3_OH_a_H_endo_O_exo_H_3_4_poz) at 23.5 kcal/mol below the reactants. The POZ

structures computed via modes I and III were found at 23.6-25.7 kcal/mol below the reactants. Figure 30 shows the calculated relative energies of the five most stable isomers of resorcinol POZs computed in water.

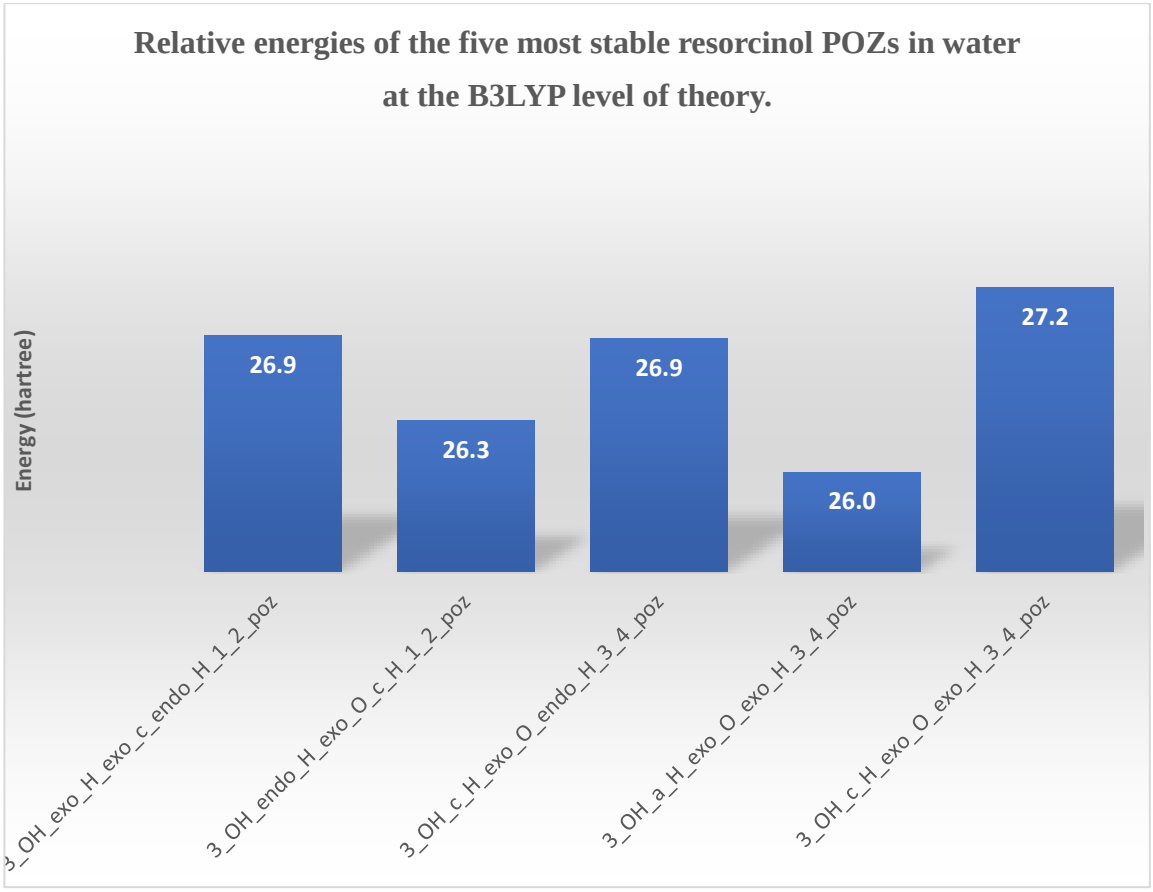


*Figure 30: Relative energies of the five most stable resorcinol POZs computed in water at 298.15 K using the B3LYP/6-31G(d,p) model.*

The transition state calculations done at the B3LYP/6-31G(d,p) level suggested mode III to be energetically the most favored pathway for POZs formation in water. Structure 18 (3_OH_a_H_endo_O_exo_H_4_5_poz) of mode III was associated with the lowest relative transition state energy barrier of 2.0 kcal/mol. In water, this structure would therefore lead to kinetically most favored POZ. The transition state structure leading to structure 13 (3_OH_c_H_exo_O_endo_H_3_4_poz) had the highest energy barrier of 9.5

kcal/mol. Consequently, the formation of structure 13 might be the least favored in water. Figure 31 shows the lowest and highest energy barriers in water at the B3LYP/6-31G(d,p) level of theory.

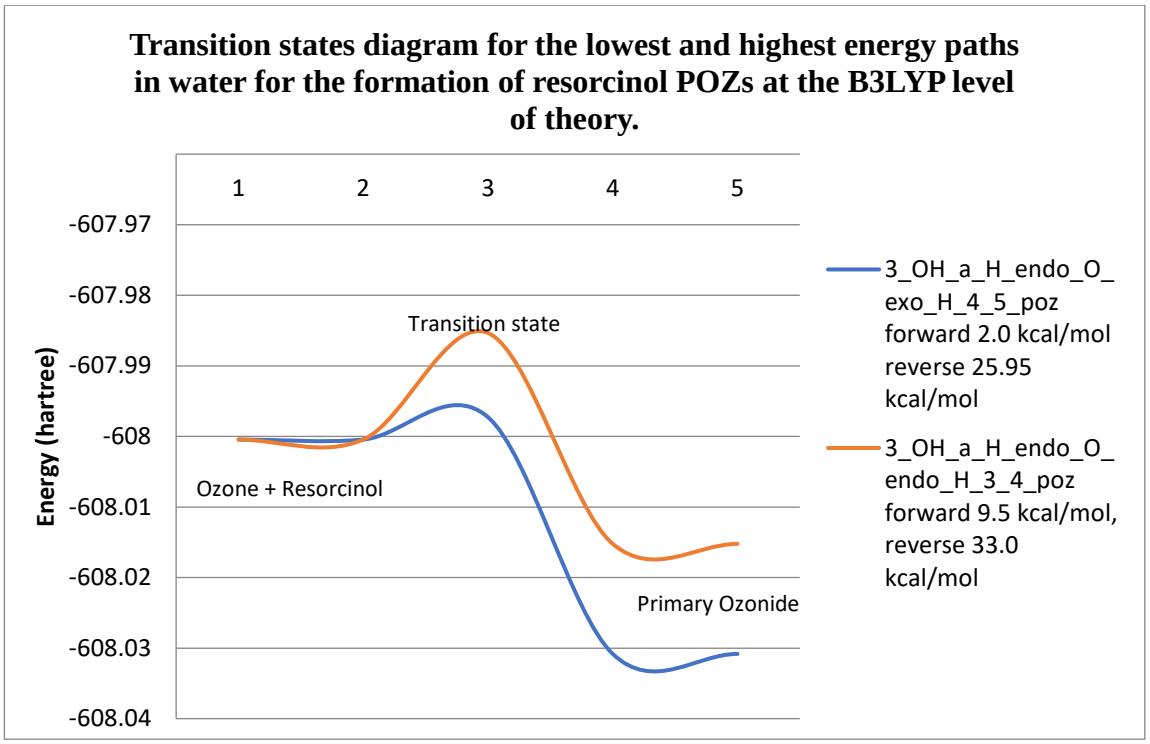


*Figure 31: Reaction profile for the most and least favored pathways for the formation of resorcinol POZs in water at the B3LYP/6-31G(d,p) level.*

Not all aryl rings maintained their planarity once the POZs were formed from the addition of ozone to resorcinol in water. Modes I and II isomers with the exo-O geometry were more likely to retain planarity of the ring structure. This was not observed for mode III isomers which only retained planarity for the endo-O geometry. Table 26 shows the most stable resorcinol POZ and the structure with the lowest energy barrier in water at the B3LYP level.

*Table 26: The most stable resorcinol isomer and the structure with the lowest energy barrier for the 1,3-cycloaddition of ozone to resorcinol in water at the B3LYP/6-31G(d,p) level.*

| **B3LYP/6-31G(d,p)** | |
|---|---|
| **The most stable resorcinol isomer in water** | **The lowest energy transition state structure in water** |
| 3_OH_c_H_exo_O_exo_H_3_4_poz | 3_OH_a_H_endo_O_exo_H_4_5_poz |
| 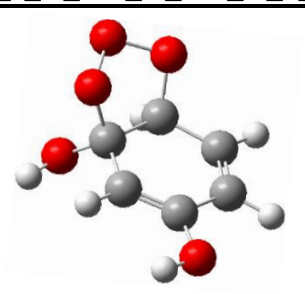 | 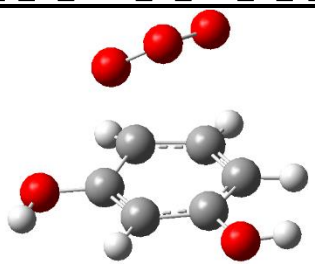 |

The change in the $R_1$ and $R_6$ bond distances were within 0.04 Å when these parameters were compared in the isolated resorcinol molecule and in the POZs computed in water. The $R_2$, $R_3$, $R_4$ and $R_5$ bond distances were roughly 1.48 Å, 1.43 Å, 1.45 Å and 1.44 Å, respectively for all the POZs formed in water. The bond angle θ for ozone decreased from 118$^o$ in the isolated molecule to between 100-103$^o$ in most POZs formed in water. For some modes I and III isomers possessing the exo-O geometry, the bond angle θ decreased to 105$^o$.

### 4.5.4 Resorcinol POZs in gas phase vs Resorcinol POZs in water.

Using the B3LYP method, all POZs computed in the gas phase and in water were much more stable than the reactants. The most stable resorcinol POZ in the gas phase was mode II structure 13 (3_OH_c_H_exo_O_endo_H_3_4_poz). On the other hand, mode II

structure 15 (3_OH_c_H_exo_O_exo_H_3_4_poz) appeared to be the most stable POZ formed in water. The B3LYP results suggested that the energy difference between the most stable and the least stable POZ in the gas phase was 5.4 kcal/mol and the corresponding value in water was 3.7 kcal/mol. With the exception of structures 1 and 5 of mode I, the POZs were more stabilized in water than in the gas phase. With regards to the energy barriers for the formation of the POZs, the B3LYP transition state calculations suggested that the pathway leading to the formation of structure 9 (3_OH_c_H_endo_O_endo_H_3_4_poz) had the lowest energy barrier in the gas phase and in water. However, in water, the B3LYP calculations indicated that structure 19 of mode III was also associated with the lowest energy barrier of 2.0 kcal/mol. Kinetically, the formation of structure 9 was favored both in the gas phase and in water and additionally, structure 19 was also favored in water. Figure 32 compares the lowest activation barriers in the gas phase and in water

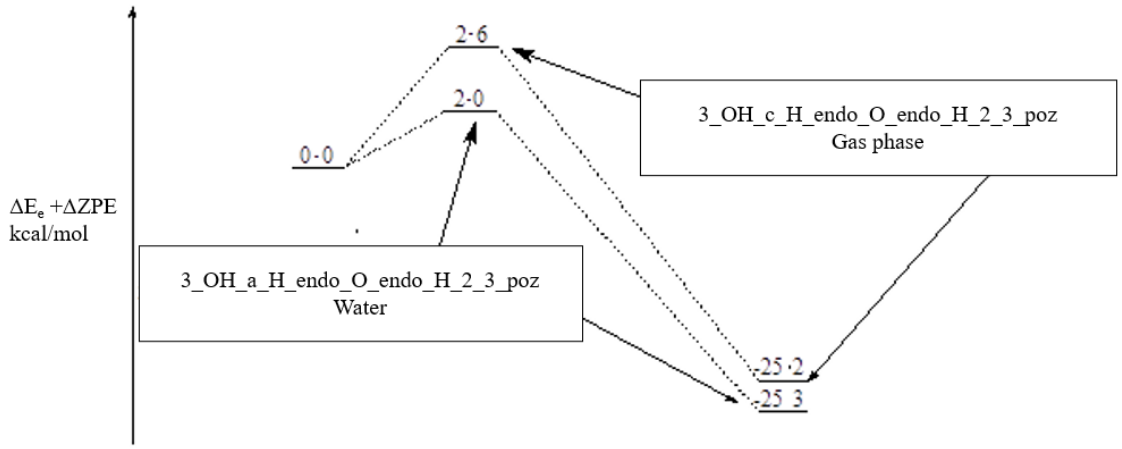


*Figure 32 A comparison of the lowest energy barriers (kcal/mol) computed for resorcinol transition state structures in the gas phase and in water at the B3LYP/6-31G(d,p) level.*

# Chapter 5

## Conclusions

In this work, the geometric structure, kinetic and thermodynamic properties have been investigated for the 1,3-Cycloaddition of ozone on phenol, thiophenol, catechol and resorcinol, in the gas phase and in water. All structures were optimized at the B3LYP/6-31G(d,p) level, and in order to improve the energetics, single point calculations were done at the CCSD(T)/6-31G(d,p) level using the B3LYP/6-31G(d,p) geometries. The calculation done in water were only completed at the B3LYP/6-31G(d,p) level of theory. All the POZ isomers studied were computationally found to be much more stable than the reactants in the gas phase and in water at all levels of theory.

From the relative energies, most of the phenol, thiophenol, catechol and resorcinol POZs were found to be nearly isoenergetic in the gas phase and in water. Consequently, at the level of theory used in this work, definitive determination of the most stable isomers is not possible. For each group of POZs, the computed relative energies of the isomers were within the margin of errors (5 kcal/mol).

Most transition state reaction barriers were more favorable in water at the B3LYP/6-31G(d,p) level of theory, in comparison to the gas phase. At the CCSD(T)/6-31G(d,p) level of theory, the transition state relative reaction barrier were higher than the reaction barriers computed at the B3LYP/6-31G(d,p) level, for all structures.

## Recommendations

Based on the results of this work, specifically the observation that the energies of various isomers in each POZ group were very close to each other, a higher level of theory is recommended for the investigation of the reaction of ozone with these phenolic compounds in the gas phase and in water. The noticeable difference between the B3LYP and the CCSD(T) results in the gas phase, strongly suggest the use of highly correlated theoretical methods in conjunction with large basis sets.

# Chapter 6

## References


Central pollution control board. (2016). *Phenols and Phenolic compounds.* PariveshBhawan: cpcb.

*Electronic Structure calculations in Gaussian.* (2017, October 4). Retrieved October 04, 2017, from http://cpb-us-e1.wpmucdn.com/blogs.cornell.edu/dist/1/3053files/2019/10/Gaussian_optimization.pdf

Embula, W., Archibong, E. F., Gariseb, N., Hishimone, P., & Ramasami, P. (2013). *A Computational Study of the 1,3-Cycloaddition of Ozone to Thiophenol: The Structure and Stability of the Primary Ozonides (POZ).* Retrieved from A Computational Study of the 1,3-Cycloaddition of Ozone to Thiophenol: The Structure and Stability of the Primary Ozonides (POZ): http://sites.uom.ac.mu/vccc/images/stories/A-Archibong.pdf

Eriksson, M. (2005). Ozone chemistry in aqueous solution-Ozone decomposition and stabilisation. Stockholm, Stock: KTH.

Gariseb, N. S. (2013). *A COMPUTATIONAL STUDY OF THE STRUCTURE, BONDING, AND THERMOCHEMICAL PROPERTIES OF PRIMARY OZONIDES DERIVED FORM SUBSTITUTED PHENOL AND THIOPHENOL (Unpublished master's thesis).* Windhoek: University of Namibia.

Hendrickx, M. F., & Vinckier, C. (2003). 1,3-Cycloaddition of OZone to Ethylene, Benzene, and Phenol: A Comparitive ab Initio Study. *Journal pf Physical Chemistry*, 7574-7580.

Ludwig-Maximilians-University Munich. (2020, 01 24). *Faculty for Chemistry and Pharmacy-Group of Prof. Zipse*. Retrieved from Faculty for Chemistry and Pharmacy-Group of Prof. Zipse: https://www.cup.uni-muenchen.de/oc/zipse/teaching/computational-chemistry-2/topics/the-polarizable-continuum-model-pcm/

Ortenberg, F. (2002). *Ozone: Space Vision (Space monitoring of Earth Atmospheric Ozone).* Israel: Design by Graphic Touch, Ltd (Haifa).

Osborn, D. L., & Taatjes, C. A. (2015). *The physical chemistry of Criegee intermediates in the gas phase.* Livemore: Combustion Research Facility.

Quan, C., Stamm, B., & Maday, Y. (2017). *Polarized Continium Modelbased on the Solvent Excluded Surface.* Retrieved 10 11, 2019, from https://hal.archives-ouvertes.fr/hal-01489262

Schwartz, C. (2010). Development of the In Situ Reductive Ozonolysis of alkenes with Tertiary Amine N-oxides. Progress toward the Assymetric Synthesis of Peroxyplakaric Acid A3 . *Student Research Projects, Dissertation and Thesis Chemistry department* , 7.

Shakhashiri, Z. (2017, 07 15). *Learn About ozone*. Retrieved from Science is fun: http://www.scifun.org

von Gunten, U. (2009). Ozonation of drinking water: Part 1. Oxidation kinetics and product formation. *A Journal of the Interntional Water Association*, 1443-1467.

Youmin, S., Xiaohua, R., & Zhaojie, C. (2012). The degradation mechanism of phenol induces by ozone in wastes systems. *Journal of Molecular Modelling*, 3821-3830.

## Appendices

**APPENDIX A** Structures of POZs.

### Minimum

**Phenol POZs**

| Gas Phase | Water |
|---|---|
| **B3LYP** | **B3LYP** |
| **1_2_POZ** | |
| 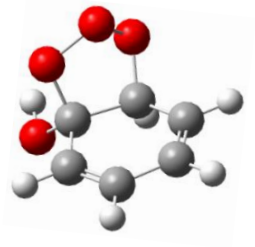 | 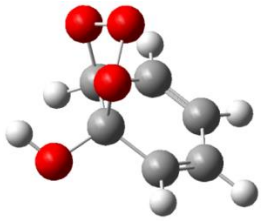 |
| Endo_O_endo_H | |
| 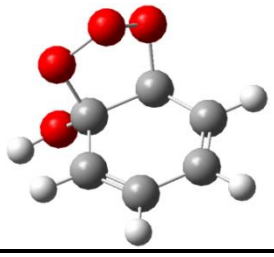 | 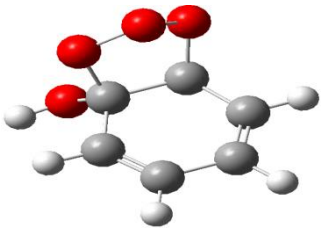 |
| Endo_O_exo_H | |
| 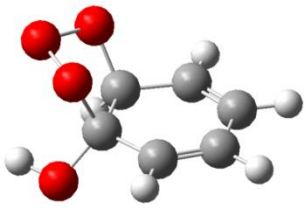 | 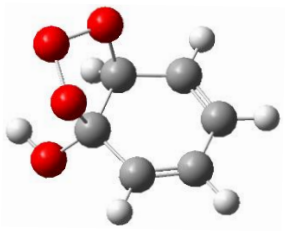 |
| Exo_O_endo_H | |
| 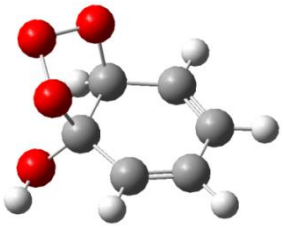 | 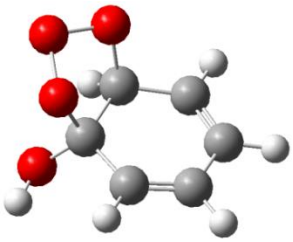 |
| Exo_O_exo_H | |

| **2_3_POZs** | |
|---|---|
| 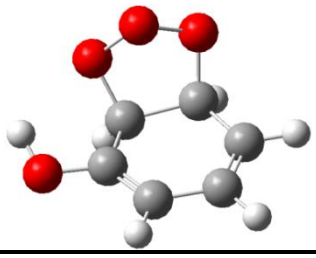 | 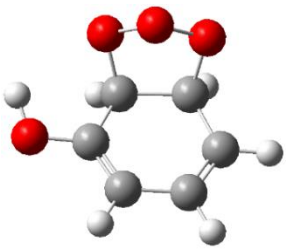 |
| Endo_O_endo_H | |
| 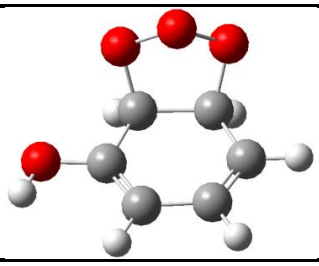 | 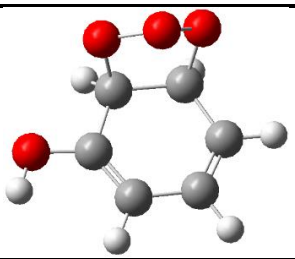 |
| Endo_O_exo_H | |
| 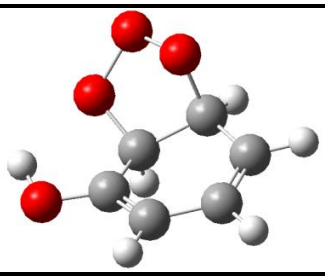 | 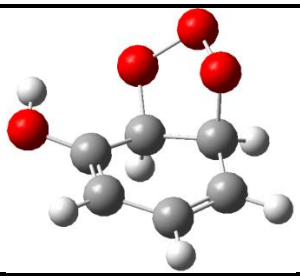 |
| Exo_O_endo_H | |
| 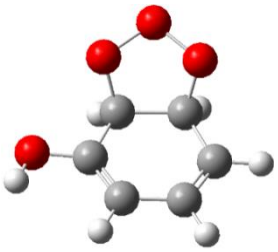 | 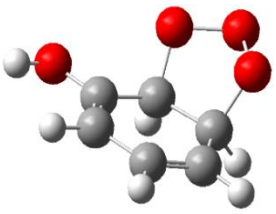 |
| Exo_O_exo_H | |
| **3_4_POZ** | |
| 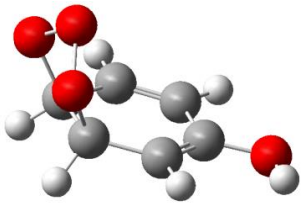 | 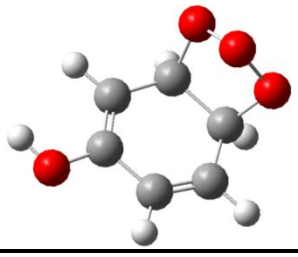 |
| Endo_O_endo_H | |

| | |
|---|---|
| 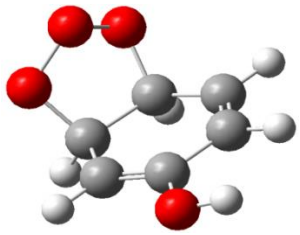 | 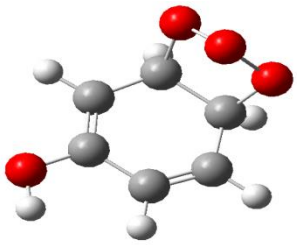 |
| Endo_O_exo_H | |
| 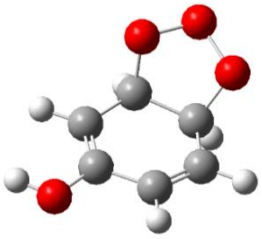 | 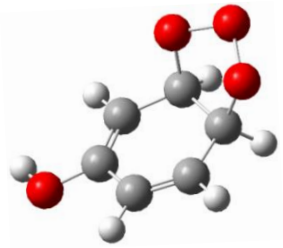 |
| Exo_O_endo_H | |
| 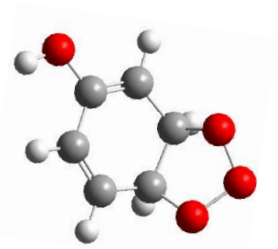 | 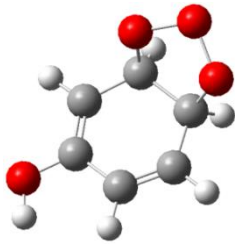 |
| Exo_O_exo_H | |

**Thiophenol POZs**

| Gas Phase | Water |
|---|---|
| **B3LYP** | **B3LYP** |
| **1_2_POZ** | |
| 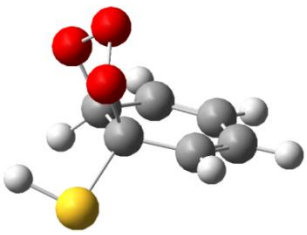 | 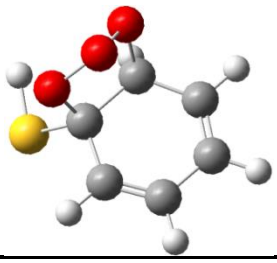 |
| Endo_O_endo_H | |
| | |

| | |
|---|---|
| 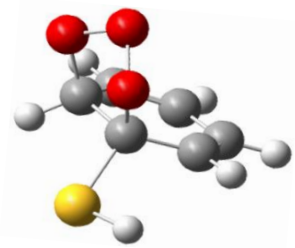 | 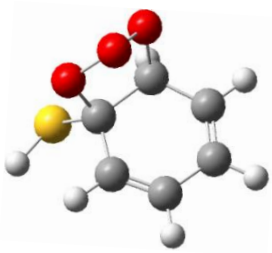 |
| Endo_O_exo_H | |
| 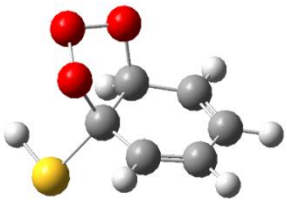 | 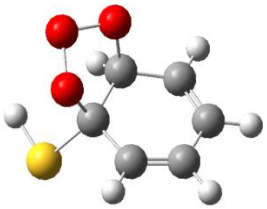 |
| Exo_O_endo_H | |
| 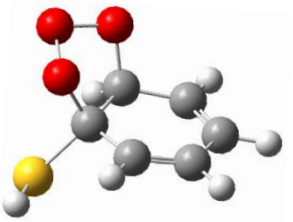 | 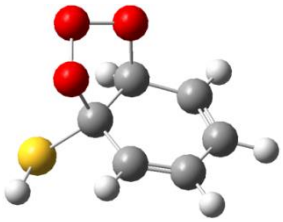 |
| Exo_O_exo_H | |
| **2_3_POZs** | |
| 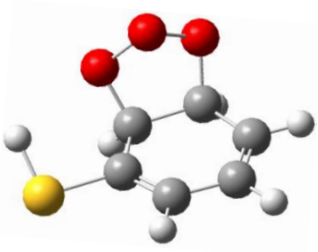 | 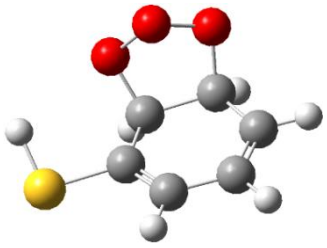 |
| Endo_O_endo_H | |
| 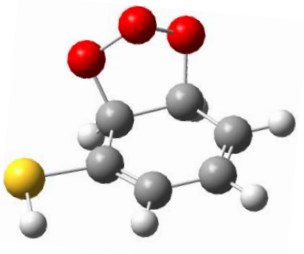 | 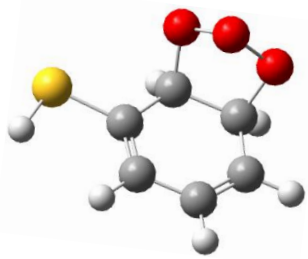 |
| Endo_O_exo_H | |

| | |
|---|---|
| 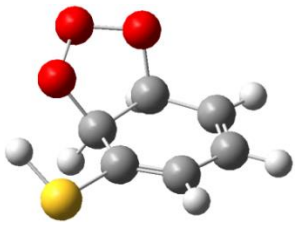 | 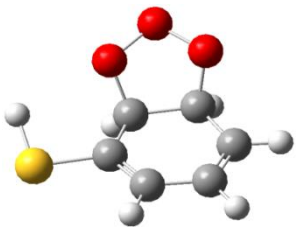 |
| Exo_O_endo_H | |
| 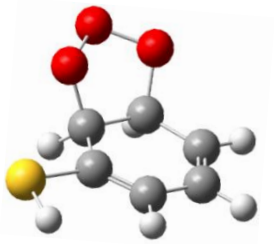 | 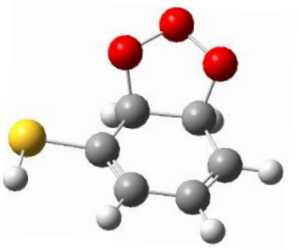 |
| Exo_O_exo_H | |
| **3_4_POZ** | |
| 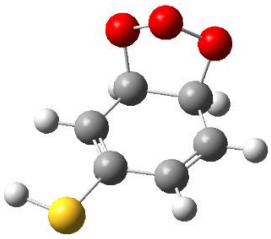 | 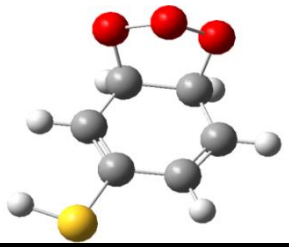 |
| Endo_O_endo_H | |
| 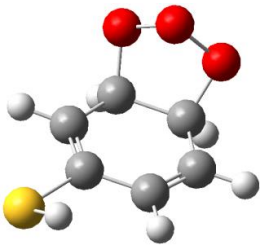 | 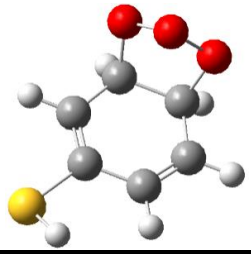 |
| Endo_O_exo_H | |
| 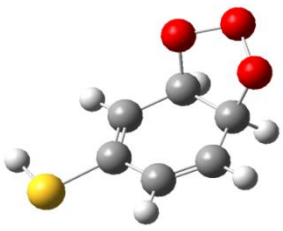 | 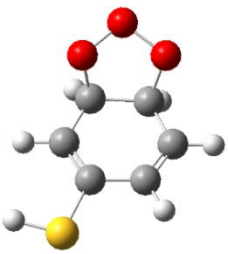 |
| Exo_O_endo_H | |

| | |
|---|---|
| 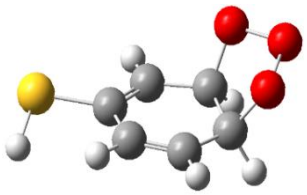 | 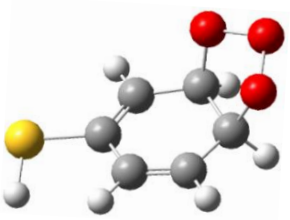 |
| Exo_O_exo_H | |

**Catechol POZs**

| Gas Phase | Water |
|---|---|
| **B3LYP** | **B3LYP** |
| **1_2_POZ** | |
| 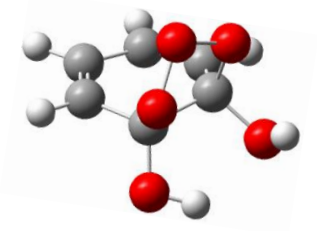 | 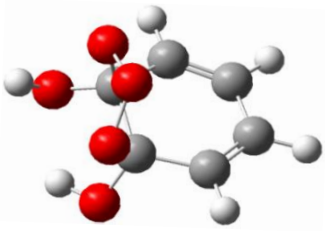 |
| Structure 1 | |
| 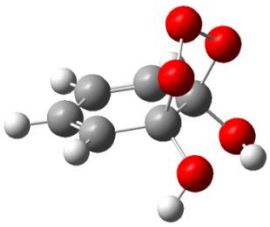 | 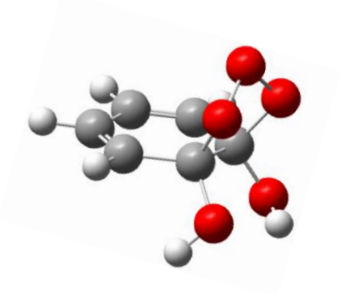 |
| Structure 2 | |
| 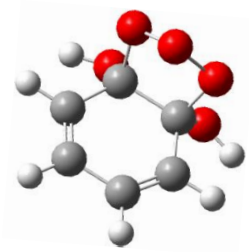 | 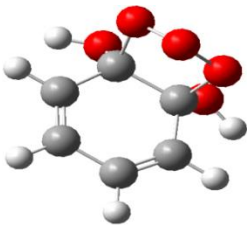 |
| structure 3 | |
| | |

| | |
|---|---|
| 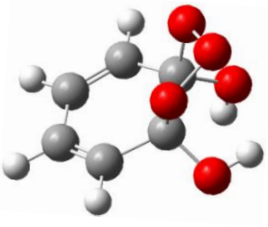 | 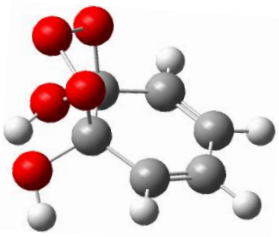 |
| Structure 4 | |
| 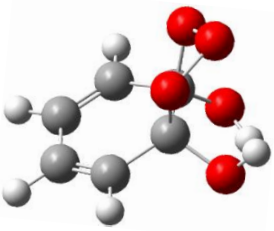 | 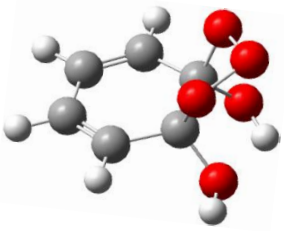 |
| Structure 5 | |
| 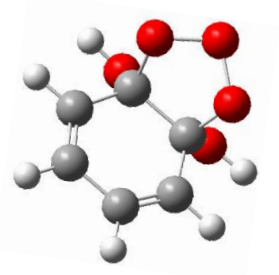 | 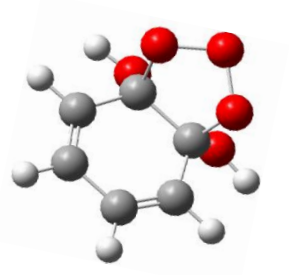 |
| Structure 6 | |
| **2_3_POZs** | |
| 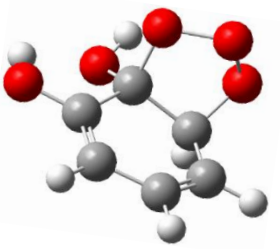 | 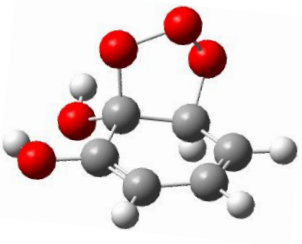 |
| Structure 7 | |
| 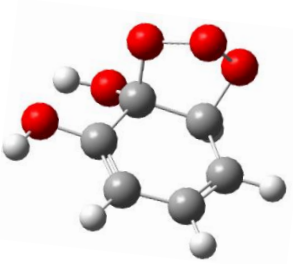 | 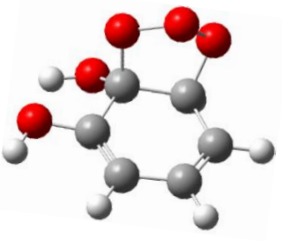 |
| Structure 8 | |

| | |
|---|---|
| 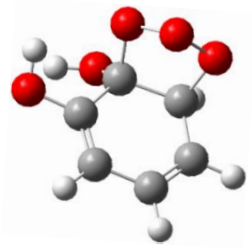 | 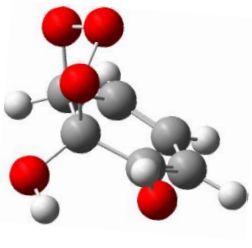 |
| Structure 9 | |
| 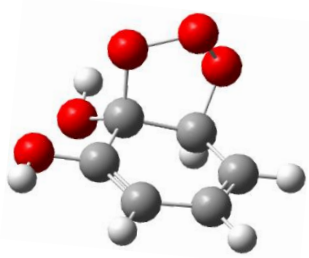 | 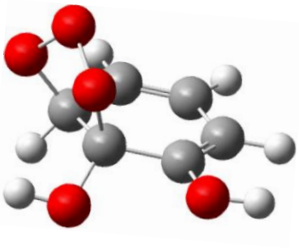 |
| Structure 10 | |
| 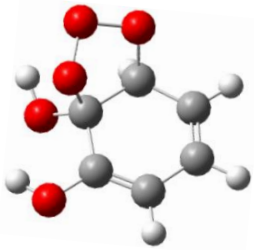 | 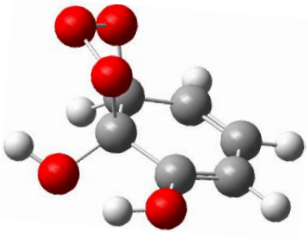 |
| Structure 11 | |
| 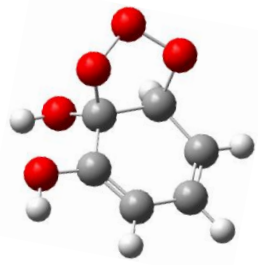 | 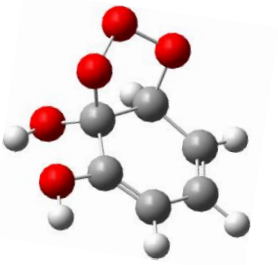 |
| Structure12 | |
| 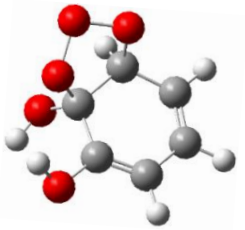 | 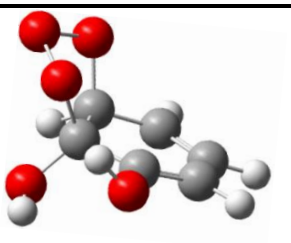 |
| Structure 13 | |

| | |
|---|---|
| 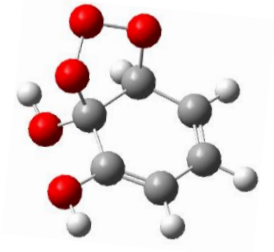 | 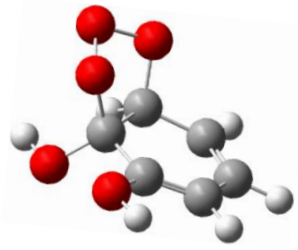 |
| Structure 14 | |
| Exo_O_exo_H | |
| **3_4_POZ** | |
| 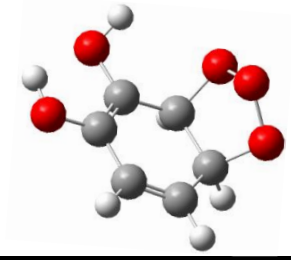 | 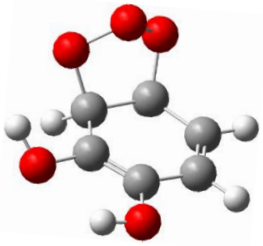 |
| Structure 15 | |
| 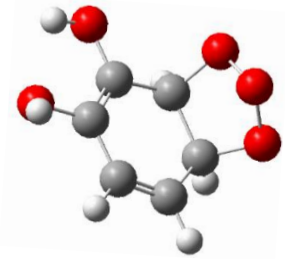 | 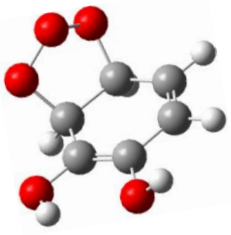 |
| Structure 16 | |
| 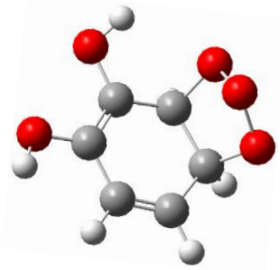 | 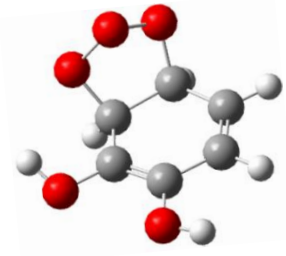 |
| Structure 17 | |
| 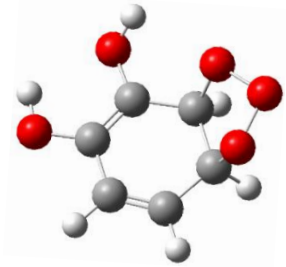 | 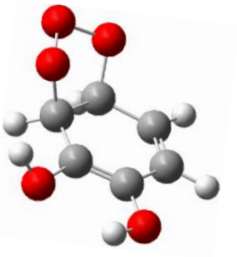 |
| Structure 18 | |

| | |
|---|---|
| 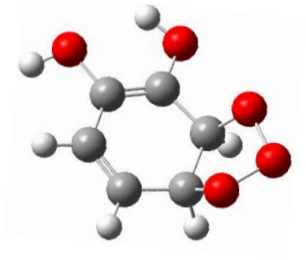 | 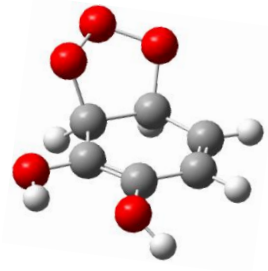 |
| Structure 19 | |
| 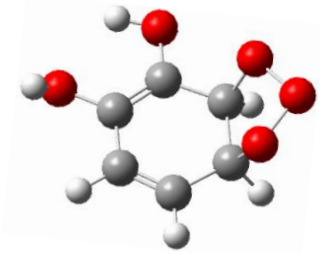 | 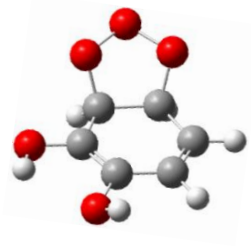 |
| Structure 20 | |
| 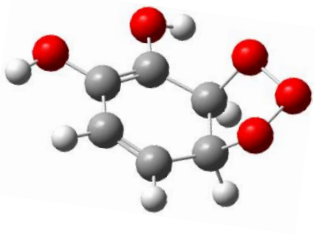 | 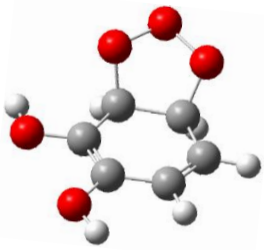 |
| Structure 21 | |
| **4_5_POZ** | |
| 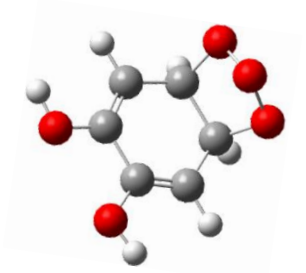 | 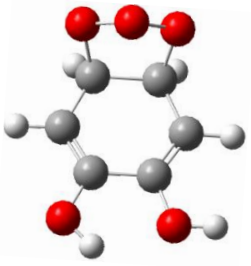 |
| Structure 22 | |
| 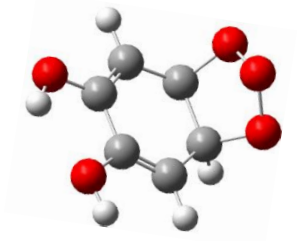 | 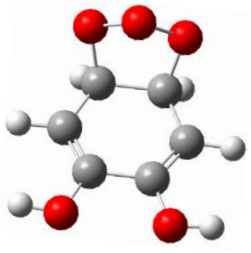 |
| Structure 23 | |

| | |
|---|---|
| 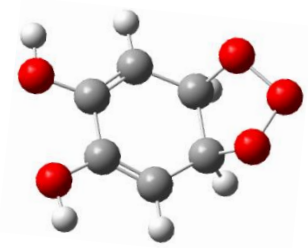 | 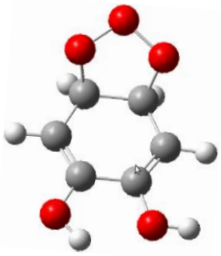 |
| Structure 24 | |
| 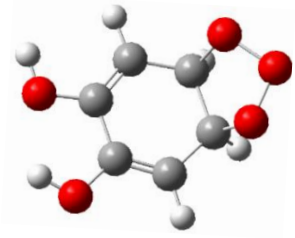 | 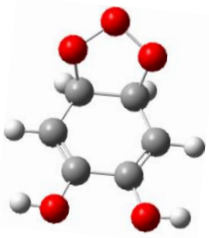 |
| Structure 25 | |

**Resorcinol POZs**

| Gas Phase | Water |
|---|---|
| **B3LYP** | **B3LYP** |
| **1_2_POZ** | |
| 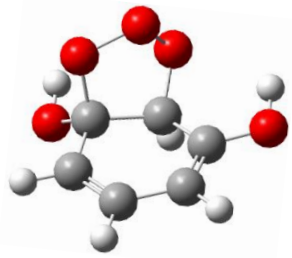 | 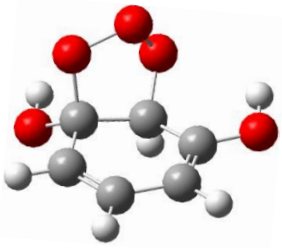 |
| Structure 1 | |
| 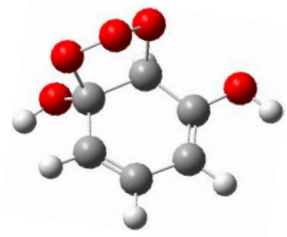 | 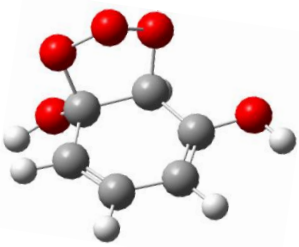 |
| Structure 2 | |

| | |
|---|---|
| 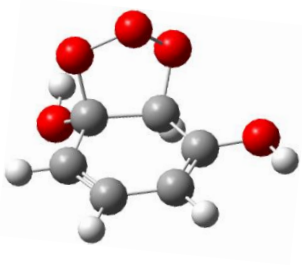 | 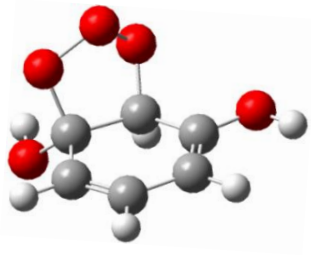 |
| structure 3 | |
| 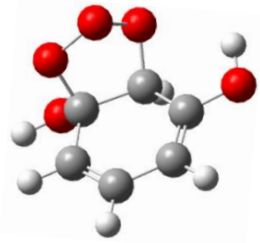 | 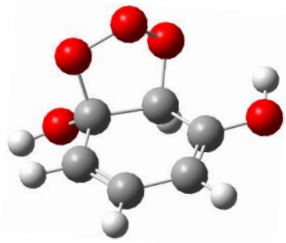 |
| Structure 4 | |
| 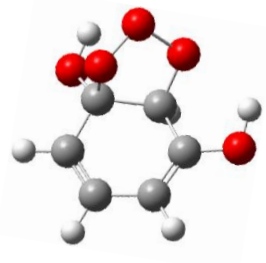 | 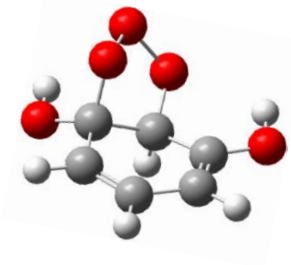 |
| Structure 5 | |
| 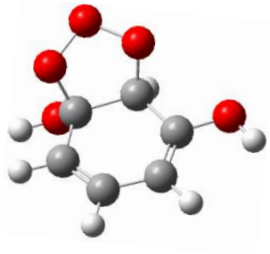 | 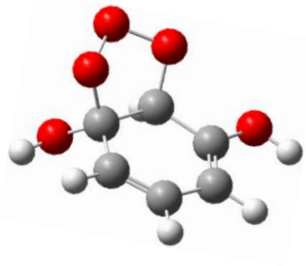 |
| Structure 6 | |
| 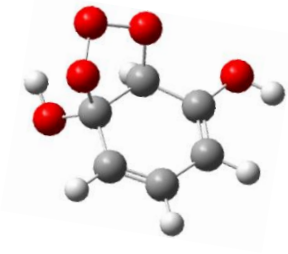 | 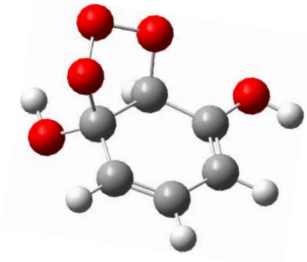 |
| Structure 7 | |

| | |
|---|---|
| 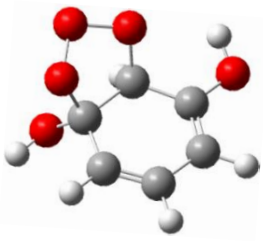 | 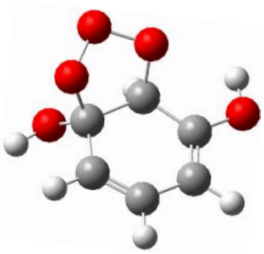 |
| Structure 8 | |
| **1_6_POZs** | |
| 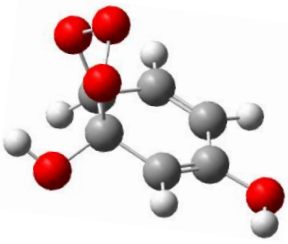 | 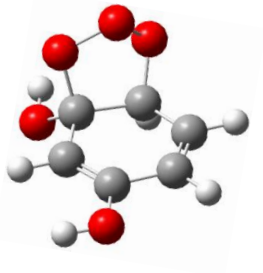 |
| Structure 9 | |
| 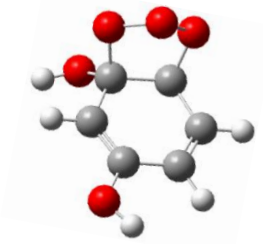 | 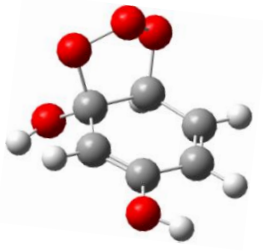 |
| Structure 10 | |
| 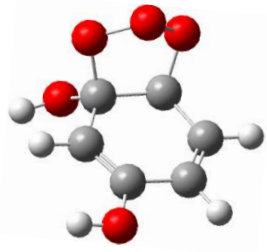 | 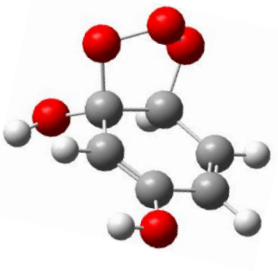 |
| Structure 11 | |
| 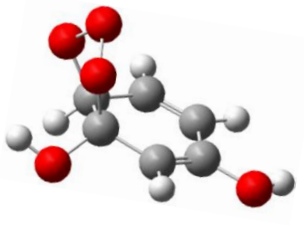 | 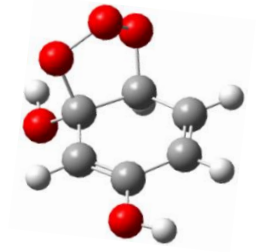 |
| Structure 12 | |

| | |
|---|---|
| 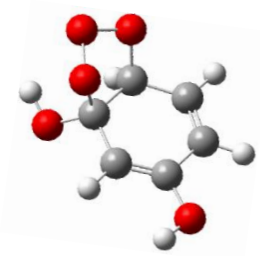 | 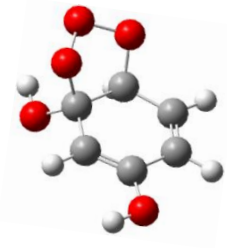 |
| Structure 13 | |
| 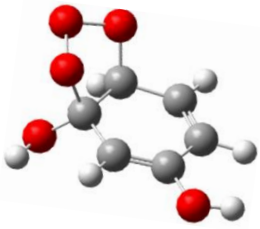 | 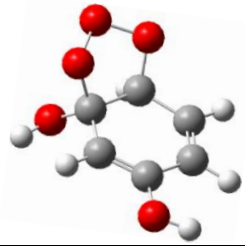 |
| Structure 14 | |
| 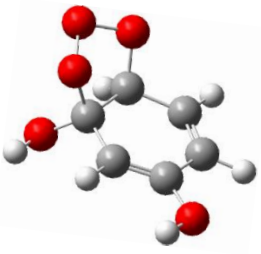 | 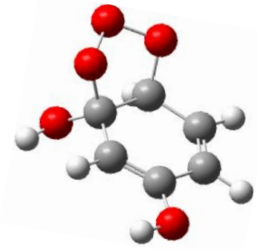 |
| Structure 15 | |
| 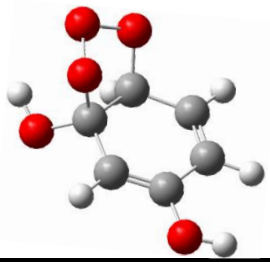 | 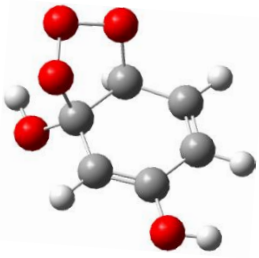 |
| Structure 16 | |
| **4_5_POZ** | |
| 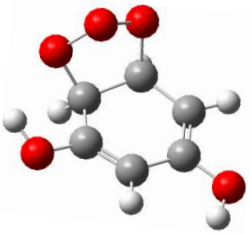 | 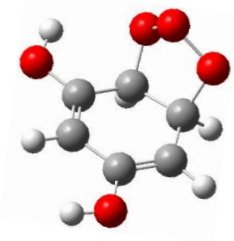 |
| Structure 17 | |

| | |
|---|---|
| 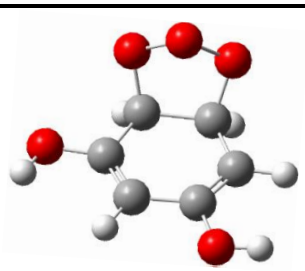 | 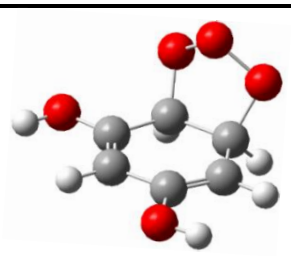 |
| Structure 18 | |
| 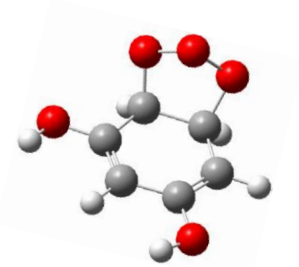 | 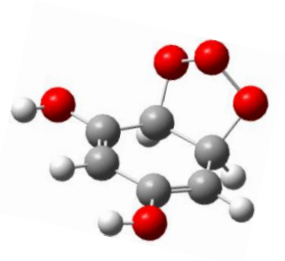 |
| Structure 19 | |
| 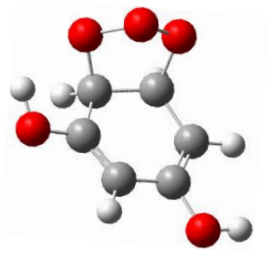 | 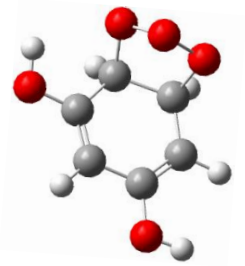 |
| Structure 20 | |
| 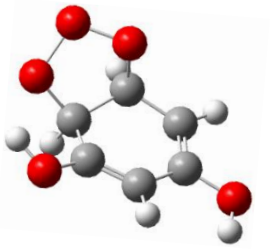 | 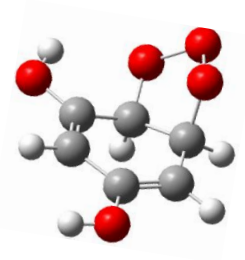 |
| Structure 21 | |
| 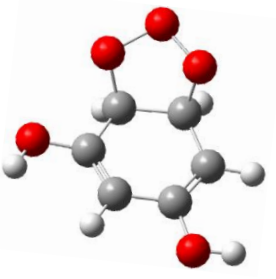 | 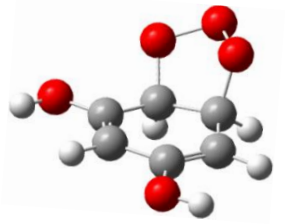 |
| Structure 22 | |

| | |
|---|---|
| 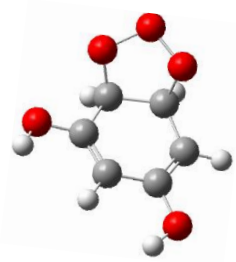 | 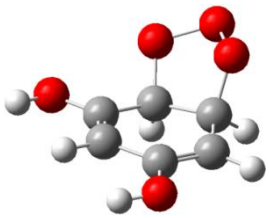 |
| Structure 23 | |
| 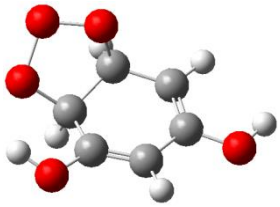 | 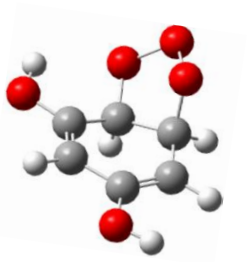 |
| Structure 24 | |

**Appendix B**

**Transition state**

**Phenol POZs**

| Gas Phase | Water |
|---|---|
| **B3LYP** | **B3LYP** |
| **1_2_POZ** | |
| 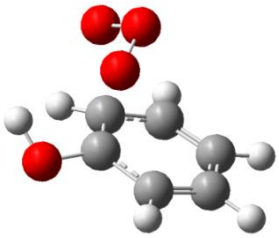 | 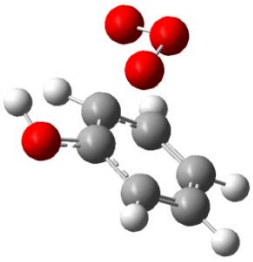 |
| Endo_O_endo_H | |
| 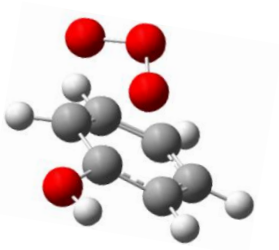 | 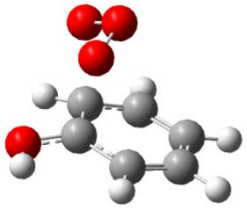 |

| Endo_O_exo_H | |
|---|---|
| 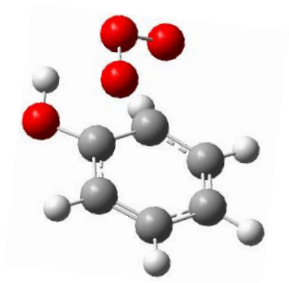 | 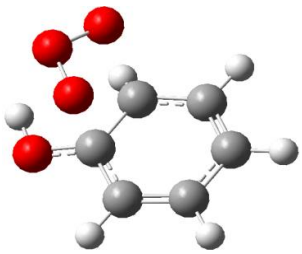 |
| Exo_O_endo_H | |
| 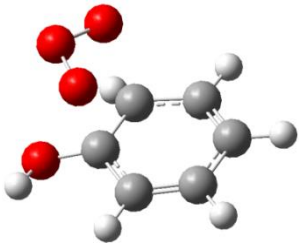 | 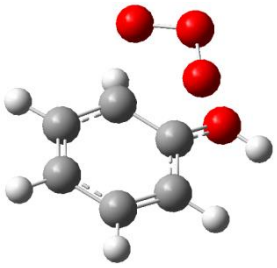 |
| Exo_O_exo_H | |
| **2_3_POZs** | |
| 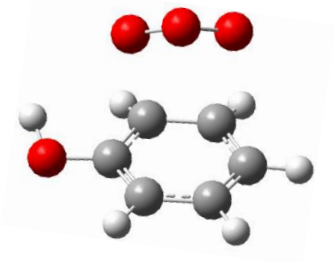 | 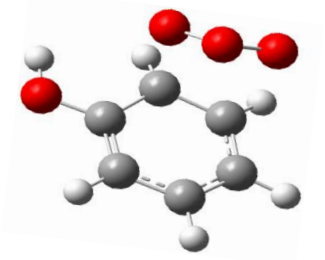 |
| Endo_O_endo_H | |
| 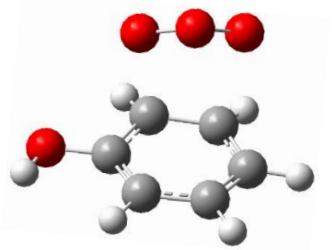 | 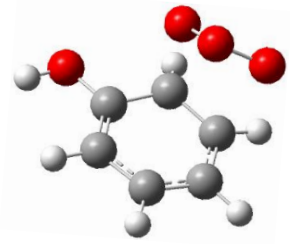 |
| Endo_O_exo_H | |

| | |
|---|---|
| 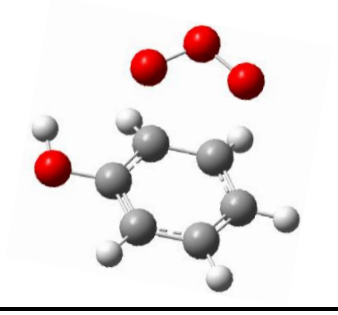 | 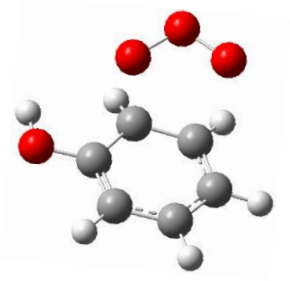 |
| Exo_O_endo_H | |
| 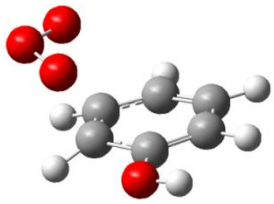 | 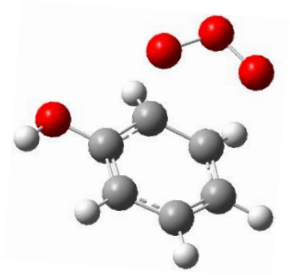 |
| Exo_O_exo_H | |
| **3_4_POZ** | |
| 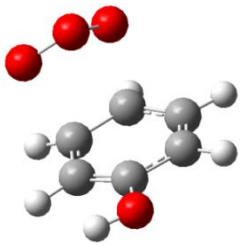 | 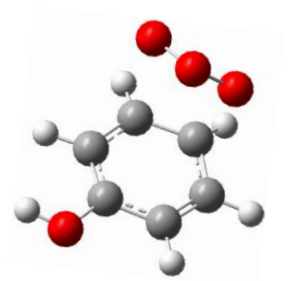 |
| Endo_O_endo_H | |
| 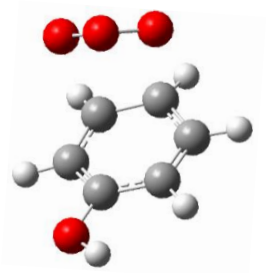 | 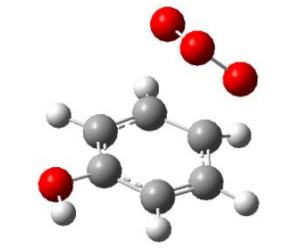 |
| Endo_O_exo_H | |
| | |

| | |
|---|---|
| 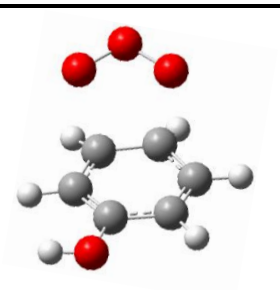 | 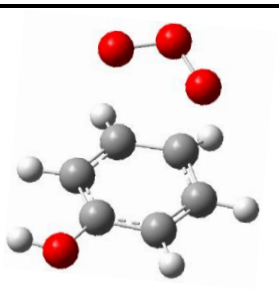 |
| Exo_O_endo_H | |
| 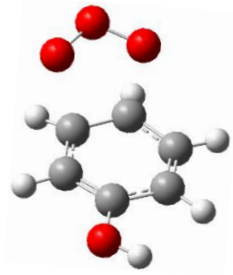 | 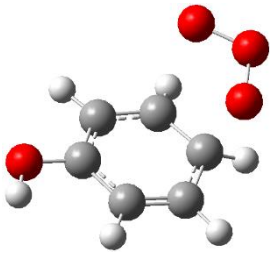 |
| Exo_O_exo_H | |

**Thiophenol POZs**

| Gas Phase | Water |
|---|---|
| **B3LYP** | **B3LYP** |
| **1_2_POZ** | |
|  | 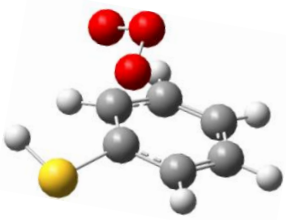 |
| Endo_O_endo_H | |
|  | 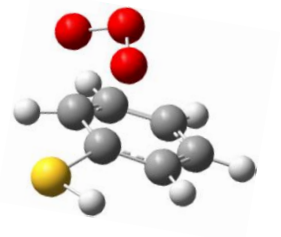 |
| Endo_O_exo_H | |

| | |
|---|---|
| 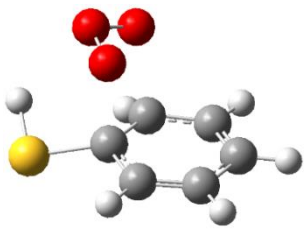 | 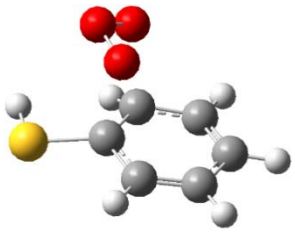 |
| Exo_O_endo_H | |
| 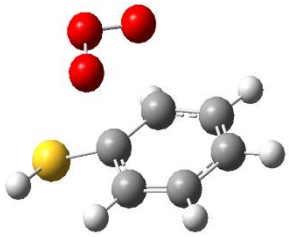 | 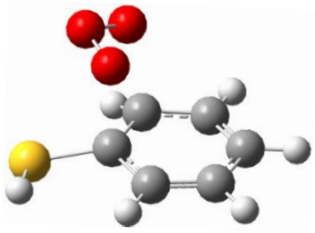 |
| Exo_O_exo_H | |
| **2_3_POZs** | |
| 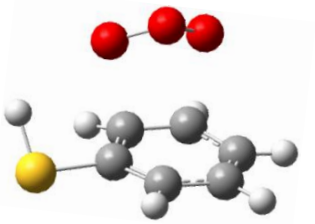 | 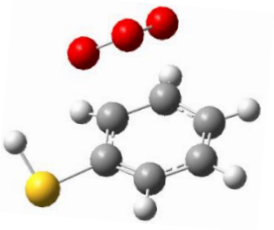 |
| Endo_O_endo_H | |
| 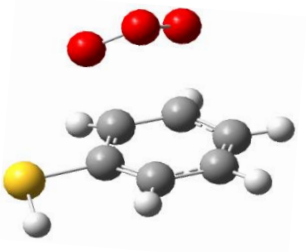 | 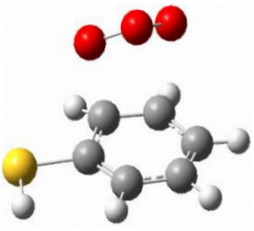 |
| Endo_O_exo_H | |
| 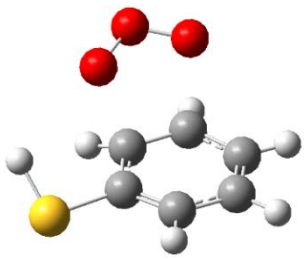 | 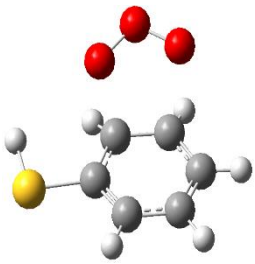 |

| Exo_O_endo_H | |
|---|---|
|  | 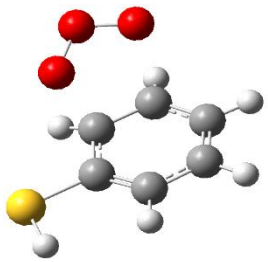 |
| Exo_O_exo_H | |
| **3_4_POZ** | |
| 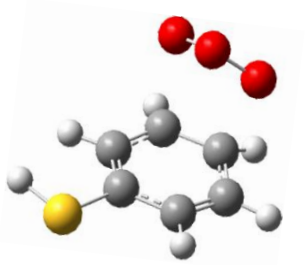 | 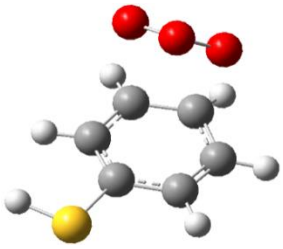 |
| Endo_O_endo_H | |
| 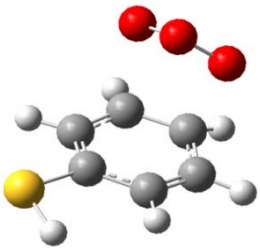 | 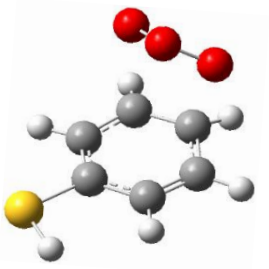 |
| Endo_O_exo_H | |
| 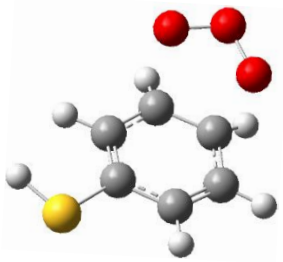 | 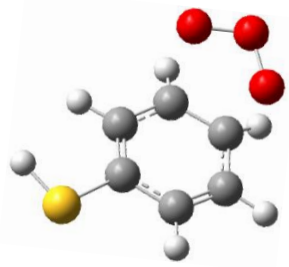 |
| Exo_O_endo_H | |
| | |

| | |
|---|---|
| 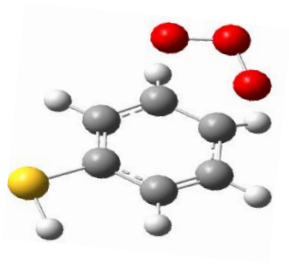 | 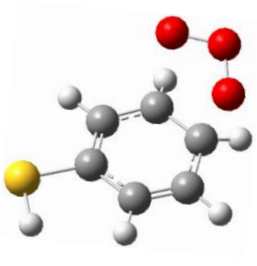 |
| Exo_O_exo_H | |

**Catechol POZs**

| Gas Phase | Water |
|---|---|
| **B3LYP** | **B3LYP** |
| **1_2_POZ** | |
| 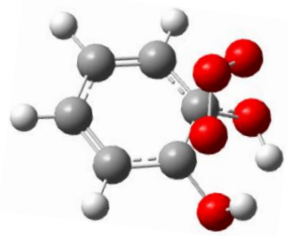 | 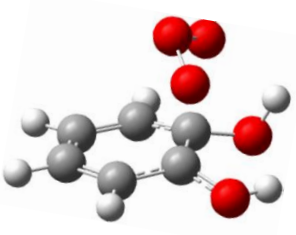 |
| Structure 1 | |
| 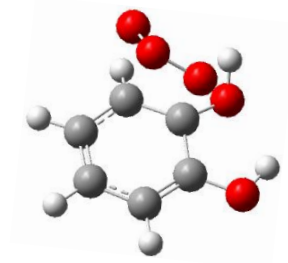 | 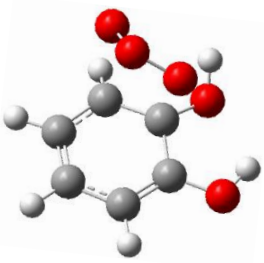 |
| Structure 2 | |
| 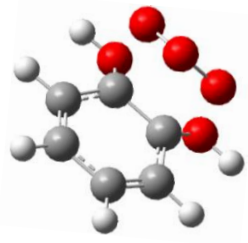 | 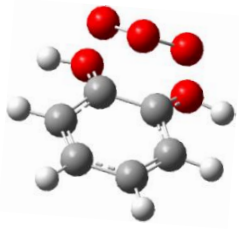 |
| structure 3 | |

| | |
|---|---|
| 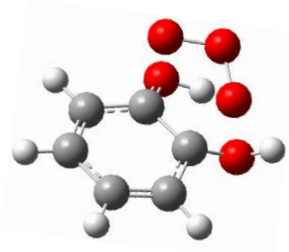 | 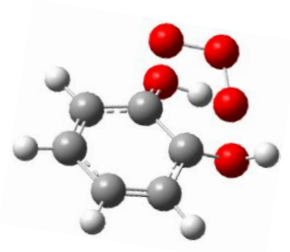 |
| Structure 4 | |
| 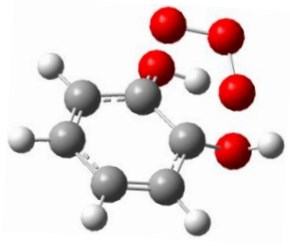 | 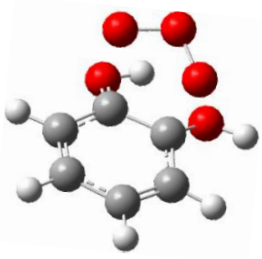 |
| Structure 5 | |
| 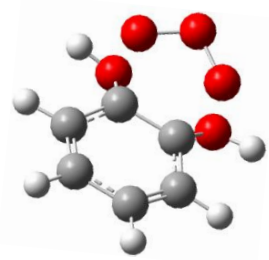 | 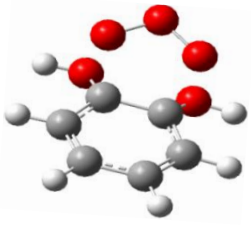 |
| Structure 6 | |
| **2_3_POZs** | |
| 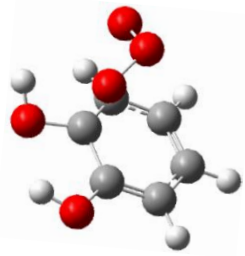 | 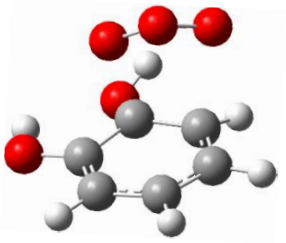 |
| Structure 7 | |
| 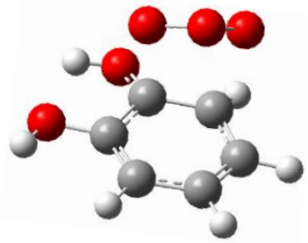 | 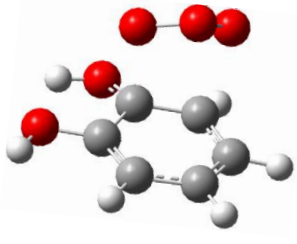 |
| Structure 8 | |

| | |
|---|---|
| 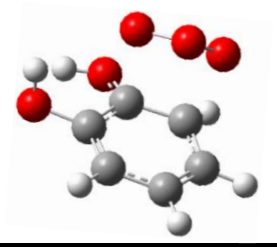 | 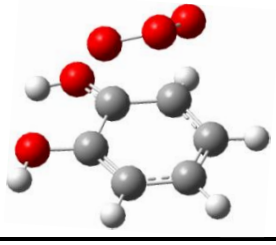 |
| Structure 9 | |
| 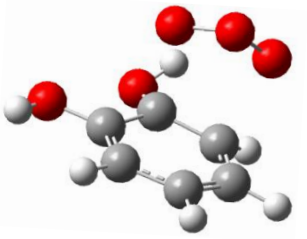 | 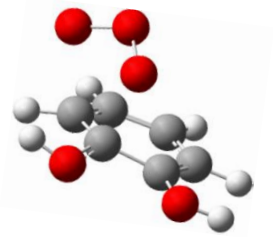 |
| Structure 10 | |
| 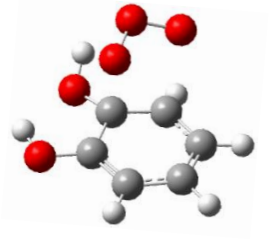 | 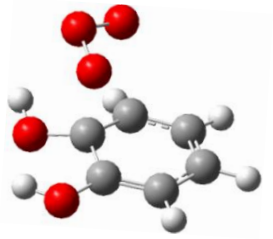 |
| Structure 11 | |
| 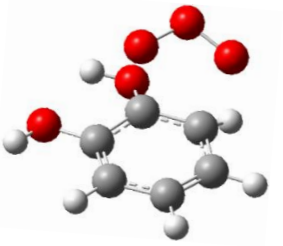 | 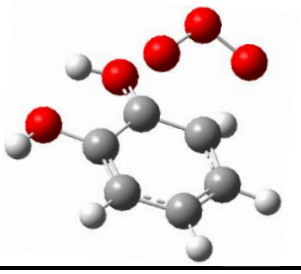 |
| Structure 12 | |
| 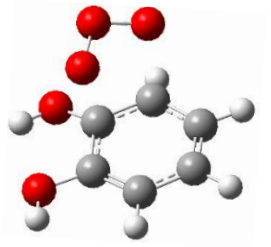 | 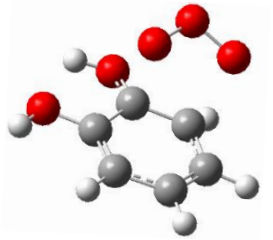 |
| Structure 13 | |

| | |
|---|---|
| 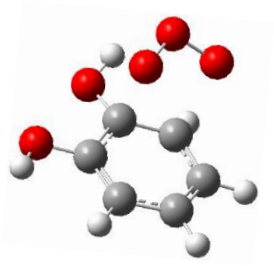 | 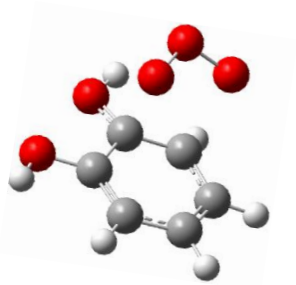 |
| Structure 14 | |
| **3_4_POZ** | |
| 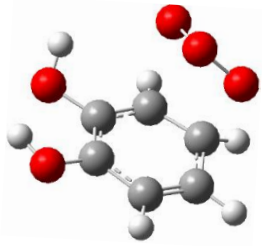 | 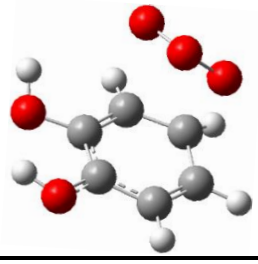 |
| Structure 15 | |
| 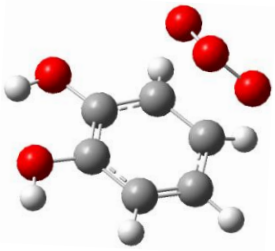 | 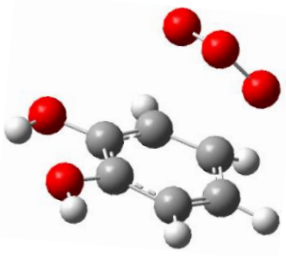 |
| Structure 16 | |
| 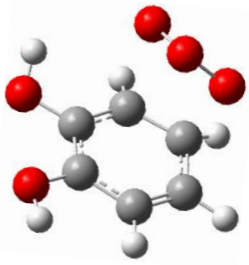 | 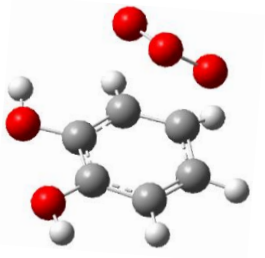 |
| Structure 17 | |
| 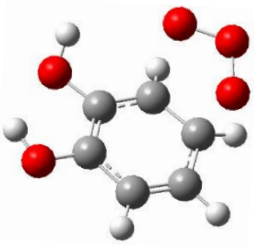 | 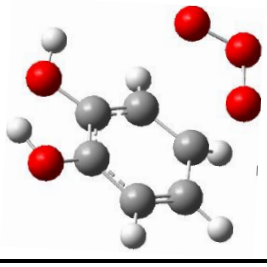 |
| Structure 18 | |

| | |
|---|---|
| 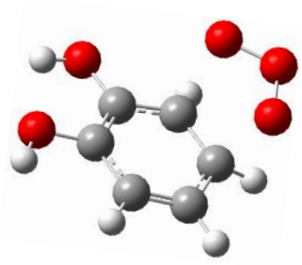 | 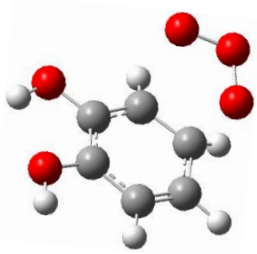 |
| Structure 19 | |
| 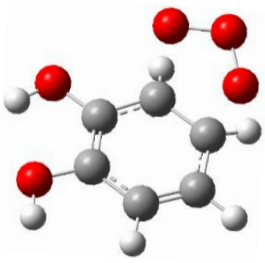 | 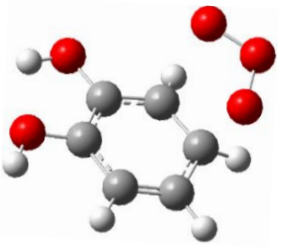 |
| Structure 20 | |
| 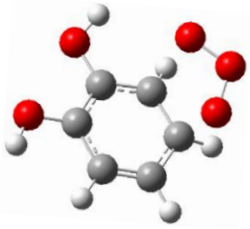 | 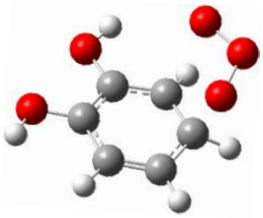 |
| Structure 21 | |
| **4_5_POZ** | |
| 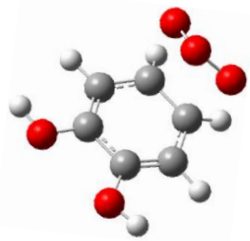 | 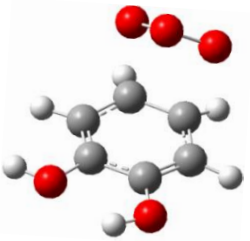 |
| Structure 22 | |
| 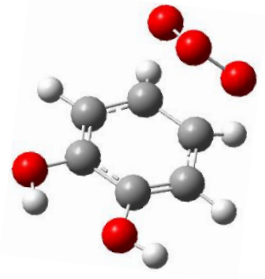 | 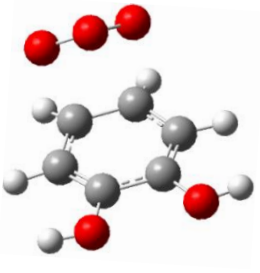 |
| Structure 23 | |

| | |
|---|---|
| 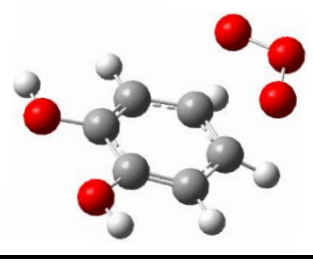 | 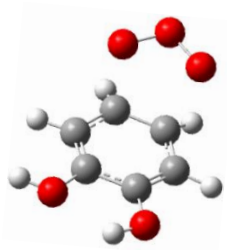 |
| Structure 24 | |
| 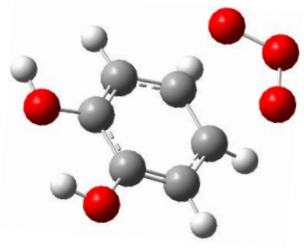 | 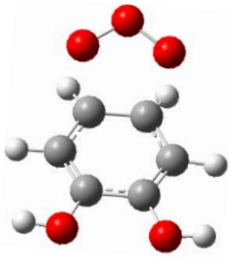 |
| Structure 25 | |

**Resorcinol POZs**

| Gas Phase | Water |
|---|---|
| **B3LYP** | **B3LYP** |
| **1_2_POZ** | |
| 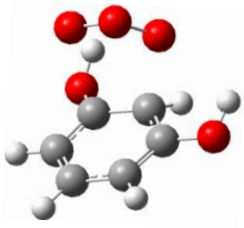 | 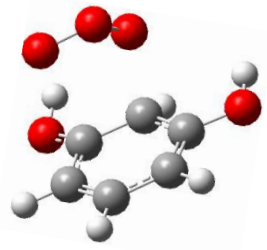 |
| Structure 1 | |
| 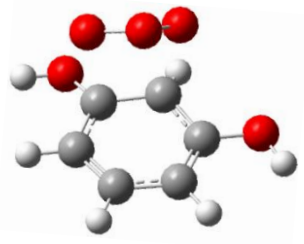 | 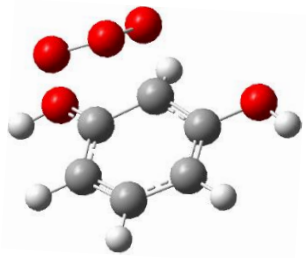 |
| Structure 2 | |

| | |
|---|---|
| 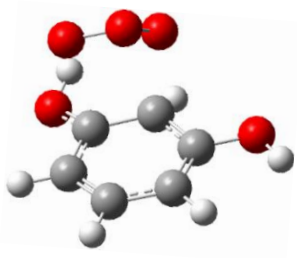 | 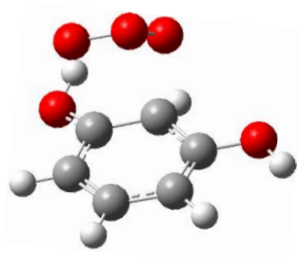 |
| structure 3 | |
| 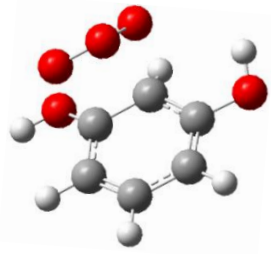 | 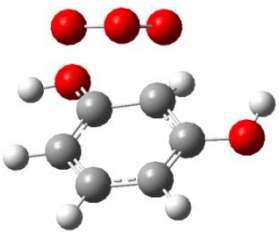 |
| Structure 4 | |
| 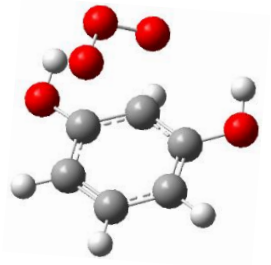 | 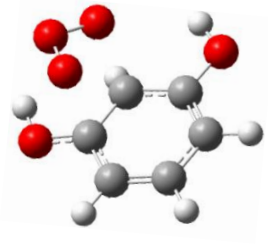 |
| Structure 5 | |
| 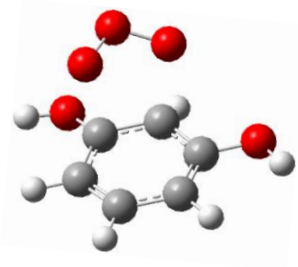 | 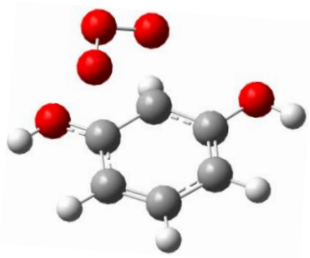 |
| Structure 6 | |
| 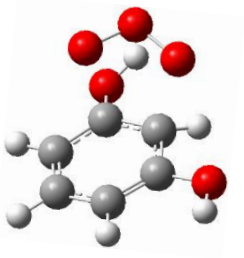 | 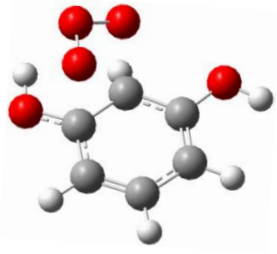 |
| Structure 7 | |

| | |
|---|---|
| 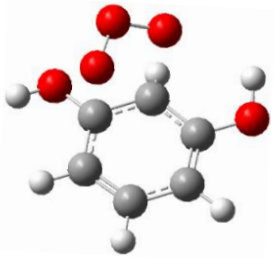 | 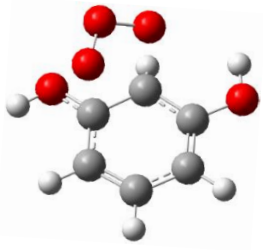 |
| Structure 8 | |
| **3_4_POZs** | |
| 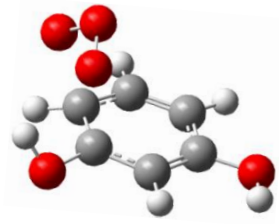 | 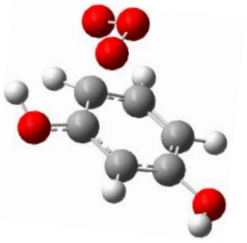 |
| Structure 9 | |
| 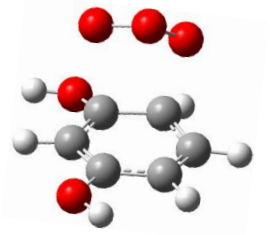 | 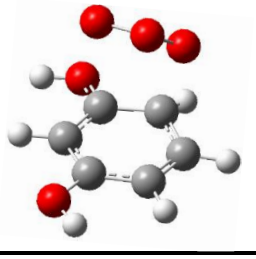 |
| Structure 10 | |
| 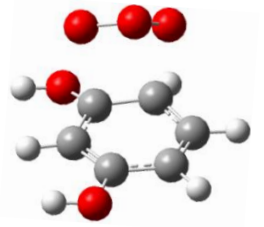 | 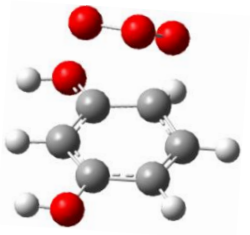 |
| Structure 11 | |
|  | 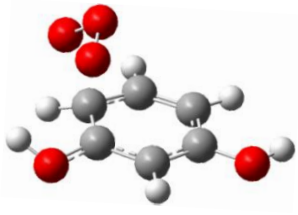 |
| Structure 12 | |

| | |
|---|---|
| 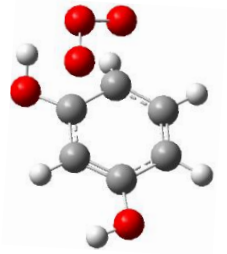 | 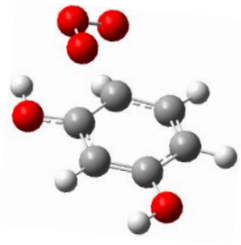 |
| Structure 13 | |
| 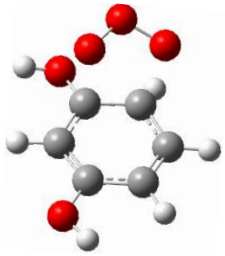 | 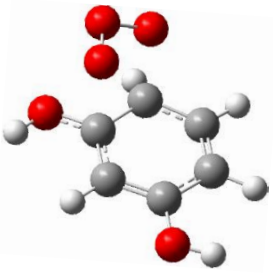 |
| Structure 14 | |
| 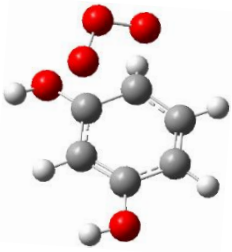 | 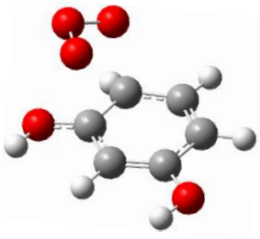 |
| Structure 15 | |
| 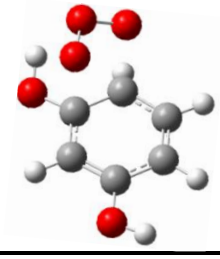 | 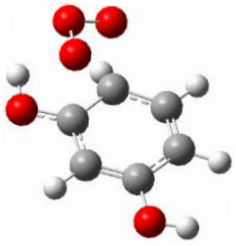 |
| Structure 16 | |
| **4_5_POZ** | |
| 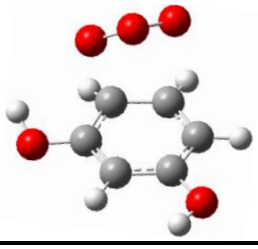 | 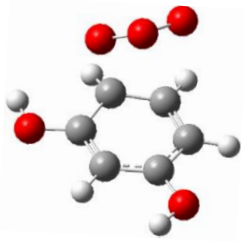 |
| Structure 17 | |

| | |
|---|---|
| 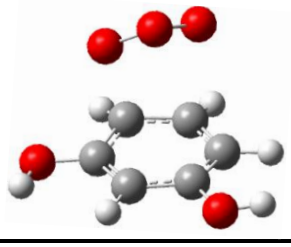 | 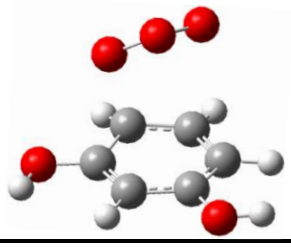 |
| Structure 18 | |
| 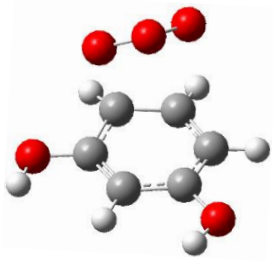 | 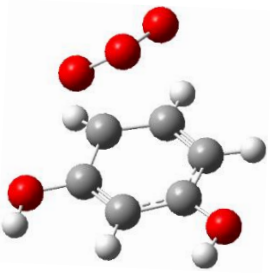 |
| Structure 19 | |
| 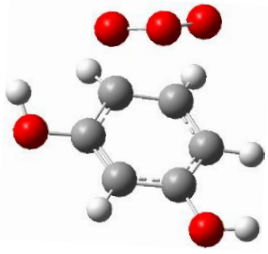 | 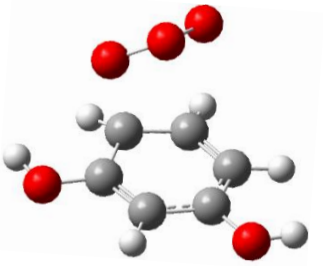 |
| Structure 20 | |
| 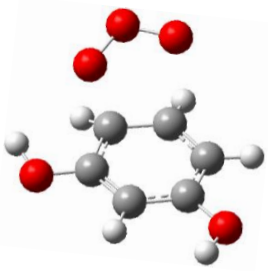 | 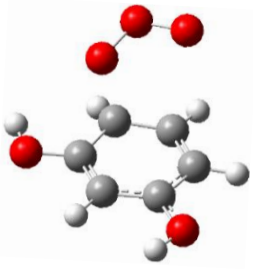 |
| Structure 21 | |
| 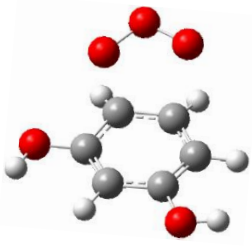 | 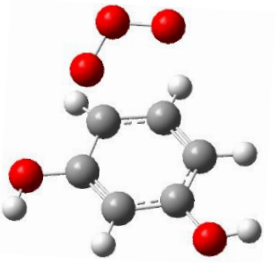 |
| Structure 22 | |

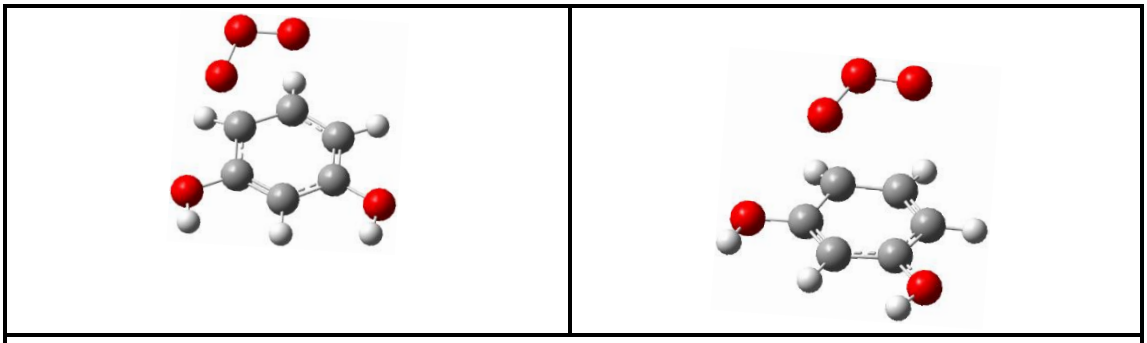

Structure 23

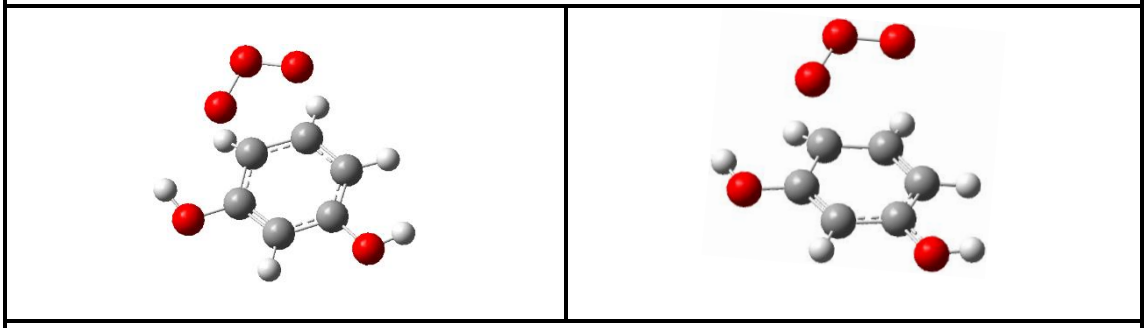

Structure 24

## Appendix C

## Group electronic energies and thermochemical properties of POZs.

## Phenol POZs

### Electronic energies and thermal properties in gas phase (a.u)

| | | | $E^{el}$ + ZPE CCSD(T) | $E^{el}$ B3LYP | $E^{el}$ + ZPE B3LYP | $\Delta E_e$+ $H^{therm}$ B3LYP | $\Delta E_e$+ $G^{therm}$ B3LYP |
|---|---|---|---|---|---|---|---|
| Ozone | | | -224.8682693 | -225.40 6453 | -225.399062 | -225.395159 | -225.422849 |
| Phenol | | | -306.5162426 | -307.478467 | -307.373671 | -307.367215 | -307.402651 |
| Ozone + Phenol | | | -531.3845119 | -532.88492 | -532.772733 | -532.762374 | -532.8255 |
| Mode I | | | | | | | |
| 1,2-addition | endo-O | endo-H | -531.4277155 | -532.9263043 | -532.810181 | -532.801254 | -532.843029 |
| | | exo-H | -531.4239855 | -532.9233107 | -532.807241 | -532.798237 | -532.840141 |
| | exo-O | endo-H | -531.430659 | -532.9286619 | -532.81241 | -532.803525 | -532.845195 |
| | | exo-H | -531.4301854 | -532.9287196 | -532.812317 | -532.80345 | - 532.844849 |
| Mode II | | | | | | | |
| 2,3-addition | endo-O | endo-H | -531.4216034 | -532.9252983 | -532.808205 | -532.799368 | -532.841075 |
| | | exo-H | -531.4205221 | -532.924352 | -532.807327 | -532.798475 | -532.840218 |
| | exo-O | endo-H | -531.4224384 | -532.9262371 | -532.809243 | -532.800405 | -532.841902 |
| | | exo-H | -531.4205223 | -532.9244335 | -532.807304 | -532.798424 | -532.840371 |
| Mode II | | | | | | | |
| 3,4-addition | endo-O | endo-H | -531.4216792 | -532.9251386 | -532.808176 | -532.799333 | -532.81112 |
| | | exo-H | -531.4182677 | -532.9215671 | -532.805144 | -532.796041 | -532.838363 |
| | exo-O | endo-H | -531.4225038 | -532.9257642 | -532.80874 | -532.799858 | -532.841807 |
| | | exo-H | -531.4192819 | -532.9223512 | -532.805817 | -532.796719 | -532.839067 |

## Electronic energies and thermal properties in water (a.u)

| | | | $E^{el}$ B3LYP | $E^{el}$ + ZPE B3LYP | $\Delta E_e$+ $H^{therm}$ B3LYP | $\Delta E_e$+ $G^{therm}$ B3LYP |
|---|---|---|---|---|---|---|
| Ozone | | | -225.4079136 | -225.4005 | -225.396657 | -225.423692 |
| Phenol | | | -307.484644 | -307.380023 | -307.37355 | -307.40901 |
| Ozone + Phenol | | | -532.8925576 | -532.780523 | -532.770207 | -532.832702 |
| Mode I | | | | | | |
| 1,2-addition | endo-O | endo-H | -532.9344513 | -532.818425 | -532.809488 | -532.851318 |
| | | exo-H | -532.933445 | -532.817302 | -532.808364 | -532.850051 |
| | exo-O | endo-H | -532.9372305 | -532.821038 | -532.8121143 | -532.853747 |
| | | exo-H | -532.9385149 | -532.822124 | -532.813283 | -532.854636 |
| Mode II | | | | | | |
| 2,3-addition | endo-O | endo-H | -532.9339244 | -532.817121 | -532.808149 | -532.850185 |
| | | exo-H | -532.9353144 | -532.81832 | -532.809472 | -532.851238 |
| | exo-O | endo-H | -532.933814 | -532.817223 | -532.808237 | -532.850097 |
| | | exo-H | -532.9354037 | -532.818423 | -532.809519 | -532.851482 |
| Mode III | | | | | | |
| 3,4-addition | endo-O | endo-H | -532.9356935 | -532.818802 | -532.809948 | -532.851773 |
| | | exo-H | -532.9334122 | -532.816904 | -532.807853 | -532.85008 |
| | exo-O | endo-H | -532.9361366 | -532.819291 | -532.810368 | -532.852409 |
| | | exo-H | -532.9339346 | -532.817413 | -532.808322 | -532.850699 |

## Thiophenol POZs

## Electronic energies and thermal properties in gas phase (a.u)

| | | | $E^{el}$ + ZPE CCSD(T) | $E^{el}$ B3LYP | $E^{el}$ + ZPE B3LYP | $\Delta E_e$+ $H^{therm}$ B3LYP | $\Delta E_e$+ $G^{therm}$ B3LYP |
|---|---|---|---|---|---|---|---|
| Ozone | | | -224.8682693 | -225.406453 | -225.399062 | -225.395159 | -225.422849 |
| Thiophenol | | | -629.1290144 | -630.4452305 | -630.345781 | -630.338532 | -630.376452 |
| Ozone + Thiophenol | | | -853.9972837 | -855.8516835 | -855.744843 | -855.733691 | -855.799301 |
| Mode I | | | | | | | |
| 1,2-addition | endo-O | endo-H | -854.0337401 | -855.8870646 | -855.7762 | -855.766632 | -855.8101 |
| | | exo-H | -854.0326852 | -855.886257 | -855.775384 | -855.765786 | -855.809279 |
| | exo-O | endo-H | -854.0358205 | -855.8892994 | -855.778304 | -855.768738 | -855.812209 |
| | | exo-H | -854.0357047 | -855.8898905 | -855.778794 | -855.769278 | -855.812492 |
| Mode II | | | | | | | |
| 2,3-addition | endo-O | endo-H | -854.0354935 | -855.8924647 | -855.780666 | -855.771193 | -855.81471 |
| | | exo-H | -854.0326723 | -855.8899858 | -855.778407 | -855.768815 | -855.812839 |
| | exo-O | endo-H | -854.0351509 | -855.8919008 | -855.78019 | -855.770548 | -855.8154826 |
| | | exo-H | -854.0328151 | -855.8901335 | -855.778398 | -855.768827 | -855.812779 |
| Mode III | | | | | | | |
| 3,4-addition | endo-O | endo-H | -854.032436 | -855.8900459 | -855.778469 | -855.768939 | -855.812675 |
| | | exo-H | -854.0323953 | -855.8893271 | -855.777832 | -855.768241 | -855.812141 |
| | exo-O | endo-H | -854.0327474 | -855.8900703 | -855.778447 | -855.768871 | -855.812846 |
| | | exo-H | -854.0323983 | -855.8891552 | -855.777574 | -855.767957 | -855.812106 |

## Electronic energies and thermal properties in water (a.u)

| | | | $E^{el}$ B3LYP | $E^{el}$ + ZPE B3LYP | $\Delta E_e$+ $H^{therm}$ B3LYP | $\Delta E_e$+ $G^{therm}$ B3LYP |
|---|---|---|---|---|---|---|
| Ozone | | | -225.4079136 | -225.40056 | -225.396657 | -225.423692 |
| Thiophenol | | | -630.4500517 | -630.350538 | -630.343361 | -630.380993 |
| Ozone + Thiophenol | | | -855.8579653 | -855.751098 | -855.740018 | -855.804685 |
| | | | | | | |
| Mode I | | | | | | |
| 1,2-addition | endo-O | endo-H | -855.8946494 | -855.783807 | -855.77423 | -855.817725 |
| | | exo-H | -855.8947661 | -855.783928 | -855.774333 | -855.81782 |
| | exo-O | endo-H | -855.8969446 | -855.785964 | -855.776413 | -855.819783 |
| | | exo-H | -855.8982315 | -855.787169 | -855.777659 | -855.820854 |
| Mode II | | | | | | |
| 2,3-addition | endo-O | endo-H | -855.9001561 | -855.788418 | -855.77887 | -855.822616 |
| | | exo-H | -855.8994384 | -855.787814 | -855.778203 | -855.822323 |
| | exo-O | endo-H | -855.8993497 | -855.787646 | -855.777981 | -855.822171 |
| | | exo-H | -855.8993857 | -855.787633 | -855.778042 | -855.822047 |
| Mode III | | | | | | |
| 3,4-addition | endo-O | endo-H | -855.8993828 | -855.787726 | -855.778223 | -855.821886 |
| | | exo-H | -855.8986287 | -855.787203 | -855.777533 | -855.821677 |
| | exo-O | endo-H | -855.8991187 | -855.787474 | -855.77789 | -855.821939 |
| | | exo-H | -855.8983287 | -855.786842 | -855.777112 | -855.821596 |

## Catechol POZs

## Electronic energies and thermal properties in gas phase (a.u)

| | $E^{el}$ + ZPE CCSD(T) | $E^{el}$ B3LYP | $E^{el}$ + ZPE B3LYP | $\Delta E_e$+ $H^{therm}$ B3LYP | $\Delta E_e$+ $G^{therm}$ B3LYP |
|---|---|---|---|---|---|
| Ozone | -224.8682693 | -225.4064534 | -225.399062 | -225.395159 | -225.422849 |
| Catechol | -381.5537917 | -382.6992865 | -382.590309 | -382.582594 | -382.620842 |
| Ozone + Catechol | -606.422061 | -608.1057399 | -607.989371 | -607.977753 | -608.043691 |
| | | | | | |
| POZ isomers | | | | | |
| 1_2_POZs | | | | | |
| 2_OH_endo_H_endo_O_a_H | -606.472898 | -608.1513548 | -608.031047 | -608.021193 | -608.064602 |
| 2_OH_c_H_endo_O_exo_H | -606.4687354 | -608.1486363 | -608.028485 | -608.018443 | -608.062284 |
| 2_OH_exo_H_endo_O_exo_H | -606.4586168 | -608.138006 | -608.01852 | -608.00815 | -608.052885 |
| 2_OH_exo_H_exo_O_a_H | -606.4747094 | -608.1531945 | -608.033068 | -608.022999 | -608.067026 |
| 2_OH_c_H_exo_O_endo_H | -606.4769011 | -608.1552943 | -608.035071 | -608.025161 | -608.06887 |
| 2_OH_exo_H_exo_O_exo_H | -606.4670655 | -608.1447029 | -608.025028 | -608.014803 | -608.059131 |
| | | | | | |
| 2_3_POZs | | | | | |
| 2_OH_c_H_endo_O_endo_H | -606.4685653 | -608.151682 | -608.030823 | -608.020866 | -608.064785 |
| 2_OH_a_H_endo_O_exo_H | -606.4643535 | -608.1474252 | -608.026613 | -608.016590 | -608.060689 |
| 2_OH_endo_H_endo_O_exo_H | -606.4637707 | -608.1463518 | -608.025161 | -608.015304 | -608.058972 |
| 2_OH_a_H_endo_O_endo_H | -606.4619347 | -608.1448306 | -608.02429 | -608.014207 | -608.058471 |
| 2_OH_c_H_exo_O_endo_H | -606.4699315 | -608.1529616 | -608.03192 | -608.022036 | -608.065827 |
| 2_OH_a_H_exo_O_exo_H | -606.469106 | -608.1517701 | -608.030611 | -608.020722 | -608.064327 |
| 2_OH_endo_H_exo_O_exo_H | -606.4678344 | -608.1501646 | -608.029026 | -608.019117 | -608.062815 |
| 2_OH_a_H_exo_O_endo_H | -606.4648016 | -608.1474277 | -608.026738 | -608.016691 | -608.060741 |
| | | | | | |
| 3_4_POZs | | | | | |
| 2_OH_c_H_endo_O_endo_H | -606.4597434 | -608.1459862 | -608.024526 | -608.014518 | -608.058762 |

| | | | | | |
|---|---|---|---|---|---|
| 2_OH_endo_H_endo_O_a_H | -606.4553888 | -608.1417105 | -608.020677 | -608.010483 | -608.055183 |
| 2_OH_a_H_endo_O_endo_H | -606.4500974 | -608.1364752 | -608.015844 | -608.005412 | -608.050699 |
| 2_OH_c_H_exo_O_endo_H | -606.4585552 | -608.144806 | -608.023482 | -608.013298 | -608.058518 |
| 2_OH_exo_H_exo_O_a_H | -606.455846 | -608.1414965 | -608.020453 | -608.010188 | -608.055217 |
| 2_OH_endo_H_exo_O_a_H | -606.4553216 | -608.141639 | -608.020508 | -608.010288 | -608.055206 |
| 2_OH_exo_H_exo_O_endo_H | -606.449836 | -608.1358521 | -608.015231 | -608.004819 | -608.049906 |
| | | | | | |
| 4_5_POZs | | | | | |
| 2_OH_exo_H_endo_O_a_H | -606.4605356 | -608.1481683 | -608.026746 | -608.016753 | -608.061071 |
| 2_OH_exo_H_endo_O_exo_H | -606.4553046 | -608.1429312 | -608.021454 | -608.011507 | -608.055799 |
| 2_OH_c_H_exo_O_exo_H | -606.4611848 | -608.1485619 | -608.027096 | -608.017053 | -608.0617 |
| 2_OH_exo_H_exo_O_exo_H | -606.4557861 | -608.1432252 | -608.021691 | -608.011696 | -608.056334 |

## Catechol POZs

## Electronic energies and thermal properties in water (a.u)

| | $E^{el}$ B3LYP | $E^{el}$ + ZPE B3LYP | $\Delta E_e$+ $\mathbf{H}^{therm}$ B3LYP | $\Delta E_e$+ $\mathbf{G}^{therm}$ B3LYP |
|---|---|---|---|---|
| Ozone | -225.4079136 | -225.40056 | -225.396657 | -225.423692 |
| Catechol | -382.7070933 | -382.598359 | -382.590642 | -382.628886 |
| Ozone + Catechol | -608.1150069 | -607.998919 | -607.987299 | -608.052578 |
| | | | | |
| POZ isomers | | | | |
| 1_2_POZs | | | | |
| 2_OH_endo_H_endo_O_endo_H | -608.159895 | -608.039879 | -608.029986 | -608.073573 |
| 2_OH_c_H_endo_O_endo_H | -608.1602165 | -608.040224 | -608.030224 | -608.073977 |
| 2_OH_exo_H_endo_O_exo_H | -608.1535089 | -608.034076 | -608.023744 | -608.068506 |
| 2_OH_exo_H_exo_O_endo_H | -608.1651332 | -608.045455 | -608.035310 | -608.079709 |
| 2_OH_c_H_exo_O_endo_H | -608.1654196 | -608.045803 | -608.035634 | -608.079773 |
| 2_OH_exo_H_exo_O_exo_H | -608.1598031 | -608.039659 | -608.029704 | -608.073404 |
| | | | | |
| 2_3_POZs | | | | |
| 2_OH_c_H_endo_O_endo_H | -608.1602517 | -608.039831 | -608.029783 | -608.074017 |
| 2_OH_a_H_endo_O_exo_H | -608.1597588 | -608.039150 | -608.029132 | -608.073229 |
| 2_OH_endo_H_endo_O_exo_H | -608.1559646 | -608.035166 | -608.025216 | -608.069119 |
| 2_OH_a_H_endo_O_endo_H | -608.1574935 | -608.036992 | -608.026953 | -608.071134 |
| 2_OH_c_H_exo_O_endo_H | -608.1617859 | -608.041135 | -608.031153 | -608.075127 |
| 2_OH_a_H_exo_O_exo_H | -608.1640506 | -608.043072 | -608.033168 | -608.076830 |
| 2_OH_endo_H_exo_O_exo_H | -608.1597731 | -608.039017 | -608.029011 | -608.072899 |
| 2_OH_a_H_exo_O_endo_H | -608.1607381 | -608.040034 | -608.030065 | -608.073872 |
| | | | | |
| 3_4_POZs | | | | |
| 2_OH_c_H_endo_O_endo_H | -608.1555572 | -608.034606 | -608.024429 | -608.069080 |
| 2_OH_a_H_endo_O_a_H | -608.154086 | -608.033469 | -608.023094 | -608.068233 |
| 2_OH_a_H_endo_O_endo_H | -608.1504177 | -608.029953 | -608.019447 | -608.064865 |
| 2_OH_c_H_exo_O_endo_H | -608.1543525 | -608.033465 | -608.023171 | -608.068284 |
| 2_OH_exo_H_exo_O_a_H | -608.1542855 | -608.033433 | -608.23115 | -608.068224 |
| 2_OH_endo_H_exo_O_a_H | -608.153878 | -608.033126 | -608.022748 | -608.068051 |
| 2_OH_a_H_c_O_endo_H | -608.1493832 | -608.029160 | -608.018396 | -608.064642 |
| | | | | |
| 4_5_POZs | | | | |
| 2_OH_a_H_endo_O_a_H | -608.1611251 | -608.040033 | -608.029992 | -608.074465 |
| 2_OH_a_H_endo_O_c_H | -608.1580975 | -608.036724 | -608.026752 | -608.071285 |
| 2_OH_a_H_exo_O_a_H | -608.1613919 | -608.040244 | -608.030160 | -608.074912 |
| 2_OH_a_H_exo_O_c_H | -608.158273 | -608.036879 | -608.026827 | -608.07247 |

## Resorcinol POZs

## Electronic energies and thermal properties in gas phase (a.u)

| Reactants | $E^{el}$ + ZPE CCSD(T) | $E^{el}$ B3LYP | $E^{el}$ + ZPE B3LYP | $\Delta E_e + H^{therm}$ B3LYP | $\Delta E_e + G^{therm}$ B3LYP |
|---|---|---|---|---|---|
| Ozone | -224.8682693 | -225.406453 | -225.399062 | -225.395159 | -225.422849 |
| Resorcinol | -381.5531427 | -382.6992394 | -382.590228 | -382.582622 | -382.620669 |
| Ozone + Resorcinol | -606.421412 | -608.1046542 | -607.988297 | -607.976753 | -608.042559 |
| | | | | | |
| POZ Isomers | | | | | |
| 1_2_POZs | | | | | |
| 3_OH_endo_H_endo_O_endo_H | -606.463055 | -608.1503324 | -608.02958 | -608.019573 | -608.063655 |
| 3_OH_exo_H_endo_O_c_H | -606.4617377 | -608.1456775 | -608.025033 | -608.014931 | -608.059238 |
| 3_OH_endo_H_endo_O_c_H | -606.4647927 | -608.1481396 | -608.02744 | -608.017411 | -608.061732 |
| 3_OH_exo_H_endo_O_endo_H | -606.4636564 | -608.1470748 | -608.026572 | -608.016389 | -608.061156 |
| 3_OH_endo_H_exo_O_endo_H | -606.4694617 | -608.1518713 | -608.031262 | -608.021306 | -608.064984 |
| 3_OH_exo_H_exo_O_c_H | -606.4674194 | -608.1506139 | -608.02972 | -608.019733 | -608.063634 |
| 3_OH_endo_H_exo_O_c_H | -606.4681144 | -608.1507885 | -608.030023 | -608.020045 | -608.064173 |
| 3_OH_exo_H_exo_O_endo_H | -606.4671222 | -608.1503511 | -608.029681 | -608.019544 | -608.063777 |
| | | | | | |
| 3_4_POZs | | | | | |
| 3_OH_c_H_endo_O_endo_H | -606.4671103 | -608.1496989 | -608.029117 | -608.019115 | -608.063343 |
| 3_OH_a_H_endo_O_exo_H | -606.4601648 | -608.1432722 | -608.023249 | -608.012903 | -608.057734 |
| 3_OH_c_H_endo_O_exo_H | -606.4629394 | -608.1461208 | -608.025641 | -608.015511 | -608.059918 |
| 3_OH_a_H_endo_O_endo_H | -606.4633125 | -608.1457133 | -608.02569 | -608.015429 | -608.060202 |
| 3_OH_c_H_exo_O_endo_H | -606.4702685 | -608.1522948 | -608.03154 | -608.021604 | -608.065651 |
| 3_OH_a_H_exo_O_exo_H | -606.4659763 | -608.1481353 | -608.02785 | -608.017615 | -608.062119 |
| 3_OH_c_H_exo_O_exo_H | -606.4689584 | -608.1512014 | -608.03046 | -608.020453 | -608.064472 |
| 3_OH_a_H_exo_O_endo_H | -606.4664634 | -608.1483166 | -608.028099 | -608.017925 | -608.062463 |
| | | | | | |
| 4_5_POZs | | | | | |
| 3_OH_c_H_endo_O_endo_H | -606.4588737 | -608.1466615 | -608.025456 | -608.015341 | -608.059897 |
| 3_OH_a_H_endo_O_exo_H | -606.460043 | -608.1479651 | -608.026457 | -608.0165 | -608.060774 |
| 3_OH_c_H_endo_O_exo_H | -606.4561283 | -608.1437655 | -608.022841 | -608.012571 | -608.057545 |
| 3_OH_a_H_endo_O_endo_H | -606.4614666 | -608.1493706 | -608.027805 | -608.017884 | -608.062042 |
| 3_OH_c_H_exo_O_endo_H | -606.461401 | -608.1494866 | -608.028297 | -608.018266 | -608.062312 |
| 3_OH_a_H_exo_O_exo_H | -606.4606757 | -608.1487243 | -608.027117 | -608.017152 | -608.061453 |
| 3_OH_c_H_exo_O_exo_H | -606.4569511 | -608.1447149 | -608.023638 | -608.013424 | -608.05822 |
| 3_OH_a_H_exo_O_endo_H | -606.4634291 | -608.151619 | -608.030161 | -608.020255 | -608.064092 |

## Electronic energies and thermal properties in water (a.u)

| | $E^{el}$ B3LYP | $E^{el}$ + ZPE B3LYP | $\Delta E_e + H^{therm}$ B3LYP | $\Delta E_e + G^{therm}$ B3LYP |
|---|---|---|---|---|
| Reactants | -225.4079136 | -225.40056 | -225.396657 | -225.423692 |
| Ozone | -382.7088032 | -382.599888 | -382.592323 | -382.630291 |
| Ozone + Resorcinol | -608.1167168 | -608.000448 | -607.98898 | -608.053983 |
| | | | | |
| POZ Isomers | | | | |
| 1_2_POZs | | | | |
| 3_OH_endo_H_endo_O_endo_H | -608.1598891 | -608.039424 | -608.029346 | -608.073619 |
| 3_OH_exo_H_endo_O_c_H | -608.1593918 | -608.038921 | -608.028812 | -608.07316 |
| 3_OH_endo_H_endo_O_c_H | -608.1601948 | -608.039591 | -608.029573 | -608.073944 |
| 3_OH_exo_H_endo_O_endo_H | -608.1582649 | -608.037974 | -608.027777 | -608.072368 |
| 3_OH_endo_H_exo_O_endo_H | -608.1601929 | -608.040109 | -608.02997 | -608.07413 |
| 3_OH_exo_H_exo_O_c_H | -608.1640586 | -608.043274 | -608.033328 | -608.07715 |

| | | | | |
|---|---|---|---|---|
| 3_OH_endo_H_exo_O_c_H | -608.162984 | -608.042423 | -608.032425 | -608.07653 |
| 3_OH_exo_H_exo_O_endo_H | -608.1617652 | -608.04131 | -608.031149 | -608.075436 |
| | | | | |
| 3_4_POZs | | | | |
| 3_OH_c_H_endo_O_endo_H | -608.1609837 | -608.040663 | -608.030638 | -608.07494 |
| 3_OH_a_H_endo_O_exo_H | -608.1576083 | -608.037832 | -608.027453 | -608.072464 |
| 3_OH_c_H_endo_O_exo_H | -608.1597539 | -608.039532 | -608.029375 | -608.073871 |
| 3_OH_a_H_endo_O_endo_H | -608.158713 | -608.03862 | -608.02844 | -608.073052 |
| 3_OH_c_H_exo_O_endo_H | -608.1637616 | -608.043241 | -608.033262 | -608.077372 |
| 3_OH_a_H_exo_O_exo_H | -608.1623152 | -608.041921 | -608.031787 | -608.076043 |
| 3_OH_c_H_exo_O_exo_H | -608.1645115 | -608.043739 | -608.033796 | -608.077654 |
| 3_OH_a_H_exo_O_endo_H | -608.161461 | -608.041215 | -608.031083 | -608.075498 |
| | | | | |
| 4_5_POZs | | | | |
| 3_OH_c_H_endo_O_endo_H | -608.1592063 | -608.038298 | -608.028108 | -608.07284 |
| 3_OH_a_H_endo_O_exo_H | -608.1620364 | -608.040787 | -608.030807 | -608.075146 |
| 3_OH_c_H_endo_O_exo_H | -608.1597776 | -608.038775 | -608.028627 | -608.073294 |
| 3_OH_a_H_endo_O_endo_H | -608.1612067 | -608.039975 | -608.029955 | -608.074337 |
| 3_OH_c_H_exo_O_endo_H | -608.1607257 | -608.039887 | -608.02977 | -608.074007 |
| 3_OH_a_H_exo_O_exo_H | -608.162895 | -608.041671 | -608.031649 | -608.076099 |
| 3_OH_c_H_exo_O_exo_H | -608.160778 | -608.03976 | -608.029603 | -608.074327 |
| 3_OH_a_H_exo_O_endo_H | -608.1624593 | -608.041412 | -608.031395 | -608.075467 |

## Appendix D

## Group transition state electronic energies and thermochemical properties of POZs.

## Phenol POZs

## Transition state electronic energies and thermal properties in gas phase (a.u)

| Reactants | | | $E^{el}$ + ZPE CCSD(T) | $E^{el}$ B3LYP | $E^{el}$ + ZPE B3LYP | $\Delta E_e$+ $\mathbf{H}^{therm}$ B3LYP | $\Delta E_e$+ $\mathbf{G}^{therm}$ B3LYP |
|---|---|---|---|---|---|---|---|
| Ozone | | | -224.8682693 | -225.406453 | -225.399062 | -225.395159 | -225.422849 |
| Phenol | | | -306.5162426 | -307.478467 | -307.373671 | -307.367215 | -307.402651 |
| Ozone + Phenol | | | -531.3845119 | -532.88492 | -532.772733 | -532.762374 | -532.8255 |
| Mode I | | | | | | | |
| 1,2-addition | endo-O | endo-H | -531.3693907 | -532.8782284 | -532.76464 | -532.755208 | -532.798068 |
| | endo-O | exo-H | -531.3666761 | -532.8756372 | -532.761891 | -532.752551 | -532.795021 |
| | exo-O | endo-H | -531.3651195 | -532.872658 | -532.759137 | -532.749763 | -532.792331 |
| | exo-O | exo-H | -531.3650242 | -532.8725798 | -532.758921 | -532.749615 | -532.79202 |
| Mode II | | | | | | | |
| 2,3-addition | endo-O | endo-H | -531.3646658 | -532.873892 | -532.760209 | -532.750655 | -532.794073 |
| | endo-O | exo-H | -531.3645554 | -532.8739078 | -532.7599 | -532.750549 | -532.793352 |
| | exo-O | endo-H | -531.3616236 | -532.8706688 | -532.757029 | -532.747497 | -532.790954 |
| | exo-O | exo-H | -531.3616399 | | | | |
| Mode III | | | | | | | |
| 3,4-addition | endo-O | endo-H | -531.3664591 | -532.877004 | -532.762832 | -532.753551 | -532.796262 |
| | endo-O | exo-H | -531.3648102 | -532.8753319 | -532.761347 | -532.752004 | -532.794815 |
| | exo-O | endo-H | -531.3632252 | -532.873042 | -532.759116 | -532.749774 | -532.792779 |
| | exo-O | exo-H | -531.3613753 | -532.8711027 | -532.757405 | -532.747977 | -532.791144 |

## Transition state electronic energies and thermal properties in water (a.u)

| | | | $E^{el}$ B3LYP | $E^{el}$ + ZPE B3LYP | $\Delta E_e$+ $\mathbf{H}^{therm}$ B3LYP | $\Delta E_e$+ $\mathbf{G}^{therm}$ B3LYP |
|---|---|---|---|---|---|---|
| Ozone | | | -225.4079136 | -225.40056 | -225.396657 | -225.423692 |
| Phenol | | | -307.484644 | -307.380023 | -307.373557 | -307.409014 |
| Ozone + Phenol | | | -532.8925576 | -532.780583 | -532.770214 | -532.832706 |
| Mode I | | | | | | |
| 1,2-addition | endo-O | endo-H | -532.8869235 | -532.773456 | -532.763966 | -532.807021 |
| | endo-O | exo-H | -532.8868227 | -532.773219 | -532.76382 | -532.806555 |
| | exo-O | endo-H | -532.8831998 | -532.769773 | -532.760312 | -532.803168 |
| | exo-O | exo-H | -532.8843434 | -532.770777 | -532.761408 | -532.804101 |
| Mode II | | | | | | |
| 2,3-addition | endo-O | endo-H | -532.8834212 | -532.769787 | -532.760264 | -532.803564 |
| | endo-O | exo-H | -532.8846184 | -532.770942 | -532.76149 | -532.80463 |
| | exo-O | endo-H | -532.8807203 | -532.767379 | -532.757749 | -532.801581 |
| | | exo-H | -532.8817907 | -532.768222 | -532.75871 | -532.802268 |
| Mode III | | | | | | |
| 3,4-addition | endo-O | endo-H | -532.8879382 | -532.774077 | -532.764688 | -532.807763 |
| | endo-O | exo-H | -532.887229 | -532.773397 | -532.763995 | -532.807068 |
| | exo-O | endo-H | -532.8846842 | -532.771022 | -532.76156 | -532.805021 |
| | exo-O | exo-H | -532.8838287 | -532.770262 | -532.76074 | -532.804361 |

## Thiophenol POZs

## Transition state Electronic energies and thermal properties in gas phase (a.u)

| Reactant | | | $E^{el}$ + ZPE CCSD(T) | $E^{el}$ B3LYP | $E^{el}$ + ZPE B3LYP | $\Delta E_e$+ $\mathbf{H}^{therm}$ B3LYP | $\Delta E_e$+ $\mathbf{G}^{therm}$ B3LYP |
|---|---|---|---|---|---|---|---|
| Ozone | | | -224.8682693 | -225.406453 | -225.399062 | -225.395159 | -225.422849 |
| Thiophenol | | | -629.1290144 | -630.4452305 | -630.345781 | -630.338532 | -630.376452 |
| Ozone + Thiophenol | | | -853.9972837 | -855.8516835 | -855.744843 | -855.733691 | -855.799301 |
| Mode I | | | | | | | |
| 1,2-addition | endo-O | endo-H | -853.9781431 | -855.8390344 | -855.730712 | -855.720584 | -855.765404 |
| | endo-O | exo-H | -853.976413 | -855.8378011 | -855.729351 | -855.71932 | -855.763743 |
| | exo-O | endo-H | -853.9738145 | -855.8337704 | -855.725544 | -855.715495 | -855.760005 |
| | exo-O | exo-H | -853.9740776 | -855.8343566 | -855.726043 | -855.716052 | -855.760405 |
| | | | | | | | |
| Mode II | | | | | | | |
| 2,3-addition | endo-O | endo-H | -853.9793715 | -855.841512 | -855.732816 | -855.722758 | -855.767613 |
| | endo-O | exo-H | -853.9769466 | -855.8397088 | -855.731075 | -855.720948 | -855.766088 |
| | exo-O | endo-H | -853.9757775 | -855.8375625 | -855.729114 | -855.718972 | -855.764206 |
| | exo-O | exo-H | -853.9740597 | -855.8363338 | -855.727918 | -855.717782 | -855.762987 |
| | | | | | | | |
| Mode III | | | | | | | |
| 3,4-addition | endo-O | endo-H | -853.9775981 | -855.841922 | -855.733106 | -855.72313 | -855.767819 |
| | endo-O | exo-H | -853.9772735 | -855.8413159 | -855.732692 | -855.722584 | -855.767707 |
| | exo-O | endo-H | -853.9742511 | -855.8377043 | -855.729255 | -855.719159 | -855.764287 |
| | exo-O | exo-H | -853.9736373 | -855.8370131 | -855.728554 | -855.718425 | -855.763685 |

## Transition state Electronic energies and thermal properties in water (a.u)

| Reactant | | | $E^{el}$ B3LYP | $E^{el}$ + ZPE B3LYP | $\Delta E_e$+ $H^{therm}$ B3LYP | $\Delta E_e$+ $G^{therm}$ B3LYP |
|---|---|---|---|---|---|---|
| Ozone | | | -225.4079136 | -225.40056 | -225.396657 | -225.423692 |
| Thiophenol | | | -630.4500517 | -630.350538 | -630.343361 | -630.380993 |
| Ozone + Thiophenol | | | -855.8579653 | -855.751098 | -855.740018 | -855.804685 |
| | | | | | | |
| Mode I | | | | | | |
| 1,2-addition | endo-O | endo-H | -855.8467264 | -855.738525 | -855.728337 | -855.773305 |
| | endo-O | exo-H | -855.8469057 | -855.73864 | -855.728532 | -855.773231 |
| | exo-O | endo-H | -855.8428813 | -855.73479 | -855.72463 | -855.769469 |
| | exo-O | exo-H | -855.8439892 | -855.735624 | -855.725643 | -855.77001 |
| | | | | | | |
| Mode II | | | | | | |
| 2,3-addition | endo-O | endo-H | -855.8480889 | -855.739601 | -855.729401 | -855.77473 |
| | endo-O | exo-H | -855.8481673 | -855.739781 | -855.729545 | -855.775053 |
| | exo-O | endo-H | -855.8452773 | -855.737187 | -855.726766 | -855.773194 |
| | exo-O | exo-H | -855.8455983 | -855.737277 | -855.727074 | -855.772595 |
| | | | | | | |
| Mode III | | | | | | |
| 3,4-addition | endo-O | endo-H | -855.8506876 | -855.742073 | -855.732033 | -855.776935 |
| | endo-O | exo-H | -855.8503507 | -855.741919 | -855.731767 | -855.776975 |
| | exo-O | endo-H | -855.847182 | -855.738784 | -855.728678 | -855.728678 |
| | exo-O | exo-H | -855.8467833 | -855.738554 | -855.72833 | -855.773929 |

## Catechol POZs

## Transition state electronic energies and thermal properties in gas phase (a.u)

| Reactant | $E^{el}$ + ZPE CCSD(T) | $E^{el}$ B3LYP | $E^{el}$ + ZPE B3LYP | $\Delta E_e$+ $H^{therm}$ B3LYP | $\Delta E_e$+ $G^{therm}$ B3LYP |
|---|---|---|---|---|---|
| Ozone | -224.8682693 | -225.4064534 | -225.399062 | -225.395159 | -225.422849 |
| Phenol | -381.5537917 | -382.6992865 | -382.590309 | -382.582594 | -382.620842 |
| Ozone + Catechol | -606.422061 | -608.1057399 | -607.989371 | -607.977753 | -608.043691 |
| | | | | | |
| POZ isomers | | | | | |
| 1_2_POZs | | | | | |
| 2_OH_endo_H_endo_O_a_H | -606.4099342 | -608.1016615 | -607.983714 | -607.973441 | -608.017818 |
| 2_OH_c_H_endo_O_exo_H | -606.4099342 | -608.1016615 | -607.983714 | -607.97344 | -608.017818 |
| 2_OH_exo_H_endo_O_exo_H | -606.40018 | -608.0918322 | -607.974356 | -607.963714 | -608.008764 |
| 2_OH_exo_H_exo_O_a_H | -606.4032323 | -608.0924777 | -607.974874 | -607.964305 | -608.009614 |
| 2_OH_c_H_exo_O_endo_H | -606.4032323 | -608.0924777 | -607.974874 | -607.964304 | -608.009614 |
| 2_OH_exo_H_exo_O_exo_H | -606.3956003 | -608.0847591 | -607.967556 | -607.956731 | -608.002735 |
| | | | | | |
| 2_3_POZs | | | | | |
| 2_OH_c_H_endo_O_endo_H | -606.4099224 | -608.1025147 | -607.98441 | -607.973953 | -608.019031 |
| 2_OH_a_H_endo_O_exo_H | -606.4065455 | -608.0987272 | -607.980615 | -607.9701 | -608.015033 |
| 2_OH_endo_H_endo_O_exo_H | -606.4065345 | -608.0974188 | -607.979296 | -607.968833 | -608.013832 |
| 2_OH_a_H_endo_O_endo_H | -606.4027478 | -608.0952293 | -607.977367 | -607.966805 | -608.01198 |
| 2_OH_c_H_exo_O_endo_H | -606.4058464 | -608.0967421 | -607.978821 | -607.968444 | -608.013238 |
| 2_OH_a_H_exo_O_exo_H | -606.4043571 | -608.095472 | -607.977404 | -607.966909 | -608.011846 |
| 2_OH_endo_H_exo_O_exo_H | -606.4043571 | -608.0954 72 | -607.977404 | -607.966909 | -608.011846 |

| | | | | | |
|---|---|---|---|---|---|
| 2_OH_a_H_exo_O_endo_H | -606.3981103 | -608.0894073 | -607.97172 | -607.961131 | -608.006266 |
| | | | | | |
| 3_4_POZs | | | | | |
| 2_OH_c_H_endo_O_endo_H | -606.4068927 | -608.0999645 | -607.981378 | -607.971014 | -608.016129 |
| 2_OH_endo_H_endo_O_a_H | -606.4005628 | -608.093362 | -607.975601 | -607.964791 | -608.010825 |
| 2_OH_a_H_endo_O_endo_H | -606.396994 | -608.0899373 | -607.972135 | -607.961427 | -608.00721 |
| 2_OH_c_H_exo_O_endo_H | -606.4024214 | -608.0950478 | -607.976855 | -607.966302 | -608.011882 |
| 2_OH_exo_H_exo_O_a_H | -606.3977499 | -608.0900406 | -607.972435 | -607.961561 | -608.007912 |
| 2_OH_endo_H_exo_O_a_H | -606.3977499 | -608.0900406 | -607.972435 | -607.961561 | -608.007912 |
| 2_OH_endo_H_exo_O_endo_H | -606.3928879 | -608.0856677 | -607.968044 | -607.957246 | -608.003314 |
| | | | | | |
| 4_5_POZs | | | | | |
| 2_OH_exo_H_endo_O_a_H | -606.4051523 | -608.0995914 | -607.981186 | -607.970649 | -608.016147 |
| 2_OH_exo_H_endo_O_exo_H | -606.399236 | -608.094006 | -607.975576 | -607.965072 | -608.01054 |
| 2_OH_c_H_exo_O_exo_H | -606.402206 | -608.0961713 | -607.977947 | -607.967386 | -608.013069 |
| 2_OH_exo_H_exo_O_exo_H | -606.3964103 | -608.0907003 | -607.972461 | -607.961929 | -608.007596 |

## Electronic energies and thermal properties in water (a.u)

| Reactant | $E^{el}$ B3LYP | $E^{el}$ + ZPE B3LYP | $\Delta E_e$+ $\mathbf{H}^{therm}$ B3LYP | $\Delta E_e$+ $\mathbf{G}^{therm}$ B3LYP |
|---|---|---|---|---|
| Ozone | -225.4079136 | -225.40056 | -225.396657 | -225.423692 |
| Catechol | -382.7070933 | -382.598359 | -382.590642 | -382.628886 |
| Ozone + Catechol | -608.1150069 | -607.998919 | -607.987299 | -608.052578 |
| | | | | |
| POZ isomers | | | | |
| 1_2_POZs | | | | |
| 2_OH_endo_H_endo_O_a_H | -608.1103775 | -607.993026 | -607.982526 | -608.027471 |
| 2_OH_c_H_endo_O_endo_H | -608.1103775 | -607.993026 | -607.982526 | -608.027471 |
| 2_OH_exo_H_endo_O_exo_H | -608.1085076 | -607.990884 | -607.980313 | -608.025374 |
| 2_OH_exo_H_exo_O_endo_H | -608.1044669 | -607.987413 | -607.976531 | -608.022980 |
| 2_OH_c_H_exo_O_endo_H | -608.1044669 | -607.987413 | -607.976531 | -608.022980 |
| 2_OH_a_H_exo_O_c_H | -608.1013842 | -607.983929 | -607.973196 | -608.019401 |
| | | | | |
| 2_3_POZs | | | | |
| 2_OH_c_H_endo_O_endo_H | -608.1116211 | -607.994073 | -607.983453 | -608.028835 |
| 2_OH_a_H_endo_O_exo_H | -608.1118991 | -607.994083 | -607.983516 | -608.028679 |
| 2_OH_endo_H_endo_O_exo_H | -608.111899 | -607.994084 | -607.983516 | -608.028680 |
| 2_OH_a_H_endo_O_endo_H | -608.1090261 | -607.991222 | -607.980656 | -608.025890 |
| 2_OH_c_H_exo_O_endo_H | -608.1072984 | -607.990154 | -607.979338 | -608.025380 |
| 2_OH_a_H_exo_O_exo_H | -608.1093128 | -607.991429 | -607.980914 | -608.025978 |
| 2_OH_endo_H_exo_O_exo_H | -608.1093128 | -607.991429 | -607.980914 | -608.025978 |
| 2_OH_a_H_exo_O_endo_H | -608.1049979 | -607.987281 | -607.976712 | -608.021874 |
| | | | | |
| 3_4_POZs | | | | |
| 2_OH_c_H_endo_O_endo_H | -608.1099903 | -607.992164 | -607.981515 | -608.027343 |
| 2_OH_a_H_endo_O_a_H | -608.1075796 | -607.990019 | -607.979279 | -608.025142 |
| 2_OH_a_H_endo_O_endo_H | -608.1052135 | -607.987532 | -607.976777 | -608.022774 |
| 2_OH_c_H_exo_O_endo_H | -608.1060674 | -607.988671 | -607.977801 | -608.024245 |
| 2_OH_exo_H_exo_O_a_H | -608.1043046 | -607.986955 | -607.976141 | -608.022387 |
| 2_OH_endo_H_exo_O_a_H | -608.1043046 | -607.986955 | -607.976141 | -608.022387 |
| 2_OH_a_H_c_O_endo_H | -608.1017187 | -607.984251 | -607.973445 | -608.019685 |
| | | | | |
| 4_5_POZs | | | | |
| 2_OH_a_H_endo_O_a_H | -608.1125158 | -607.994564 | -607.983893 | -608.029881 |
| 2_OH_a_H_endo_O_c_H | -608.1094556 | -607.991261 | -607.980649 | -608.026668 |

| | | | | |
|---|---|---|---|---|
| 2_OH_a_H_exo_O_a_H | -608.1098263 | -607.992021 | -607.981328 | -608.027523 |
| 2_OH_a_H_exo_O_c_H | -608.1068036 | -607.988916 | -607.978210 | -608.024917 |

## Resorcinol POZs

### Transition state electronic energies and thermal properties in gas phase (a.u)

| | $E^{el}$ + ZPE CCSD(T) | $E^{el}$ B3LYP | $E^{el}$ + ZPE B3LYP | $\Delta E_e$+ $\mathbf{H}^{therm}$ B3LYP | $\Delta E_e$+ $\mathbf{G}^{therm}$ B3LYP |
|---|---|---|---|---|---|
| Ozone | -224.8682693 | -225.406453 | -225.399062 | -225.395159 | -225.422849 |
| Resorcinol | -381.5531427 | -382.6982012 | -382.589235 | -382.581594 | -382.61971 |
| Ozone + Resorcinol | -606.421412 | -608.1046542 | -607.988297 | -607.976753 | -608.042559 |
| | | | | | |
| POZ Isomers | | | | | |
| 1_2_POZs | | | | | |
| 3_OH_endo_H_endo_O_endo_H | -606.4076955 | -608.0998816 | -607.982219 | -607.971533 | -608.01743 |
| 3_OH_exo_H_endo_O_c_H | -606.4032595 | -608.0952575 | -607.977379 | -607.966775 | -608.012099 |
| 3_OH_endo_H_endo_O_c_H | -606.4060233 | -608.0981879 | -607.980511 | -607.969819 | -608.015635 |
| 3_OH_exo_H_endo_O_endo_H | -606.4044736 | -608.0964449 | -607.978699 | -607.968021 | -608.013556 |
| 3_OH_endo_H_exo_O_endo_H | -606.4031442 | -608.0945168 | -607.976993 | -607.966228 | -608.012226 |
| 3_OH_exo_H_exo_O_c_H | -606.4025079 | -608.093857 | -607.975912 | -607.965413 | -608.010474 |
| 3_OH_endo_H_exo_O_c_H | -606.4024659 | -608.0937383 | -607.975977 | -607.965369 | -608.010758 |
| 3_OH_exo_H_exo_O_endo_H | -606.4032748 | -608.0946943 | -607.97693 | -607.966293 | -608.011755 |
| | | | | | |
| 3_4_POZs | | | | | |
| 3_OH_c_H_endo_O_endo_H | -606.4086543 | -608.1020001 | -607.984132 | -607.973567 | -608.019105 |
| 3_OH_a_H_endo_O_exo_H | -606.4039861 | -608.0966497 | -607.978855 | -607.968218 | -608.013637 |
| 3_OH_c_H_endo_O_exo_H | -606.4047313 | -608.0973947 | -607.979491 | -607.968882 | -608.014265 |
| 3_OH_a_H_endo_O_endo_H | -606.4070488 | -608.10015 | -607.98248 | -607.97186 | -608.017491 |
| 3_OH_c_H_exo_O_endo_H | -606.4032725 | -608.0953911 | -607.977607 | -607.967016 | -608.012467 |
| 3_OH_a_H_exo_O_exo_H | -606.4016927 | -608.0934638 | -607.975746 | -607.965134 | -608.010508 |
| 3_OH_c_H_exo_O_exo_H | -606.4027123 | -608.0944192 | -607.976564 | -607.965999 | -608.011289 |
| 3_OH_a_H_exo_O_endo_H | -606.4014404 | -608.0935145 | -607.975939 | -607.965288 | -608.010842 |
| | | | | | |
| 4_5_POZs | | | | | |
| 3_OH_c_H_endo_O_endo_H | -606.4041146 | -608.0980964 | -607.980068 | -607.969394 | -608.015322 |
| 3_OH_a_H_endo_O_exo_H | -606.4048283 | -608.0990777 | -607.980608 | -607.970161 | -608.0154 |
| 3_OH_c_H_endo_O_exo_H | -606.4027483 | -608.0967345 | -607.978473 | -607.967946 | -608.013314 |
| 3_OH_a_H_endo_O_endo_H | -606.4048137 | -608.0990682 | -607.98097 | -607.970324 | -608.016204 |
| 3_OH_c_H_exo_O_endo_H | -606.4030895 | -608.0948259 | -607.976859 | -607.966180 | -608.012189 |
| 3_OH_a_H_exo_O_exo_H | -606.4011627 | -608.0954391 | -607.977191 | -607.966673 | -608.012275 |
| 3_OH_c_H_exo_O_exo_H | -606.4025713 | -608.0928216 | -607.974823 | -607.964197 | -608.010009 |
| 3_OH_a_H_exo_O_endo_H | -606.4009394 | -608.095977 | -607.977899 | -607.967272 | -608.013161 |

## Resorcinol POZs

### Transition state electronic energies and thermal properties in water (a.u)

| | $E^{el}$ B3LYP | $E^{el}$ + ZPE B3LYP | $\Delta E_e$+ $\mathbf{H}^{therm}$ B3LYP | $\Delta E_e$+ $\mathbf{G}^{therm}$ B3LYP |
|---|---|---|---|---|
| | | | | |
| Ozone | -225.4079136 | -225.40056 | -225.396657 | -225.423692 |
| Resorcinol | -382.7088032 | -382.599888 | -382.592323 | -382.630291 |
| Ozone + Resorcinol | -608.1167168 | -608.000448 | -607.98898 | -608.053983 |
| POZ Isomers | | | | |

| | | | | |
|---|---|---|---|---|
| 1_2_POZs | | | | |
| 3_OH_endo_H_endo_O_endo_H | -608.110281 | -607.993142 | -607.982148 | -608.029021 |
| 3_OH_exo_H_endo_O_c_H | -608.111024 | -607.993172 | -607.982524 | -608.028189 |
| 3_OH_endo_H_endo_O_c_H | -608.1108883 | -607.993348 | -607.982522 | -608.02884 |
| 3_OH_exo_H_endo_O_endo_H | -608.1101473 | -607.992657 | -607.981816 | -608.028009 |
| 3_OH_endo_H_exo_O_endo_H | -608.107242 | -607.99014 | -607.979174 | -608.025708 |
| 3_OH_exo_H_exo_O_c_H | -608.10996 | -607.99207 | -607.98151 | -608.026946 |
| 3_OH_endo_H_exo_O_c_H | -608.1086067 | -607.991004 | -607.980292 | -608.026114 |
| 3_OH_exo_H_exo_O_endo_H | -608.1087005 | -607.991176 | -607.98044 | -608.026328 |
| | | | | |
| 3_4_POZs | | | | |
| 3_OH_c_H_endo_O_endo_H | -608.1144459 | -607.996798 | -607.985997 | -608.032333 |
| 3_OH_a_H_endo_O_exo_H | -608.1136662 | -607.995976 | -607.985283 | -608.031098 |
| 3_OH_c_H_endo_O_exo_H | -608.1141632 | -607.996303 | -607.98567 | -608.031361 |
| 3_OH_a_H_endo_O_endo_H | -608.1137191 | -607.996228 | -607.985345 | -608.031923 |
| 3_OH_c_H_exo_O_endo_H | -608.1102905 | -607.992819 | -607.982005 | -608.028296 |
| 3_OH_a_H_exo_O_exo_H | -608.1104418 | -607.992828 | -607.98214 | -608.028055 |
| 3_OH_c_H_exo_O_exo_H | -608.1111186 | -607.993275 | -607.982678 | -608.028333 |
| 3_OH_a_H_exo_O_endo_H | -608.1094644 | -607.992191 | -607.998132 | -608.027691 |
| | | | | |
| 4_5_POZs | | | | |
| 3_OH_c_H_endo_O_endo_H | -608.113991 | -607.996028 | -607.985389 | -608.031266 |
| 3_OH_a_H_endo_O_exo_H | -608.1152724 | -607.99728 | -607.986699 | -608.032402 |
| 3_OH_c_H_endo_O_exo_H | -608.1148375 | -607.996823 | -607.986241 | -608.031943 |
| 3_OH_a_H_endo_O_endo_H | -608.1141938 | -607.996318 | -607.985647 | -608.031638 |
| 3_OH_c_H_exo_O_endo_H | -608.1114794 | -607.993697 | -607.982929 | -608.029448 |
| 3_OH_a_H_exo_O_exo_H | -608.1124518 | -607.99471 | -607.983989 | -608.03039 |
| 3_OH_c_H_exo_O_exo_H | -608.1119031 | -607.994272 | -607.98351 | -608.029982 |
| 3_OH_a_H_exo_O_endo_H | -608.1117337 | -607.99395 | -607.983203 | -608.029625 |

## APPENDIX E

### Geometrical parameters

Note: All bond lengths ($R_i$) are given in angstroms (Å) and all bond angle sizes (θ) are given in degrees (°).

### Phenol POZs

### Phenol POZ geometries and planarity in gas phase

| 1_2_POZ | | | | | |
|---|---|---|---|---|---|
| **Bond** | **Molecule** | **POZ isomers** | | | |
| | | | | | |
| | Phenol | endo_O_endo_H | endo_O_exo_H | exo_O_endo_H | exo_O_exo_H |
| $R_1$ (Å ) | 1.36788 | 1.3946 | 1.396 | 1.3984 | 1.4035 |
| | Ozone | | | | |
| $R_2$ (Å ) | | 1.464 | 1.458 | 1.43637 | 1.4301 |
| $R_3$ (Å ) | 1.26405 | 1.4471 | 1.4387 | 1.454 | 1.4591 |
| $R_4$ (Å ) | 1.26405 | 1.44 | 1.4426 | 1.4424 | 1.4367 |
| $R_5$ (Å ) | | 1.4385 | 1.44218 | 1.4413 | 1.4396 |
| Θ (degrees) | | 102.29 | 101.69 | 101.16 | 101.03 |

| | | | | | |
|---|---|---|---|---|---|
| Planarity | | Non planar | Planar | Planar | Non planar |

## Phenol POZ geometries and planarity in gas phase

| 2_3_POZ | | | | | |
|---|---|---|---|---|---|
| **Bond** | **Molecule** | **POZ isomers** | | | |
| | | | | | |
| | Phenol | endo_O_endo_H | endo_O_exo_H | exo_O_endo_H | exo_O_exo_H |
| $R_1$ (Å ) | 1.36788 | 1.35948 | 1.35872 | 1.35208 | 1.35658 |
| | Ozone | | | | |
| $R_2$ (Å ) | | 1.4377 | 1.443 | 1.4283 | 1.4414 |
| $R_3$ (Å ) | 1.26405 | 1.4523 | 1.4466 | 1.5097 | 1.4486 |
| $R_4$ (Å ) | 1.26405 | 1.4392 | 1.437 | 1.4145 | 1.4381 |
| $R_5$ (Å ) | | 1.4611 | 1.447 | 1.45319 | 1.4432 |
| Θ (degrees) | 118 | 101.34 | 101.24 | 104.4 | 101.61 |
| Planarity | | Non planar | Planar | Non planar | Non planar |

## Phenol POZ geometries and planarity in gas phase

| 3_4_POZ | | | | | |
|---|---|---|---|---|---|
| **Bond** | **Molecule** | **POZ isomers** | | | |
| | | | | | |
| | Phenol | endo_O_endo_H | endo_O_exo_H | exo_O_endo_H | exo_O_exo_H |
| $R_1$ (Å ) | 1.36788 | 1.36265 | 1.36561 | 1.3603 | 1.36277 |
| | Ozone | | | | |
| $R_2$ (Å ) | | 1.45403 | 1.45574 | 1.44701 | 1.44797 |
| $R_3$ (Å ) | 1.26405 | 1.43859 | 1.43662 | 1.43363 | 1.43073 |
| $R_4$ (Å ) | 1.26405 | 1.44424 | 1.44603 | 1.4568 | 1.46161 |
| $R_5$ (Å ) | | 1.44363 | 1.44261 | 1.44373 | 1.44286 |
| Θ (degrees) | 118 | 101.12 | 101.15 | 101.93 | 102.02 |
| Planarity | | Non planar | Non planar | Non planar | Non planar |

## Phenol POZ geometries and planarity in water

| 1_2_POZ | | | | | |
|---|---|---|---|---|---|
| **Bond** | **Molecule** | **POZ isomers** | | | |
| | | | | | |
| | Phenol | endo_O_endo_H | endo_O_exo_H | exo_O_endo_H | exo_O_exo_H |
| $R_1$ (Å ) | 1.36755 | 1.39034 | 1.39131 | 1.39552 | 1.35978 |
| | Ozone | | | | |
| $R_2$ (Å ) | | 1.47444 | 1.47246 | 1.44469 | 1.45738 |
| $R_3$ (Å ) | 1.26436 | 1.44255 | 1.43683 | 1.454558 | 1.43362 |
| $R_4$ (Å ) | 1.26436 | 1.44193 | 1.445 | 1.44173 | 1.45914 |
| $R_5$ (Å ) | | 1.44369 | 1.44713 | 1.44547 | 1.45171 |

| | | | | | |
|---|---|---|---|---|---|
| Θ (degrees) | | 102.14 | 101.74 | 101.07 | 101.91 |
| Planarity | | Non planar | Planar | Planar | Non planar |

## Phenol POZ geometries and planarity in water

| 2_3_POZ | | | | | |
|---|---|---|---|---|---|
| **Bond** | **Molecule** | **POZ isomers** | | | |
| | | | | | |
| | Phenol | endo_O_endo_H | endo_O_exo_H | exo_O_endo_H | exo_O_exo_H |
| $R_1$ (Å ) | 1.36755 | 1.35966 | 1.35795 | 1.35368 | 1.35587 |
| | Ozone | | | | |
| $R_2$ (Å ) | | 1.44184 | 1.44884 | 1.4333 | 1.44958 |
| $R_3$ (Å ) | 1.26436 | 1.44887 | 1.44725 | 1.50742 | 1.45092 |
| $R_4$ (Å ) | 1.26436 | 1.44157 | 1.43798 | 1.41711 | 1.43801 |
| $R_5$ (Å ) | | 1.46658 | 1.45541 | 1.45915 | 1.45152 |
| Θ (degrees) | | 101.5 | 101.21 | 104.4 | 101.66 |
| Planarity | | Non planar | Planar | Non planar | Non planar |

## Phenol POZ geometries and planarity in water

| 3_4_POZ | | | | | |
|---|---|---|---|---|---|
| **Bond** | **Molecule** | **POZ isomers** | | | |
| | | | | | |
| | Phenol | endo_O_endo_H | endo_O_exo_H | exo_O_endo_H | exo_O_exo_H |
| $R_1$ (Å ) | 1.36788 | 1.36265 | 1.36561 | 1.3603 | 1.36277 |
| | Ozone | | | | |
| $R_2$ (Å ) | | 1.45403 | 1.45574 | 1.44701 | 1.44797 |
| $R_3$ (Å ) | 1.26346 | 1.43859 | 1.43662 | 1.43363 | 1.43073 |
| $R_4$ (Å ) | 1.26346 | 1.44424 | 1.44603 | 1.4568 | 1.46161 |
| $R_5$ (Å ) | | 1.44363 | 1.44261 | 1.44373 | 1.44286 |
| Θ (degrees) | | 101.12 | 101.15 | 101.8 | 102.02 |
| Planarity | | planar | planar | Non planar | Non planar |

## Thiophenol POZs

## Thiophenol POZ geometries and planarity in gas phase

| 1_2_POZ | | | | | |
|---|---|---|---|---|---|
| **Bond** | **Molecule** | **POZ isomers** | | | |
| | | | | | |
| | Thiophenol | endo_O_endo_H | endo_O_exo_H | exo_O_endo_H | exo_O_exo_H |
| $R_1$ (Å ) | 1.78928 | 1.84167 | 1.84067 | 1.85962 | 1.85883 |
| | Ozone | | | | |
| $R_2$ (Å ) | | 1.45075 | 1.44426 | 1.43334 | 1.42872 |

| | | | | | |
|---|---|---|---|---|---|
| $R_3$ (Å ) | 1.26405 | 1.44292 | 1.44507 | 1.45346 | 1.45278 |
| $R_4$ (Å ) | 1.26405 | 1.44326 | 1.44201 | 1.43745 | 1.43683 |
| $R_5$ (Å ) | | 1.44385 | 1.44564 | 1.43856 | 1.43855 |
| Θ (degrees) | 118 | 101.05 | 101 | 101.39 | 101.28 |
| Planarity | Planar | Planar | Non-Planar | Non-Planar | Non-Planar |

## Thiophenol POZ geometries and planarity in gas phase

| 2_3_POZ | | | | | |
|---|---|---|---|---|---|
| **Bond** | **Molecule** | **POZ isomers** | | | |
| | | | | | |
| | Thiophenol | endo_O_endo_H | endo_O_exo_H | exo_O_endo_H | exo_O_exo_H |
| $R_1$ (Å ) | 1.78928 | 1.78073 | 1.77748 | 1.77921 | 1.77481 |
| | Ozone | | | | |
| $R_2$ (Å ) | | 1.44017 | 1.43876 | 1.44509 | 1.44152 |
| $R_3$ (Å ) | 1.26405 | 1.44405 | 1.44357 | 1.45953 | 1.4445 |
| $R_4$ (Å ) | 1.26405 | 1.44042 | 1.4398 | 1.43054 | 1.44133 |
| $R_5$ (Å ) | | 1.45265 | 1.45012 | 1.44178 | 1.44194 |
| Θ (degrees) | 118 | 101.09 | 100.97 | 102.33 | 101.37 |
| Planarity | Planar | Non-Planar | Non-Planar | Non-Planar | Non-Planar |

## Thiophenol POZ geometries and planarity in gas phase

| 3_4_POZ | | | | | |
|---|---|---|---|---|---|
| **Bond** | **Molecule** | **POZ isomers** | | | |
| | | | | | |
| | Thiophenol | endo_O_endo_H | endo_O_exo_H | exo_O_endo_H | exo_O_exo_H |
| $R_1$ (Å ) | 1.78928 | 1.78244 | 1.78855 | 1.78063 | 1.78526 |
| | Ozone | | | | |
| $R_2$ (Å ) | | 1.44998 | 1.44728 | 1.44431 | 1.44328 |
| $R_3$ (Å ) | 1.26405 | 1.43993 | 1.44024 | 1.43718 | 1.43717 |
| $R_4$ (Å ) | 1.26405 | 1.44291 | 1.44326 | 1.45143 | 1.45159 |
| $R_5$ (Å ) | | 1.44502 | 1.44532 | 1.4446 | 1.44424 |
| Θ (degrees) | 118 | 101.16 | 101.17 | 101.66 | 101.71 |
| Planarity | Planar | Planar | Planar | Non-Planar | Non-Planar |
| | | | | | |

## Thiophenol POZ geometries and planarity in water

| 1_2_POZ | | | | | |
|---|---|---|---|---|---|
| **Bond** | **Molecule** | **POZ isomers** | | | |
| | | | | | |
| | Thiophenol | endo_O_endo_H | endo_O_exo_H | exo_O_endo_H | exo_O_exo_H |
| $R_1$ (Å ) | 1.79248 | 1.83852 | 1.83949 | 1.85693 | 1.85758 |

| | Ozone | | | | |
|---|---|---|---|---|---|
| $R_2$ (Å ) | | 1.45723 | 1.45237 | 1.4397 | 1.43604 |
| $R_3$ (Å ) | 1.26436 | 1.44313 | 1.44445 | 1.45484 | 1.45324 |
| $R_4$ (Å ) | 1.26436 | 1.44288 | 1.44344 | 1.43727 | 1.43753 |
| $R_5$ (Å ) | | 1.45034 | 1.45257 | 1.44449 | 1.44497 |
| Θ (degrees) | 118 | 101.01 | 100.99 | 101.35 | 101.25 |
| Planarity | Planar | Planar | Non-Planar | Non-Planar | Non-Planar |

## Thiophenol POZ geometries and planarity in water

| **2_3_POZ** | | | | | |
|---|---|---|---|---|---|
| **Bond** | **Molecule** | **POZ isomers** | | | |
| | | | | | |
| | Thiophenol | endo_O_endo_H | endo_O_exo_H | exo_O_endo_H | exo_O_exo_H |
| $R_1$ (Å ) | 1.79248 | 1.78324 | 1.78047 | 1.78034 | 1.77796 |
| | Ozone | | | | |
| $R_2$ (Å ) | | 1.44451 | 1.4462 | 1.44839 | 1.44986 |
| $R_3$ (Å ) | 1.26436 | 1.44374 | 1.44497 | 1.44382 | 1.44602 |
| $R_4$ (Å ) | 1.26436 | 1.44217 | 1.43962 | 1.44293 | 1.44117 |
| $R_5$ (Å ) | | 1.45959 | 1.45653 | 1.4498 | 1.44966 |
| Θ (degrees) | 118 | 101.1 | 101 | 101.5 | 101.42 |
| Planarity | Planar | Non-Planar | Non-Planar | Planar | Planar |

## Thiophenol POZ geometries and planarity in water

| **3_4_POZ** | | | | | |
|---|---|---|---|---|---|
| **Bond** | **Molecule** | **POZ isomers** | | | |
| | | | | | |
| | Thiophenol | endo_O_endo_H | endo_O_exo_H | exo_O_endo_H | exo_O_exo_H |
| $R_1$ (Å ) | 1.79248 | 1.78439 | 1.78886 | 1.78194 | 1.78559 |
| | Ozone | | | | |
| $R_2$ (Å ) | | 1.45751 | 1.45512 | 1.45272 | 1.45212 |
| $R_3$ (Å ) | 1.26436 | 1.4413 | 1.44157 | 1.43843 | 1.43879 |
| $R_4$ (Å ) | 1.26436 | 1.44334 | 1.44352 | 1.45128 | 1.45092 |
| $R_5$ (Å ) | | 1.45135 | 1.4517 | 1.45212 | 1.45228 |
| Θ (degrees) | 118 | 101.2 | 101.2 | 101.67 | 101.68 |
| Planarity | Planar | Planar | Planar | Non-Planar | Non-Planar |

## Catechol POZs

### Catechol POZ geometries and planarity in gas phase

| 1_2_POZ_endo_O | | | | | |
|---|---|---|---|---|---|
| **Bond** | **Molecule** | **POZ isomers** | | | |
| | Catechol | Structure 1 | Structure 2 | Structure 3 | |
| $R_1$ (Å ) | 1.37861 | 1.41618 | 1.37695 | 1.3851 | |
| $R_6$ (Å ) | 1.36359 | 1.37324 | 1.40941 | 1.385 | |
| | Ozone | | | | |
| $R_2$ (Å ) | | 1.42975 | 1.45812 | 1.45563 | |
| $R_3$ (Å ) | 1.26405 | 1.48176 | 1.43064 | 1.43752 | |
| $R_4$ (Å ) | 1.26405 | 1.41493 | 1.44714 | 1.43779 | |
| $R_5$ (Å ) | | 1.46253 | 1.43476 | 1.45548 | |
| Θ (degrees) | 118 | 103.08 | 102.36 | 101.91 | |
| Planarity | | Non-planar | Non-planar | Planar | |

### Catechol POZ geometries and planarity in gas phase

| 1_2_POZ_exo_O | | | | | |
|---|---|---|---|---|---|
| **Bond** | **Molecule** | **POZ isomers** | | | |
| | Catechol | Structure 4 | Structure 5 | Structure 6 | |
| $R_1$ (Å ) | 1.37861 | 1.38083 | 1.41964 | 1.39215 | |
| $R_6$ (Å ) | 1.36359 | 1.42098 | 1.38542 | 1.39215 | |
| | Ozone | | | | |
| $R_2$ (Å ) | | 1.44868 | 1.40837 | 1.43578 | |
| $R_3$ (Å ) | 1.26405 | 1.43626 | 1.45897 | 1.44666 | |
| $R_4$ (Å ) | 1.26405 | 1.46765 | 1.44042 | 1.44666 | |
| $R_5$ (Å ) | | 1.41525 | 1.43739 | 1.43578 | |
| Θ (degrees) | 118 | 100.91 | 100.94 | 100.32 | |
| Planarity | | Non-planar | Planar | Planar | |

### Catechol POZ geometries and planarity in gas phase

| 2_3_POZ_endo_O | | | | | |
|---|---|---|---|---|---|
| **Bond** | **Molecule** | **POZ isomers** | | | |
| | Catechol | Structure 7 | Structure 8 | Structure 9 | Structure10 |
| $R_1$ (Å ) | 1.37861 | 1.35118 | 1.36339 | 1.37432 | 1.35328 |
| $R_6$ (Å ) | 1.36359 | 1.40803 | 1.39003 | 1.38772 | 1.39106 |
| | Ozone | | | | |
| $R_2$ (Å ) | | 1.44433 | 1.45463 | 1.4624 | 1.45648 |
| $R_3$ (Å ) | 1.26405 | 1.47121 | 1.44832 | 1.43901 | 1.45295 |
| $R_4$ (Å ) | 1.26405 | 1.42764 | 1.43499 | 1.44648 | 1.43497 |
| $R_5$ (Å ) | | 1.44083 | 1.44128 | 1.44847 | 1.4408 |
| Θ (degrees) | 118 | 103.01 | 102.001 | 101.34 | 102.31 |
| Planarity | | Non-planar | Non-planar | Non-planar | Non-planar |

## Catechol POZ geometries and planarity in gas phase

| 2_3_POZ_exo_O | | | | | |
|---|---|---|---|---|---|
| **Bond** | **Molecule** | **POZ isomers** | | | |
| | Catechol | Structure 11 | Structure 12 | Structure 13 | Structure 14 |
| $R_1$ (Å ) | 1.37861 | 1.35288 | 1.3612 | 1.37151 | 1.35234 |
| $R_6$ (Å ) | 1.36359 | 1.40812 | 1.39754 | 1.39718 | 1.39618 |
| | Ozone | | | | |
| $R_2$ (Å ) | | 1.4296 | 1.42984 | 1.43734 | 1.43359 |
| $R_3$ (Å ) | 1.26405 | 1.45692 | 1.45686 | 1.46144 | 1.4577 |
| $R_4$ (Å ) | 1.26405 | 1.44036 | 1.43647 | 1.43428 | 1.4386 |
| $R_5$ (Å ) | | 1.45056 | 1.44144 | 1.4405 | 1.43816 |
| Θ (degrees) | 118 | 101.01 | 101 | 101.28 | 101.24 |
| Planarity | | Non-planar | Non-planar | Non-planar | Non-planar |

## Catechol POZ geometries and planarity in gas phase

| 3_4_POZ_endo_O | | | | | |
|---|---|---|---|---|---|
| **Bond** | **Molecule** | **POZ isomers** | | | |
| | Catechol | Structure 15 | Structure 16 | Structure 17 | |
| $R_1$ (Å ) | 1.37861 | 1.3611 | 1.39004 | 1.3695 | |
| $R_6$ (Å ) | 1.36359 | 1.38415 | 1.35717 | 1.36708 | |
| | Ozone | | | | |
| $R_2$ (Å ) | | 1.45244 | 1.44589 | 1.44734 | |
| $R_3$ (Å ) | 1.26405 | 1.44444 | 1.44311 | 1.44459 | |
| $R_4$ (Å ) | 1.26405 | 1.4408 | 1.44011 | 1.44254 | |
| $R_5$ (Å ) | | 1.45094 | 1.44526 | 1.45404 | |
| Θ (degrees) | 118 | 101.5 | 101.15 | 101.1 | |
| Planarity | | Non-planar | Non-planar | Non-planar | |

## Catechol POZ geometries and planarity in gas phase

| 3_4_POZ_exo_O | | | | | |
|---|---|---|---|---|---|
| **Bond** | **Molecule** | **POZ isomers** | | | |
| | Catechol | Structure 18 | Structure 19 | Structure 20 | Structure21 |
| $R_1$ (Å ) | 1.37861 | 1.36091 | 1.38641 | 1.3911 | 1.3759 |
| $R_6$ (Å ) | 1.36359 | 1.38502 | 1.35758 | 1.35494 | 1.35666 |
| | Ozone | | | | |
| $R_2$ (Å ) | | 1.45145 | 1.44258 | 1.44347 | 1.43358 |
| $R_3$ (Å ) | 1.26405 | 1.4465 | 1.4392 | 1.44359 | 1.50304 |
| $R_4$ (Å ) | 1.26405 | 1.43959 | 1.44726 | 1.44228 | 1.41672 |
| $R_5$ (Å ) | | 1.44285 | 1.44318 | 1.44237 | 1.45007 |
| Θ (degrees) | 118 | 101.43 | 101.46 | 101.47 | 104.39 |
| Planarity | | Non-planar | Non-planar | Non-planar | Non-planar |

## Catechol POZ geometries and planarity in gas phase

| 4_5_POZ_endo_O | | | | | |
|---|---|---|---|---|---|
| **Bond** | **Molecule** | **POZ isomers** | | | |
| | Catechol | Structure 22 | Structure23 | | |
| $R_1$ (Å ) | 1.37861 | 1.36864 | 1.3573 | | |
| $R_6$ (Å ) | 1.36359 | 1.35687 | 1.3573 | | |
| | Ozone | | | | |
| $R_2$ (Å ) | | 1.4526 | 1.45027 | | |
| $R_3$ (Å ) | 1.26405 | 1.43806 | 1.44087 | | |
| $R_4$ (Å ) | 1.26405 | 1.44348 | 1.44087 | | |
| $R_5$ (Å ) | | 1.44716 | 1.45027 | | |
| Θ (degrees) | 118 | 101.01 | 100.98 | | |
| Planarity | | Non-planar | Planar | | |

## Catechol POZ geometries and planarity in gas phase

| 4_5_POZ_exo_O | | | | | |
|---|---|---|---|---|---|
| **Bond** | **Molecule** | **POZ isomers** | | | |
| | Catechol | Structure 24 | Structure25 | | |
| $R_1$ (Å ) | 1.37861 | 1.35507 | 1.35641 | | |
| $R_6$ (Å ) | 1.36359 | 1.36852 | 1.35643 | | |
| | Ozone | | | | |
| $R_2$ (Å ) | | 1.44541 | 1.449 | | |
| $R_3$ (Å ) | 1.26405 | 1.44954 | 1.44359 | | |
| $R_4$ (Å ) | 1.26405 | 1.43812 | 1.44368 | | |
| $R_5$ (Å ) | | 1.44711 | 1.44686 | | |
| Θ (degrees) | 118 | 101.32 | 101.19 | | |
| Planarity | | Non-planar | Planar | | |

## Catechol POZs

## Catechol POZ geometries and planarity in water

| 1_2_POZ_endo_O | | | | | |
|---|---|---|---|---|---|
| **Bond** | **Molecule** | **POZ isomers** | | | |
| | Catechol | Structure 1 | Structure 2 | Structure 3 | |
| $R_1$ (Å ) | 1.37317 | 1.37445 | 1.37445 | 1.38356 | |
| $R_6$ (Å ) | 1.3669 | 1.40902 | 1.40902 | 1.38404 | |
| | | | | | |
| $R_2$ (Å ) | Ozone | 1.46706 | 1.46706 | 1.46526 | |
| $R_3$ (Å ) | 1.26436 | 1.41753 | 1.41753 | 1.43556 | |
| $R_4$ (Å ) | 1.26436 | 1.47458 | 1.47458 | 1.43997 | |
| $R_5$ (Å ) | | 1.43869 | 1.43869 | 1.46539 | |
| Θ (degrees) | | 103.1 | 103.1 | 101.94 | |
| Planarity | | Non-planar | Non-planar | Planar | |

## Catechol POZ geometries and planarity in water

| 1_2_POZ_exo_O | | | | | |
|---|---|---|---|---|---|
| **Bond** | **Molecule** | **POZ isomers** | | | |
| | Catechol | Structure 4 | Structure 5 | Structure 6 | |
| $R_1$ (Å ) | 1.37317 | 1.41057 | 1.38416 | 1.39066 | |
| $R_6$ (Å ) | 1.3669 | 1.38313 | 1.40127 | 1.39066 | |
| | | | | | |
| $R_2$ (Å ) | Ozone | 1.42403 | 1.44970 | 1.44416 | |
| $R_3$ (Å ) | 1.26436 | 1.45488 | 1.44246 | 1.44693 | |
| $R_4$ (Å ) | 1.26436 | 1.44368 | 1.45498 | 1.44693 | |
| $R_5$ (Å ) | | 1.44603 | 1.43027 | 1.44416 | |
| Θ (degrees) | | 100.8 | 100.53 | 100.4 | |
| Planarity | | Planar | Planar | Planar | |

## Catechol POZ geometries and planarity in water

| 2_3_POZ_endo_O | | | | | |
|---|---|---|---|---|---|
| **Bond** | **Molecule** | **POZ isomers** | | | |
| | Catechol | Structure 7 | Structure 8 | Structure 9 | Structure10 |
| $R_1$ (Å ) | 1.37317 | 1.35436 | 1.35987 | 1.37169 | 1.35508 |
| $R_6$ (Å ) | 1.3669 | 1.39768 | 1.38713 | 1.38533 | 1.38787 |
| | | | | | |
| $R_2$ (Å ) | Ozone | 1.45757 | 1.46842 | 1.46970 | 1.46727 |
| $R_3$ (Å ) | 1.26436 | 1.46265 | 1.44615 | 1.43557 | 1.44836 |
| $R_4$ (Å ) | 1.26436 | 1.43049 | 1.43751 | 1.44888 | 1.43711 |
| $R_5$ (Å ) | | 1.44449 | 1.44728 | 1.45288 | 1.44590 |
| Θ (degrees) | | 102.81 | 101.98 | 101.33 | 102.15 |
| Planarity | | Non-Planar | Non-Planar | Non-Planar | Non-Planar |

## Catechol POZ geometries and planarity in water

| 2_3_POZ_exo_O | | | | | |
|---|---|---|---|---|---|
| **Bond** | **Molecule** | **POZ isomers** | | | |
| | Catechol | Structure 11 | Structure 12 | Structure 13 | Structure 14 |
| $R_1$ (Å ) | 1.37317 | 1.35583 | 1.35756 | 1.36765 | 1.35358 |
| $R_6$ (Å ) | 1.3669 | 1.39985 | 1.39457 | 1.39493 | 1.39308 |
| | | | | | |
| $R_2$ (Å ) | Ozone | 1.43756 | 1.44068 | 1.44310 | 1.44337 |
| $R_3$ (Å ) | 1.26436 | 1.45579 | 1.45511 | 1.45848 | 1.45645 |
| $R_4$ (Å ) | 1.26436 | 1.43982 | 1.43932 | 1.43735 | 1.43995 |
| $R_5$ (Å ) | | 1.45259 | 1.44754 | 1.44512 | 1.44340 |
| Θ (degrees) | | 100.88 | 100.98 | 101.16 | 101.18 |
| Planarity | | Non-Planar | Non-Planar | Non-Planar | Non-Planar |

## Catechol POZ geometries and planarity in water

| 3_4_POZ_endo_O | | | | | |
|---|---|---|---|---|---|
| **Bond** | **Molecule** | **POZ isomers** | | | |
| | Catechol | Structure 15 | Structure 16 | Structure 17 | |
| $R_1$ (Å ) | 1.37317 | 1.36352 | 1.38132 | 1.37008 | |
| $R_6$ (Å ) | 1.3669 | 1.38205 | 1.36372 | 1.37194 | |
| | | | | | |
| $R_2$ (Å ) | Ozone | 1.45752 | 1.45428 | 1.452778 | |
| $R_3$ (Å ) | 1.26436 | 1.44233 | 1.44423 | 1.44347 | |
| $R_4$ (Å ) | 1.26436 | 1.44350 | 1.44076 | 1.44395 | |
| $R_5$ (Å ) | | 1.45572 | 1.45172 | 1.45966 | |
| Θ (degrees) | | 101.04 | 101.15 | 101.05 | |
| Planarity | | Planar | Planar | Non-Planar | |

## Catechol POZ geometries and planarity in water

| 3_4_POZ_exo_O | | | | | |
|---|---|---|---|---|---|
| **Bond** | **Molecule** | **POZ isomers** | | | |
| | Catechol | Structure 18 | Structure 19 | Structure 20 | Structure21 |
| $R_1$ (Å ) | 1.37317 | 1.36101 | 1.37969 | 138216 | 1.36989 |
| $R_6$ (Å ) | 1.3669 | 1.38344 | 1.36198 | 1.36099 | 1.37005 |
| | | | | | |
| $R_2$ (Å ) | Ozone | 1.45671 | 1.45274 | 1.45263 | 1.45551 |
| $R_3$ (Å ) | 1.26436 | 1.43924 | 1.44231 | 1.44460 | 1.44049 |
| $R_4$ (Å ) | 1.26436 | 1.44829 | 1.44564 | 1.44289 | 1.44757 |
| $R_5$ (Å ) | | 1.45073 | 1.45101 | 1.45020 | 1.45204 |
| Θ (degrees) | | 101.31 | 101.39 | 101.44993 | 101.25 |
| Planarity | | Planar | Planar | Planar | Planar |

## Catechol POZ geometries and planarity in water

| 4_5_POZ_endo_O | | | | | |
|---|---|---|---|---|---|
| **Bond** | **Molecule** | **POZ isomers** | | | |
| | Catechol | Structure 22 | Structure23 | | |
| $R_1$ (Å ) | 1.37317 | 1.36197 | 1.35759 | | |
| $R_6$ (Å ) | 1.3669 | 1.35709 | 1.35759 | | |
| | | | | | |
| $R_2$ (Å ) | Ozone | 1.45973 | 1.45810 | | |
| $R_3$ (Å ) | 1.26436 | 1.44065 | 1.44171 | | |
| $R_4$ (Å ) | 1.26436 | 1.44254 | 1.44171 | | |
| $R_5$ (Å ) | | 1.45646 | 1.45810 | | |
| Θ (degrees) | | 101.04 | 101.04 | | |
| Planarity | | Planar | Planar | | |

## Catechol POZ geometries and planarity in water

| 4_5_POZ_exo_O | | | | | |
|---|---|---|---|---|---|
| **Bond** | **Molecule** | **POZ isomers** | | | |
| | Catechol | Structure 24 | Structure25 | | |
| $R_1$ (Å ) | 1.37317 | 1.36084 | 1.35597 | | |
| $R_6$ (Å ) | 1.3669 | 1.35492 | 1.35597 | | |
| | | | | | |
| $R_2$ (Å ) | Ozone | 1.45612 | 1.45574 | | |
| $R_3$ (Å ) | 1.26436 | 1.44190 | 1.44449 | | |
| $R_4$ (Å ) | 1.26436 | 1.44699 | 1.44449 | | |
| $R_5$ (Å ) | | 1.45507 | 1.45573 | | |
| Θ (degrees) | | 101.24 | 101.2 | | |
| Planarity | | Planar | Planar | | |

## Resorcinol POZs

## Resorcinol POZ geometries and planarity in gas phase

| 1_2_POZ_endo_O | | | | | |
|---|---|---|---|---|---|
| **Bond** | **Molecule** | **POZ isomers** | | | |
| | Resorcinol | Structure 1 | Structure 2 | Structure 3 | Structure 4 |
| $R_1$ (Å ) | 1.36712 | 1.39351 | 1.39423 | 1.393875 | 1.397 |
| $R_6$ (Å ) | 1.36643 | 1.35657 | 1.356852 | 1.35679 | 1.35789 |
| | Ozone | | | | |
| $R_2$ (Å ) | | 1.47426 | 1.46065 | 1.46819 | 1.4665 |
| $R_3$ (Å ) | 1.26405 | 1.44858 | 1.42862 | 1.44079 | 1.442 |
| $R_4$ (Å ) | 1.26405 | 1.45101 | 1.45357 | 1.44374 | 1.4488 |
| $R_5$ (Å ) | | 1.43351 | 1.43639 | 1.43186 | 1.43485 |
| Θ (degrees) | 118 | 102.84 | 101.5 | 102.03 | 102.16 |
| Planarity | Planar | Non-planar | Non-planar | Non-planar | Non-planar |

## Resorcinol POZ geometries and planarity in gas phase

| 1_2_POZ_exo_O | | | | | |
|---|---|---|---|---|---|
| **Bond** | **Molecule** | **POZ isomers** | | | |
| | Resorcinol | Structure 5 | Structure 6 | Structure 7 | Structure 8 |
| $R_1$ (Å ) | 1.36712 | 1.38556 | 1.40319 | 1.39735 | 1.4025 |
| $R_6$ (Å ) | 1.36643 | 1.35254 | 1.35712 | 1.35708 | 1.36099 |
| | Ozone | | | | |
| $R_2$ (Å ) | | 1.46165 | 1.43246 | 1.438 | 1.43507 |
| $R_3$ (Å ) | 1.26405 | 1.41901 | 1.45572 | 1.45127 | 1.45151 |
| $R_4$ (Å ) | 1.26405 | 1.51976 | 1.43802 | 1.4449 | 1.44264 |
| $R_5$ (Å ) | | 1.42583 | 1.43643 | 1.43959 | 1.43998 |
| Θ (degrees) | 118 | 104.45 | 101.03 | 101.21 | 100.83 |
| Planarity | Planar | Non-planar | Non-planar | Non-planar | Non-planar |

## Resorcinol POZ geometries and planarity in gas phase

| 3_4_POZ_endo_O | | | | | |
|---|---|---|---|---|---|
| **Bond** | **Molecule** | **POZ isomers** | | | |
| | Resorcinol | Structure 9 | Structure 10 | Structure 11 | Structure 12 |
| $R_1$ (Å ) | 1.36712 | 1.36126 | 1.36437 | 1.36159 | 1.36423 |
| $R_6$ (Å ) | 1.36643 | 1.397 | 1.3965 | 1.39704 | 1.39621 |
| | Ozone | | | | |
| $R_2$ (Å ) | | 1.47259 | 1.46456 | 1.46283 | 1.47484 |
| $R_3$ (Å ) | 1.26405 | 1.44131 | 1.42831 | 1.43052 | 1.44005 |
| $R_4$ (Å ) | 1.26405 | 1.44464 | 1.45331 | 1.45105 | 1.44604 |
| $R_5$ (Å ) | | 1.43573 | 1.43903 | 1.44039 | 1.43468 |
| Θ (degrees) | 118 | 102.08 | 101.46 | 101.42 | 102.14 |
| Planarity | Planar | Non-planar | Non-planar | Planar | Non-planar |

## Resorcinol POZ geometries and planarity in gas phase

| 3_4_POZ_exo_O | | | | | |
|---|---|---|---|---|---|
| **Bond** | **Molecule** | **POZ isomers** | | | |
| | Resorcinol | Structure 13 | Structure 14 | Structure 15 | Structure 16 |
| $R_1$ (Å ) | 1.36712 | 1.36005 | 1.36498 | 1.36227 | 1.36268 |
| $R_6$ (Å ) | 1.36643 | 1.39988 | 1.40457 | 1.40517 | 1.39877 |
| | | | | | |
| | Ozone | 1.4428 | 1.43647 | 1.43499 | 1.44432 |
| $R_2$ (Å ) | | 1.44836 | 1.45231 | 1.45449 | 1.44619 |
| $R_3$ (Å ) | 1.26405 | 1.44965 | 1.4421 | 1.44025 | 1.45261 |
| $R_4$ (Å ) | 1.26405 | 1.44235 | 1.4378 | 1.43865 | 1.44221 |
| $R_5$ (Å ) | | 1.36005 | 1.36498 | 1.36227 | 1.36268 |
| Θ (degrees) | 118 | 101.22 | 100.95 | 100.9 | 101.33 |
| Planarity | Planar | Non-planar | Planar | Planar | Non-planar |

## Resorcinol POZ geometries and planarity in gas phase

| 4_5_POZ_endo_O | | | | | |
|---|---|---|---|---|---|
| **Bond** | **Molecule** | **POZ isomers** | | | |
| | Resorcinol | Structure 17 | Structure 18 | Structure 19 | Structure 20 |
| $R_1$ (Å ) | 1.36712 | 1.36342 | 1.36348 | 1.36639 | 1.36086 |
| $R_6$ (Å ) | 1.36643 | 1.35424 | 1.35633 | 1.35567 | 1.35587 |
| | Ozone | | | | |
| $R_2$ (Å ) | | 1.43209 | 1.43975 | 1.43857 | 1.43367 |
| $R_3$ (Å ) | 1.26405 | 1.45949 | 1.44877 | 1.45072 | 1.45699 |
| $R_4$ (Å ) | 1.26405 | 1.43538 | 1.43369 | 1.43186 | 1.43659 |
| $R_5$ (Å ) | | 1.47522 | 1.45408 | 1.45557 | 1.47212 |
| Θ (degrees) | 118 | 101.61 | 101.06 | 101.08 | 101.48 |
| Planarity | Planar | Non-planar | Planar | Planar | Non-planar |

## Resorcinol POZ geometries and planarity in gas phase

| 4_5_POZ_exo_O | | | | | |
|---|---|---|---|---|---|
| **Bond** | **Molecule** | **POZ isomers** | | | |
| | Resorcinol | Structure 21 | Structure 22 | Structure 23 | Structure 24 |
| $R_1$ (Å ) | 1.36712 | 1.36086 | 1.361 | 1.36328 | 1.35755 |
| $R_6$ (Å ) | 1.36643 | 1.35587 | 1.35345 | 1.35239 | 1.34954 |
| | Ozone | | | | |
| $R_2$ (Å ) | | 1.43367 | 1.43996 | 1.43849 | 1.42416 |
| $R_3$ (Å ) | 1.26405 | 1.45699 | 1.46099 | 1.46624 | 1.51761 |
| $R_4$ (Å ) | 1.26405 | 1.43659 | 1.43011 | 1.4271 | 1.41105 |
| $R_5$ (Å ) | | 1.47212 | 1.44858 | 1.44966 | 1.46247 |
| Θ (degrees) | 118 | 101.48 | 101.89 | 102.1 | 104.33 |
| Planarity | Planar | Non-planar | Non-planar | Non-planar | Non-planar |

## Resorcinol POZ geometries and planarity in water

| 1_2_POZ_endo_O | | | | | |
|---|---|---|---|---|---|
| **Bond** | **Molecule** | **POZ isomers** | | | |
| | Resorcinol | Structure 1 | Structure 2 | Structure 3 | Structure 4 |
| $R_1$ (Å ) | 1.36653 | 1.39030 | 1.39059 | 1.38993 | 1.39212 |
| $R_6$ (Å ) | 1.36647 | 1.35573 | 1.35615 | 1.3555 | 1.35782 |
| | Ozone | | | | |
| $R_2$ (Å ) | | 1.48153 | 1.47483 | 1.47856 | 1.48005 |
| $R_3$ (Å ) | 1.26436 | 1.45014 | 1.42786 | 1.43651 | 1.44122 |
| $R_4$ (Å ) | 1.26436 | 1.44718 | 1.45445 | 1.44689 | 1.44826 |
| $R_5$ (Å ) | | 1.43481 | 1.44127 | 1.437 | 1.43751 |
| Θ (degrees) | 117.75 | 102.8 | 101.53 | 101.91 | 102.05 |
| Planarity | Planar | Non-planar | Planar | Non-planar | Non-planar |

## Resorcinol POZ geometries and planarity in water

| 1_2_POZ_exo_O | | | | | |
|---|---|---|---|---|---|
| **Bond** | **Molecule** | **POZ isomers** | | | |
| | Resorcinol | Structure 5 | Structure 6 | Structure 7 | Structure 8 |
| $R_1$ (Å ) | 1.36653 | 1.38424 | 1.39882 | 1.39507 | 1.39807 |
| $R_6$ (Å ) | 1.36647 | 1.35258 | 1.35598 | 1.35537 | 1.35899 |
| | Ozone | | | | |
| $R_2$ (Å ) | | 1.46582 | 1.44362 | 1.44579 | 1.44454 |
| $R_3$ (Å ) | 1.26436 | 1.42241 | 1.45337 | 1.45246 | 1.45216 |
| $R_4$ (Å ) | 1.26436 | 1.51352 | 1.44097 | 1.44371 | 1.44214 |
| $R_5$ (Å ) | | 1.42863 | 1.44275 | 1.44407 | 1.44385 |
| Θ (degrees) | 117.75 | 104.6 | 101.00 | 101.059 | 100.85 |
| Planarity | Planar | Non-planar | Planar | Planar | Planar |

**Resorcinol POZ geometries and planarity in water**

| 3_4_POZ_endo_O | | | | | |
|---|---|---|---|---|---|
| **Bond** | **Molecule** | **POZ isomers** | | | |
| | Resorcinol | Structure 9 | Structure 10 | Structure 11 | Structure 12 |
| $R_1$ (Å ) | 1.36653 | 1.35881 | 1.36066 | 1.35875 | 1.36075 |
| $R_6$ (Å ) | 1.36647 | 1.39350 | 1.39382 | 1.39370 | 1.39346 |
| | Ozone | | | | |
| $R_2$ (Å ) | | 1.48361 | 1.47946 | 1.47783 | 1.48509 |
| $R_3$ (Å ) | 1.26436 | 1.43756 | 1.42851 | 1.42859 | 1.43721 |
| $R_4$ (Å ) | 1.26436 | 1.44656 | 1.45317 | 1.45325 | 1.44694 |
| $R_5$ (Å ) | | 1.44065 | 1.44470 | 1.44544 | 1.44017 |
| Θ (degrees) | 117.75 | 101.96 | 101.5 | 101.46 | 101.99 |
| Planarity | Planar | Non-Planar | Planar | Planar | Non-Planar |
| | | | | | |

**Resorcinol POZ geometries and planarity in water**

| 3_4_POZ_exo_O | | | | | |
|---|---|---|---|---|---|
| **Bond** | **Molecule** | **POZ isomers** | | | |
| | Resorcinol | Structure 13 | Structure 14 | Structure 15 | Structure 16 |
| $R_1$ (Å ) | 1.36653 | 1.35758 | 1.36070 | 1.35902 | 1.35927 |
| $R_6$ (Å ) | 1.36647 | 1.39839 | 1.40125 | 1.40117 | 1.39833 |
| | Ozone | | | | |
| $R_2$ (Å ) | | 1.45050 | 1.44836 | 1.44759 | 1.45133 |
| $R_3$ (Å ) | 1.26436 | 1.45057 | 1.45108 | 1.45172 | 1.44998 |
| $R_4$ (Å ) | 1.26436 | 1.44685 | 1.44419 | 1.44363 | 1.44758 |
| $R_5$ (Å ) | | 1.44595 | 1.44424 | 1.44431 | 1.44599 |
| Θ (degrees) | 117.75 | 100.98 | 100.94 | 100.92 | 101.01 |
| Planarity | Planar | Planar | Planar | Planar | Planar |

**Resorcinol POZ geometries and planarity in water**

| 4_5_POZ_endo_O | | | | | |
|---|---|---|---|---|---|
| **Bond** | **Molecule** | **POZ isomers** | | | |
| | Resorcinol | Structure 17 | Structure 18 | Structure 19 | Structure 20 |
| $R_1$ (Å ) | 1.36653 | 1.36208 | 1.36206 | 1.363778 | 1.36041 |
| $R_6$ (Å ) | 1.36647 | 1.35374 | 1.35482 | 1.35363 | 1.35532 |
| | Ozone | | | | |
| $R_2$ (Å ) | | 1.43558 | 1.44476 | 1.44428 | 1.43649 |
| $R_3$ (Å ) | 1.26436 | 1.45381 | 1.44904 | 1.44964 | 1.45298 |
| $R_4$ (Å ) | 1.26436 | 1.44009 | 1.43514 | 1.43442 | 1.44031 |
| $R_5$ (Å ) | | 1.48323 | 1.46546 | 1.46679 | 1.48088 |
| Θ (degrees) | 117.75 | 101.58 | 101.07 | 101.08 | 101.5 |
| Planarity | Planar | Non-planar | Planar | Planar | Non-planar |

## Resorcinol POZ geometries and planarity in water

| 4_5_POZ_exo_O | | | | | |
|---|---|---|---|---|---|
| **Bond** | **Molecule** | **POZ isomers** | | | |
| | Resorcinol | Structure 21 | Structure 22 | Structure 23 | Structure 24 |
| $R_1$ (Å ) | 1.36653 | 1.35803 | 1.35858 | 1.36010 | 1.35637 |
| $R_6$ (Å ) | 1.36647 | 1.34902 | 1.35240 | 1.35104 | 1.35060 |
| | Ozone | | | | |
| $R_2$ (Å ) | | 1.42600 | 1.44729 | 1.44654 | 1.42721 |
| $R_3$ (Å ) | 1.26436 | 1.51757 | 1.46442 | 1.46668 | 1.51593 |
| $R_4$ (Å ) | 1.26436 | 1.41331 | 1.42980 | 1.42866 | 1.41371 |
| $R_5$ (Å ) | | 1.47126 | 1.45901 | 1.46001 | 1.46993 |
| Θ (degrees) | 117.75 | 104.52 | 102.05 | 102.15 | 104.5 |
| Planarity | Planar | Non-Planar | Non-Planar | Non-Planar | Non-Planar |

## APPENDIX F

## Mulliken charges

## Phenol POZs

## Phenol POZ Mulliken charge in gas phase

| 1_2_POZ | | | | | |
|---|---|---|---|---|---|
| **Atom** | **Molecule** | **POZ isomers** | | | |
| | Phenol | endo_O_endo_H | endo_O_exo_H | exo_O_endo_H | exo_O_exo_H |
| **$O_1$** | -0.558 | -0.536 | -0.531 | -0.534 | -0.526 |
| **$C_1$** | 0.326 | 0.455 | 0.461 | 0.434 | 0.442 |
| | Ozone | | | | |
| **$O_2$** | -0.116 | -0.294 | -0.29 | -0.277 | -0.291 |
| **$O_3$** | 0.231 | -0.054 | -0.06 | -0.082 | -0.064 |
| **$O_4$** | -0.116 | -0.278 | -0.272 | -0.268 | -0.268 |

## Phenol POZ Mulliken charge in gas phase

| 2_3_POZ | | | | | |
|---|---|---|---|---|---|
| **Atom** | **Molecule** | **POZ isomers** | | | |
| | Phenol | endo_O_endo_H | endo_O_exo_H | exo_O_endo_H | exo_O_exo_H |
| **$O_1$** | -0.558 | -0.542 | -0.529 | -0.534 | -0.524 |
| **$C_1$** | 0.326 | 0.371 | 0.347 | 0.353 | 0.338 |
| | Ozone | | | | |
| **$O_2$** | -0.116 | -0.288 | -0.265 | -0.33 | -0.27 |
| **$O_3$** | 0.231 | -0.058 | -0.064 | -0.05 | -0.067 |
| **$O_4$** | -0.116 | -0.268 | -0.269 | -0.247 | -0.266 |

## Phenol POZ Mulliken charge in gas phase

| 3_4_POZ | | | | | |
|---|---|---|---|---|---|
| **Atom** | **Molecule** | **POZ isomers** | | | |
| | Phenol | endo_O_endo_H | endo_O_exo_H | exo_O_endo_H | exo_O_exo_H |
| **$O_1$** | -0.558 | -0.549 | -0.55 | -0.544 | -0.545 |
| **$C_1$** | 0.326 | 0.346 | 0.351 | 0.355 | 0.361 |
| | Ozone | | | | |
| **$O_2$** | -0.116 | -0.271 | -0.264 | -0.264 | -0.259 |
| **$O_3$** | 0.231 | -0.065 | -0.065 | -0.068 | -0.067 |
| **$O_4$** | -0.116 | -0.272 | -0.273 | -0.286 | -0.29 |

## Phenol POZ Mulliken charge in water

| 1_2_POZ | | | | | |
|---|---|---|---|---|---|
| **Atom** | **Molecule** | **POZ isomers** | | | |
| | Phenol_water | endo_O_endo_H | endo_O_exo_H | exo_O_endo_H | exo_O_exo_H |
| **$O_1$** | -0.583 | -0.552 | -0.553 | -0.55 | -0.548 |
| **$C_1$** | 0.323 | 0.462 | 0.465 | 0.445 | 0.451 |
| | Ozone_water | | | | |
| **$O_2$** | -0.125 | -0.307 | -0.307 | -0.302 | -0.304 |
| **$O_3$** | 0.249 | -0.079 | -0.081 | -0.09 | -0.088 |
| **$O_4$** | -0.125 | -0.288 | -0.29 | -0.285 | -0.287 |

## Phenol POZ Mulliken charge in water

| 2_3_POZ | | | | | |
|---|---|---|---|---|---|
| **Atom** | **Molecule** | **POZ isomers** | | | |
| | Phenol | endo_O_endo_H | endo_O_exo_H | exo_O_endo_H | exo_O_exo_H |
| **$O_1$** | -0.602 | -0.555 | -0.554 | -0.549 | -0.55 |
| **$C_1$** | 0.318 | 0.377 | 0.35 | 0.357 | 0.343 |
| | Ozone | | | | |
| **$O_2$** | -0.128 | -0.286 | -0.287 | -0.329 | -0.297 |
| **$O_3$** | 0.256 | -0.082 | -0.086 | -0.074 | -0.085 |
| **$O_4$** | -0.128 | -0.287 | -0.288 | -0.27 | -0.286 |

## Phenol POZ Mulliken charge in water

| 3_4_POZ | | | | | |
|---|---|---|---|---|---|
| **Atom** | **Molecule** | **POZ isomers** | | | |
| | Phenol | endo_O_endo_H | endo_O_exo_H | exo_O_endo_H | exo_O_exo_H |

| | | | | | |
|---|---|---|---|---|---|
| **$O_1$** | -0.602 | -0.569 | -0.573 | -0.563 | -0.567 |
| **$C_1$** | 0.318 | 0.344 | 0.352 | 0.355 | 0.363 |
| | Ozone | | | | |
| **$O_2$** | -0.128 | -0.293 | -0.393 | -0.286 | -0.285 |
| **$O_3$** | 0.256 | -0.09 | -0.089 | -0.089 | -0.089 |
| **$O_4$** | -0.128 | -0.291 | -0.29 | -0.308 | -0.309 |

## Thiophenol POZs

### Thiophenol POZ Mulliken charge in gas phase

| **1_2_POZ** | | | | | |
|---|---|---|---|---|---|
| **Atom** | **Molecule** | **POZ isomers** | | | |
| | Thiophenol | endo_O_endo_H | endo_O_exo_H | exo_O_endo_H | exo_O_exo_H |
| **S** | 0.012 | 0.008 | 0.027 | -0.013 | 0 |
| **$C_1$** | -0.086 | 0.045 | 0.042 | 0.069 | 0.072 |
| | Ozone | | | | |
| **$O_1$** | -0.116 | -0.271 | -0.266 | -0.262 | -0.263 |
| **$O_2$** | 0.231 | -0.061 | -0.061 | -0.063 | -0.053 |
| **$O_3$** | -0.116 | -0.253 | -0.252 | -0.257 | -0.259 |

### Thiophenol POZ Mulliken charge in gas phase

| **2_3_POZ** | | | | | |
|---|---|---|---|---|---|
| **Atom** | **Molecule** | **POZ isomers** | | | |
| | Thiophenol | endo_O_endo_H | endo_O_exo_H | exo_O_endo_H | exo_O_exo_H |
| **S** | 0.012 | 0.001 | 0.049 | 0.014 | 0.054 |
| **$C_1$** | -0.086 | -0.085 | -0.081 | -0.091 | -0.093 |
| | Ozone | | | | |
| **$O_1$** | -0.116 | -0.268 | -0.269 | -0.258 | -0.0267 |
| **$O_2$** | 0.231 | -0.059 | -0.059 | -0.057 | -0.064 |
| **$O_3$** | -0.116 | -0.275 | -0.0263 | -0.299 | -0.0267 |

### Thiophenol POZ Mulliken charge in gas phase

| **3_4_POZ** | | | | | |
|---|---|---|---|---|---|
| **Atom** | **Molecule** | **POZ isomers** | | | |
| | Thiophenol | endo_O_endo_H | endo_O_exo_H | exo_O_endo_H | exo_O_exo_H |
| **S** | 0.012 | 0.029 | 0.015 | 0.035 | 0.03 |
| **$C_1$** | -0.086 | -0.071 | -0.078 | -0.065 | -0.077 |
| | Ozone | | | | |
| **$O_1$** | -0.116 | -0.27 | -0.27 | -0.28 | -0.28 |
| **$O_2$** | 0.231 | -0.062 | -0.062 | -0.066 | -0.065 |

| | | | | | |
|---|---|---|---|---|---|
| **$O_3$** | -0.116 | -0.269 | -0.267 | -0.265 | -0.263 |

## Thiophenol POZ Mulliken charge in water

| **1_2_POZ** | | | | | |
|---|---|---|---|---|---|
| **Atom** | **Molecule** | **POZ isomers** | | | |
| | Thiophenol | endo_O_endo_H | endo_O_exo_H | exo_O_endo_H | exo_O_exo_H |
| **S** | -0.038 | -0.015 | -0.008 | -0.043 | -0.041 |
| **$C_1$** | -0.099 | 0.0453 | 0.043 | 0.073 | 0.073 |
| | Ozone | | | | |
| **$O_1$** | -0.125 | -0.269 | -0.268 | -0.276 | -0.273 |
| **$O_2$** | 0.249 | -0.081 | -0.081 | -0.076 | -0.074 |
| **$O_3$** | -0.125 | -0.284 | -0.283 | -0.278 | -0.278 |

## Thiophenol POZ Mulliken charge in water

| **2_3_POZ** | | | | | |
|---|---|---|---|---|---|
| **Atom** | **Molecule** | **POZ isomers** | | | |
| | Thiophenol | endo_O_endo_H | endo_O_exo_H | exo_O_endo_H | exo_O_exo_H |
| **S** | -0.038 | -0.029 | -0.004 | -0.001 | -0.011 |
| **$C_1$** | -0.099 | -0.086 | -0.088 | -0.102 | -0.101 |
| | Ozone | | | | |
| **$O_1$** | -0.125 | -0.285 | -0.282 | -0.286 | -0.291 |
| **$O_2$** | 0.249 | -0.081 | -0.082 | -0.081 | -0.081 |
| **$O_3$** | -0.125 | -0.287 | -0.286 | -0.29 | -0.287 |

## Thiophenol POZ Mulliken charge in water

| **3_4_POZ** | | | | | |
|---|---|---|---|---|---|
| **Atom** | **Molecule** | **POZ isomers** | | | |
| | Thiophenol | endo_O_endo_H | endo_O_exo_H | exo_O_endo_H | exo_O_exo_H |
| **S** | -0.038 | -0.013 | -0.021 | -0.003 | -0.009 |
| **$C_1$** | -0.099 | -0.082 | -0.085 | -0.075 | -0.077 |
| | Ozone | | | | |
| **$O_1$** | -0.125 | -0.0288 | -0.287 | -0.287 | -0.286 |
| **$O_2$** | 0.249 | -0.086 | -0.086 | -0.085 | -0.084 |
| **$O_3$** | -0.125 | -0.288 | -0.288 | -0.3 | -0.3 |

## Catechol POZs

### Catechol POZ Mulliken charge in gas phase

| 1_2_POZ_endo_O | | | | | |
|---|---|---|---|---|---|
| **Atom** | **Molecule** | **POZ isomers** | | | |
| | Catechol | Structure 1 | Structure 2 | Structure 3 | |
| **$O_1$** | -0.595 | -0.558 | -0.534 | -0.511 | |
| **$C_1$** | 0.287 | 0.447 | 0.442 | 0.465 | |
| **$O_2$** | -0.568 | -0.526 | -0.558 | -0.511 | |
| **$C_2$** | 0.313 | 0.432 | 0.493 | 0.465 | |
| | Ozone | | | | |
| **$O_3$** | -0.116 | -0.311 | -0.283 | -0.288 | |
| **$O_4$** | 0.231 | -0.05 | -0.06 | -0.063 | |
| **$O_5$** | -0.116 | -0.282 | -0.284 | -0.288 | |

### Catechol POZ Mulliken charge in gas phase

| 1_2_POZ_exo_O | | | | | |
|---|---|---|---|---|---|
| **Atom** | **Molecule** | **POZ isomers** | | | |
| | Catechol | Structure 4 | Structure 5 | Structure 6 | |
| **$O_1$** | -0.595 | -0.553 | -0.532 | -0.506 | |
| **$C_1$** | 0.287 | 0.48 | 0.445 | 0.444 | |
| **$O_2$** | -0.568 | -0.536 | -0.562 | -0.506 | |
| **$C_2$** | 0.313 | 0.433 | 0.428 | 0.444 | |
| | Ozone | | | | |
| **$O_3$** | -0.116 | -0.279 | -0.273 | -0.287 | |
| **$O_4$** | 0.231 | -0.07 | -0.083 | -0.061 | |
| **$O_5$** | -0.116 | -0.274 | -0.284 | -0.287 | |

### Catechol POZ Mulliken charge in gas phase

| 2_3_POZ_endo_O | | | | | |
|---|---|---|---|---|---|
| **Atom** | **Molecule** | **POZ isomers** | | | |
| | Catechol | Structure 7 | Structure 8 | Structure 9 | Structure 10 |
| **$O_1$** | -0.568 | -0.541 | -0.556 | -0.566 | -0.518 |
| **$C_1$** | 0.313 | 0.384 | 0.356 | 0.352 | 0.366 |
| **$O_2$** | -0.595 | -0.0554 | -0.533 | -0.525 | -0.524 |
| **$C_2$** | 0.287 | 0.406 | 0.453 | 0.425 | 0.45 |
| | Ozone | | | | |
| **$O_3$** | -0.116 | -0.294 | -0.284 | -0.3 | -0.289 |
| **$O_4$** | 0.231 | -0.043 | -0.058 | -0.061 | -0.053 |

| | | | | | |
|---|---|---|---|---|---|
| **$O_5$** | -0.116 | -0.275 | -0.268 | -0.272 | -0.277 |

## Catechol POZ Mulliken charge in gas phase

| **2_3_POZ_exo_O** | | | | | |
|---|---|---|---|---|---|
| **Atom** | **Molecule** | **POZ isomers** | | | |
| | Catechol | Structure 11 | Structure 12 | Structure 13 | Structure 14 |
| **$O_1$** | -0.568 | -0.539 | -0.546 | -0.536 | -0.518 |
| **$C_1$** | 0.313 | 0.389 | 0.355 | 0.364 | 0.377 |
| **$O_2$** | -0.595 | -0.551 | -0.529 | -0.548 | -0.523 |
| **$C_2$** | 0.287 | 0.383 | 0.443 | 0.429 | 0.437 |
| | Ozone | | | | |
| **$O_3$** | -0.116 | -0.266 | -0.283 | -0.275 | -0.277 |
| **$O_4$** | 0.231 | -0.083 | -0.065 | -0.058 | -0.079 |
| **$O_5$** | -0.116 | -0.265 | -0.267 | -0.261 | -0.261 |

## Catechol POZ Mulliken charge in gas phase

| **3_4_POZ_endo_O** | | | | | |
|---|---|---|---|---|---|
| **Atom** | **Molecule** | **POZ isomers** | | | |
| | Catechol | Structure 15 | Structure 16 | Structure 17 | |
| **$O_1$** | -0.568 | -0.561 | -0.596 | -0.552 | |
| **$C_1$** | 0.313 | 0.305 | 0.249 | 0.295 | |
| **$O_2$** | -0.595 | -0.586 | -0.54 | -0.547 | |
| **$C_2$** | 0.287 | 0.272 | 0.316 | 0.315 | |
| | Ozone | | | | |
| **$O_3$** | -0.116 | -0.283 | -0.26 | -0.282 | |
| **$O_4$** | 0.231 | -0.061 | -0.066 | -0.059 | |
| **$O_5$** | -0.116 | -0.268 | -0.27 | -0.27 | |

## Catechol POZ Mulliken charge in gas phase

| **3_4_POZ_exo_O** | | | | | |
|---|---|---|---|---|---|
| **Atom** | **Molecule** | **POZ isomers** | | | |
| | Catechol | Structure 18 | Structure 19 | Structure 20 | Structure 21 |
| **$O_1$** | -0.568 | -0.56 | -0.592 | -0.595 | -0.562 |
| **$C_1$** | 0.313 | 0.305 | 0.263 | 0.246 | 0.287 |
| **$O_2$** | -0.595 | -0.584 | -0.538 | -0.535 | -0.534 |
| **$C_2$** | 0.287 | 0.253 | 0.291 | 0.304 | 0.306 |
| | Ozone | | | | |
| **$O_3$** | -0.116 | -0.295 | -0.26 | -0.265 | -0.326 |
| **$O_4$** | 0.231 | -0.062 | -0.067 | -0.066 | -0.05 |
| **$O_5$** | -0.116 | -0.265 | -0.274 | -0.27 | -0.25 |

## Catechol POZ Mulliken charge in gas phase

| 4_5_POZ_endo_O | | | | | |
|---|---|---|---|---|---|
| **Atom** | **Molecule** | **POZ isomers** | | | |
| | Catechol | Structure 22 | Structure 23 | | |
| **$O_1$** | -0.568 | -0.556 | -0.534 | | |
| **$C_1$** | 0.313 | 0.351 | 0.349 | | |
| **$O_2$** | -0.595 | -0.583 | -0.534 | | |
| **$C_2$** | 0.287 | 0.335 | 0.349 | | |
| | Ozone | | | | |
| **$O_3$** | -0.116 | -0.274 | -0.272 | | |
| **$O_4$** | 0.231 | -0.067 | -0.067 | | |
| **$O_5$** | -0.116 | -0.269 | -0.272 | | |

## Catechol POZ Mulliken charge in gas phase

| 4_5_POZ_exo_O | | | | | |
|---|---|---|---|---|---|
| **Atom** | **Molecule** | **POZ isomers** | | | |
| | Catechol | Structure 24 | Structure 25 | | |
| **$O_1$** | -0.568 | -0.582 | -0.532 | | |
| **$C_1$** | 0.313 | 0.335 | 0.352 | | |
| **$O_2$** | -0.595 | -0.553 | -0.532 | | |
| **$C_2$** | 0.287 | 0.357 | 0.352 | | |
| | Ozone | | | | |
| **$O_3$** | -0.116 | -0.266 | -0.274 | | |
| **$O_4$** | 0.231 | -0.071 | -0.072 | | |
| **$O_5$** | -0.116 | -0.288 | -0.274 | | |

## Catechol POZ Mulliken charge in water

| 1_2_POZ_endo_O | | | | | |
|---|---|---|---|---|---|
| **Atom** | **Molecule** | **POZ isomers** | | | |
| | Catechol | Structure 1 | Structure 2 | Structure 3 | |
| **$O_1$** | -0.60000 | -0.544774 | -0.544774 | -0.541353 | |
| **$C_1$** | 0.286505 | 0.438084 | 0.438084 | 0.467233 | |
| **$O_2$** | -0.588007 | -0.563440 | -0.563440 | -0.541378 | |
| **$C_2$** | 0.301226 | 0.456088 | 0.456088 | 0.466280 | |
| | Ozone | | | | |
| **$O_3$** | -0.125 | -0.294369 | -0.294369 | -0.304926 | |
| **$O_4$** | 0.249 | -0.067837 | -0.067837 | -0.082447 | |
| **$O_5$** | -0.125 | -0.317330 | -0.317330 | -0.307298 | |

## Catechol POZ Mulliken charge in water

| 1_2_POZ_exo_O | | | | | |
|---|---|---|---|---|---|
| **Atom** | **Molecule** | **POZ isomers** | | | |
| | Catechol | Structure 4 | Structure 5 | Structure 6 | |
| **$O_1$** | -0.60000 | -0.573002 | -0.555274 | -0.536891 | |
| **$C_1$** | 0.286505 | 0.480124 | 0.449814 | 0.449057 | |
| **$O_2$** | -0.588007 | -0.560348 | -0.565416 | -0.536891 | |
| **$C_2$** | 0.301226 | 0.446810 | 0.444146 | 0.449057 | |
| | Ozone | | | | |
| **$O_3$** | -0.124633 | -0.292700 | -0.295526 | -0.297582 | |
| **$O_4$** | 0.249265 | -0.089421 | -0.089333 | -0.088413 | |
| **$O_5$** | -0.124633 | -0.297251 | -0.296140 | -0.297582 | |

## Catechol POZ Mulliken charge in water

| 2_3_POZ_endo_O | | | | | |
|---|---|---|---|---|---|
| **Atom** | **Molecule** | **POZ isomers** | | | |
| | Catechol | Structure 7 | Structure 8 | Structure 9 | Structure 10 |
| **$O_1$** | -0.60000 | -0.559666 | -0.564293 | -0.573815 | -0.547321 |
| **$C_1$** | 0.286505 | 0.376540 | 0.346625 | 0.356084 | 0.358847 |
| **$O_2$** | -0.588007 | -0.552896 | -0.549566 | -0.540050 | -0.541005 |
| **$C_2$** | 0.301226 | 0.413703 | 0.455212 | 0.425937 | 0.449649 |
| | Ozone | | | | |
| **$O_3$** | -0.124633 | -0.303989 | -0.303084 | -0.303554 | -0.303635 |
| **$O_4$** | 0.249265 | -0.066408 | -0.078790 | -0.078520 | -0.074882 |
| **$O_5$** | -0.124633 | -0.280482 | -0.286580 | -0.291094 | -0.285258 |

## Catechol POZ Mulliken charge in water

| 2_3_POZ_exo_O | | | | | |
|---|---|---|---|---|---|
| **Atom** | **Molecule** | **POZ isomers** | | | |
| | Catechol | Structure 11 | Structure 12 | Structure 13 | Structure 14 |
| **$O_1$** | -0.60000 | -0.556335 | -0.556044 | -0.565399 | -0.546862 |
| **$C_1$** | 0.286505 | 0.382047 | 0.345747 | 0.355872 | 0.365447 |
| **$O_2$** | -0.588007 | -0.551121 | -0.545199 | -0.534232 | -0.542013 |
| **$C_2$** | 0.301226 | 0.392195 | 0.446607 | 0.414220 | 0.439410 |
| | Ozone | | | | |
| **$O_3$** | -0.124633 | -0.282555 | -0.299424 | -0.314200 | -0.299201 |
| **$O_4$** | 0.249265 | -0.086822 | -0.086806 | -0.077179 | -0.087714 |
| **$O_5$** | -0.124633 | -0.287225 | -.284684 | -0.279301 | -0.280049 |

## Catechol POZ Mulliken charge in water

| 3_4_POZ_endo_O | | | | | |
|---|---|---|---|---|---|
| **Atom** | **Molecule** | **POZ isomers** | | | |
| | Catechol | Structure 15 | Structure 16 | Structure 17 | |
| **$O_1$** | -0.60000 | -0.579072 | -0.603197 | -0.582171 | |
| **$C_1$** | 0.286505 | 0.297188 | 0.265449 | 0.287413 | |
| **$O_2$** | -0.588007 | -0.591724 | -0.566049 | -0.573085 | |
| **$C_2$** | 0.301226 | 0.272792 | 0.300153 | 0.300816 | |
| | Ozone | | | | |
| **$O_3$** | -0.124633 | -0.288659 | -0.284722 | -0.288145 | |
| **$O_4$** | 0.249265 | -0.083643 | -0.086591 | -0.081954 | |
| **$O_5$** | -0.124633 | -0.288049 | -0.287016 | -0.289268 | |

## Catechol POZ Mulliken charge in water

| 3_4_POZ_exo_O | | | | | |
|---|---|---|---|---|---|
| **Atom** | **Molecule** | **POZ isomers** | | | |
| | Catechol | Structure 18 | Structure 19 | Structure 20 | Structure 21 |
| **$O_1$** | -0.60000 | -0.573634 | -0.600885 | -0.602902 | -0.580046 |
| **$C_1$** | 0.286505 | 0.305017 | 0.271641 | 0.254109 | 0.286996 |
| **$O_2$** | -0.588007 | -0.589665 | -0.562228 | -0.56174 | -0.562379 |
| **$C_2$** | 0.301226 | 0.243986 | 0.283466 | 0.290049 | 0.286638 |
| | Ozone | | | | |
| **$O_3$** | -0.124633 | -0,293773 | -0.288497 | -0.290460 | -0.286928 |
| **$O_4$** | 0.249265 | -0.082678 | -0.085355 | -0.084735 | -0.083019 |
| **$O_5$** | -0.124633 | -0.294313 | -0.292030 | -0.289464 | -0.293615 |

## Catechol POZ Mulliken charge in water

| 4_5_POZ_endo_O | | | | | |
|---|---|---|---|---|---|
| **Atom** | **Molecule** | **POZ isomers** | | | |
| | Catechol | Structure 22 | Structure 23 | | |
| **$O_1$** | -0.60000 | -0.573064 | -0.559359 | | |
| **$C_1$** | 0.286505 | 0.346058 | 0.340764 | | |
| **$O_2$** | -0.588007 | -0.584853 | -0.559359 | | |
| **$C_2$** | 0.301226 | 0.336327 | 0.340764 | | |
| | Ozone | | | | |
| **$O_3$** | -0.124633 | -0.291551 | -0.291934 | | |
| **$O_4$** | 0.249265 | -0.091259 | -0.091663 | | |
| **$O_5$** | -0.124633 | -0.291473 | -0.291663 | | |

### Catechol POZ Mulliken charge in water

| 4_5_POZ_exo_O | | | | | |
|---|---|---|---|---|---|
| **Atom** | **Molecule** | **POZ isomers** | | | |
| | Catechol | Structure 24 | Structure 25 | | |
| **$O_1$** | -0.60000 | -0.568765 | -0.555680 | | |
| **$C_1$** | 0.286505 | 0.352624 | 0.345838 | | |
| **$O_2$** | -0.588007 | -0.582759 | -0.555679 | | |
| **$C_2$** | 0.301226 | 0.340439 | 0.345842 | | |
| | Ozone | | | | |
| **$O_3$** | -0.124633 | -0.292611 | -0.295432 | | |
| **$O_4$** | 0.249265 | -0.092528 | -0.092937 | | |
| **$O_5$** | -0.124633 | -0.297391 | -0.295427 | | |

## Resorcinol POZs

### Resorcinol POZ Mulliken charge in gas phase

| 1_2_POZ_endo_O | | | | | |
|---|---|---|---|---|---|
| **Atom** | **Molecule** | **POZ isomers** | | | |
| | Resorcinol | Structure 1 | Structure 2 | Structure 3 | Structure 4 |
| **$O_1$** | -0.56 | -0.532 | -0.532 | -0.536 | -0.53 |
| **$C_1$** | 0.333 | 0.461 | 0.465 | 0.454 | 0.461 |
| **$O_2$** | -0.561 | -0.54 | -0.526 | -0.527 | -0.541 |
| **$C_2$** | 0.326 | 0.366 | 0.346 | 0.345 | 0.367 |
| | Ozone | | | | |
| **$O_3$** | -0.116 | -0.29 | -0.285 | -0.294 | -0.286 |
| **$O_4$** | 0.231 | -0.05 | -0.064 | -0.057 | -0.052 |
| **$O_5$** | -0.116 | -0.295 | -0.269 | -0.268 | -0.285 |

### Resorcinol POZ Mulliken charge in gas phase

| 1_2_POZ_exo_O | | | | | |
|---|---|---|---|---|---|
| **Atom** | **Molecule** | **POZ isomers** | | | |
| | Resorcinol | Structure 5 | Structure 6 | Structure 7 | Structure 8 |
| **$O_1$** | -0.56 | -0.54 | -0.527 | -0.535 | -0.528 |
| **$C_1$** | 0.333 | 0.43 | 0.439 | 0.431 | 0.443 |
| **$O_2$** | -0.561 | -0.537 | -0.525 | -0.526 | -0.537 |
| **$C_2$** | 0.326 | 0.355 | 0.328 | 0.334 | 0.357 |
| | Ozone | | | | |
| **$O_3$** | -0.116 | -0.248 | -0.289 | -0.272 | -0.289 |
| **$O_4$** | 0.231 | -0.069 | -0.064 | -0.084 | -0.059 |
| **$O_5$** | -0.116 | -0.331 | -0.264 | -0.263 | -0.285 |

## Resorcinol POZ Mulliken charge in gas phase

| 3_4_POZ_endo_O | | | | | |
|---|---|---|---|---|---|
| **Atom** | **Molecule** | **POZ isomers** | | | |
| | Resorcinol | Structure 9 | Structure 10 | Structure11 | Structure 12 |
| **$O_1$** | -0.56 | -0.548 | -0.55 | -0.547 | -0.548 |
| **$C_1$** | 0.333 | 0.337 | 0.344 | 0.341 | 0.34 |
| **$O_2$** | -0.561 | -0.538 | -0.535 | -0.534 | -0.536 |
| **$C_2$** | 0.326 | 0.449 | 0.459 | 0.461 | 0.446 |
| | Ozone | | | | |
| **$O_3$** | -0.116 | -0.297 | -0.283 | -0.287 | -0.294 |
| **$O_4$** | 0.231 | -0.058 | -0.064 | -0.064 | -0.059 |
| **$O_5$** | -0.116 | -0.28 | -0.277 | -0.276 | -0.28 |

## Resorcinol POZ Mulliken charge in gas phase

| 3_4_POZ_exo_O | | | | | |
|---|---|---|---|---|---|
| **Atom** | **Molecule** | **POZ isomers** | | | |
| | Resorcinol | Structure 13 | Structure 14 | Structure 15 | Structure 16 |
| **$O_1$** | -0.56 | -0.546 | -0.55 | -0.547 | -0.546 |
| **$C_1$** | 0.333 | 0.346 | 0.345 | 0.34 | 0.35 |
| **$O_2$** | -0.561 | -0.539 | -0.53 | -0.529 | -0.538 |
| **$C_2$** | 0.326 | 0.426 | 0.432 | 0.435 | 0.423 |
| | Ozone | | | | |
| **$O_3$** | -0.116 | -0.272 | -0.283 | -0.89 | -0.267 |
| **$O_4$** | 0.231 | -0.087 | -0.066 | -0.066 | -0.086 |
| **$O_5$** | -0.116 | -0.275 | -0.274 | -0.271 | -0.278 |

## Resorcinol POZ Mulliken charge in gas phase

| 4_5_POZ_endo_O | | | | | |
|---|---|---|---|---|---|
| **Atom** | **Molecule** | **POZ isomers** | | | |
| | Resorcinol | Structure 17 | Structure 18 | Structure 19 | Structure 20 |
| **$O_1$** | -0.56 | -0.549 | -0.553 | -0.553 | -0.546 |
| **$C_1$** | 0.333 | 0.364 | 0.353 | 0.363 | 0.355 |
| **$O_2$** | -0.561 | -0.541 | -0.53 | -0.527 | -0.542 |
| **$C_2$** | 0.326 | 0.375 | 0.355 | 0.356 | 0.374 |
| | Ozone | | | | |
| **$O_3$** | -0.116 | -0.292 | -0.266 | -0.267 | -0.29 |
| **$O_4$** | 0.231 | -0.061 | -0.066 | -0.066 | -0.06 |
| **$O_5$** | -0.116 | -0.267 | -0.269 | -0.265 | -0.27 |

## Resorcinol POZ Mulliken charge in gas phase

| 4_5_POZ_exo_O | | | | | |
|---|---|---|---|---|---|
| **Atom** | **Molecule** | **POZ isomers** | | | |
| | Resorcinol | Structure 21 | Structure 22 | Structure 23 | Structure 24 |
| **$O_1$** | -0.56 | -0.544 | -0.549 | -0.549 | -0.541 |
| **$C_1$** | 0.333 | 0.37 | 0.364 | 0.375 | 0.362 |
| **$O_2$** | -0.561 | -0.535 | -0.524 | -0.521 | -0.536 |
| **$C_2$** | 0.326 | 0.357 | 0.35 | 0.352 | 0.356 |
| | Ozone | | | | |
| **$O_3$** | -0.116 | -0.336 | -0.278 | -0.282 | -0.334 |
| **$O_4$** | 0.231 | -0.052 | -0.069 | -0.068 | -0.053 |
| **$O_5$** | -0.116 | -0.245 | -0.26 | -0.256 | -0.247 |

## Resorcinol POZs

## Resorcinol POZ Mulliken charge in water

| 1_2_POZ_endo_O | | | | | |
|---|---|---|---|---|---|
| **Atom** | **Molecule** | **POZ isomers** | | | |
| | Resorcinol | Structure 1 | Structure 2 | Structure 3 | Structure 4 |
| **$O_1$** | -0.580 | -0.547 | -0.552 | -0.55 | -0.55 |
| **$C_1$** | 0.318 | 0.463 | 0.470 | 0.460 | 0.466 |
| **$O_2$** | -0.581 | -0.552 | -0.548 | -0.547 | -0.553 |
| **$C_2$** | 0.324 | 0.364 | 0.344 | 0.344 | 0.366 |
| | Ozone | | | | |
| **$O_3$** | -0.125 | -0.308 | -0.302 | -0.307 | -0.304 |
| **$O_4$** | 0.249 | -0.068 | -0.083 | -0.078 | -0.074 |
| **$O_5$** | -0.125 | -0.287 | -0.290 | -0.283 | -0.289 |

## Resorcinol POZ Mulliken charge in water

| 1_2_POZ_exo_O | | | | | |
|---|---|---|---|---|---|
| **Atom** | **Molecule** | **POZ isomers** | | | |
| | Resorcinol | Structure 5 | Structure 6 | Structure 7 | Structure 8 |
| **$O_1$** | -0.580 | -0.553 | -0.548 | -0.551 | -0.548 |
| **$C_1$** | 0.318 | 0.432 | 0.447 | 0.439 | 0.450 |
| **$O_2$** | -0.581 | -0.548 | -0.546 | -0.545 | -0.548 |
| **$C_2$** | 0.324 | 0.354 | 0.327 | 0.331 | 0.353 |
| | Ozone | | | | |
| **$O_3$** | -0.125 | -0.270 | -0.301 | -0.294 | -0.298 |
| **$O_4$** | 0.249 | -0.079 | -0.086 | -0.091 | -0.082 |
| **$O_5$** | -0.125 | -0.328 | -0.285 | -0.283 | -0.287 |

## Resorcinol POZ Mulliken charge in water

| 3_4_POZ_endo_O | | | | | |
|---|---|---|---|---|---|
| **Atom** | **Molecule** | **POZ isomers** | | | |
| | Resorcinol | Structure 9 | Structure 10 | Structure11 | Structure 12 |
| **$O_1$** | -0.580 | -0.562 | -0.566 | -0.562 | -0.566 |
| **$C_1$** | 0.318 | 0.335 | 0.342 | 0.338 | 0.341 |
| **$O_2$** | -0.581 | -0.552 | -0.555 | -0.555 | -0.552 |
| **$C_2$** | 0.324 | 0.450 | 0.464 | 0.464 | 0.450 |
| | Ozone | | | | |
| **$O_3$** | -0.125 | -0.311 | -0.304 | -0.304 | -0.311 |
| **$O_4$** | 0.249 | -0.081 | -0.086 | -0.086 | -0.081 |
| **$O_5$** | -0.125 | -0.289 | -0.294 | -0.295 | -0.289 |

## Resorcinol POZ Mulliken charge in water

| 3_4_POZ_exo_O | | | | | |
|---|---|---|---|---|---|
| **Atom** | **Molecule** | **POZ isomers** | | | |
| | Resorcinol | Structure 13 | Structure 14 | Structure 15 | Structure 16 |
| **$O_1$** | -0.580 | -0.560 | -0.565 | -0.561 | -0.563 |
| **$C_1$** | 0.318 | 0.334 | 0.346 | 0.339 | 0.350 |
| **$O_2$** | -0.581 | -0.554 | -0.552 | -0.551 | -0.554 |
| **$C_2$** | 0.324 | 0.429 | 0.441 | 0.441 | 0.430 |
| | Ozone | | | | |
| **$O_3$** | -0.125 | -0.295 | -0.301 | -0.302 | -0.294 |
| **$O_4$** | 0.249 | -0.096 | -0.091 | -0.091 | -0.096 |
| **$O_5$** | -0.125 | -0.289 | -0.290 | -0.290 | -0.290 |

## Resorcinol POZ Mulliken charge in water

| 4_5_POZ_endo_O | | | | | |
|---|---|---|---|---|---|
| **Atom** | **Molecule** | **POZ isomers** | | | |
| | Resorcinol | Structure 17 | Structure 18 | Structure 19 | Structure 20 |
| **$O_1$** | -0.580 | -0.570 | -0.569 | -0.573 | -0.565 |
| **$C_1$** | 0.318 | 0.360 | 0.345 | 0.357 | 0.348 |
| **$O_2$** | -0.581 | -0.550 | -0.549 | -0.547 | -0.553 |
| **$C_2$** | 0.324 | 0.372 | 0.355 | 0.356 | 0.373 |
| | Ozone | | | | |
| **$O_3$** | -0.125 | -0.291 | -0.287 | -0.287 | -0.291 |
| **$O_4$** | 0.249 | -0.083 | -0.089 | -0.089 | -0.083 |
| **$O_5$** | -0.125 | -0.295 | -0.289 | -0.289 | -0.295 |

## Resorcinol POZ Mulliken charge in water

| 4_5_POZ_exo_O | | | | | |
|---|---|---|---|---|---|
| **Atom** | **Molecule** | **POZ isomers** | | | |
| | Resorcinol | Structure 21 | Structure 22 | Structure 23 | Structure 24 |
| **$O_1$** | -0.580 | -0.563 | -0.563 | -0.567 | -0.559 |
| **$C_1$** | 0.318 | 0.366 | 0.357 | 0.369 | 0.356 |
| **$O_2$** | -0.581 | -0.545 | -0.545 | -0.543 | -0.548 |
| **$C_2$** | 0.324 | 0.352 | 0.347 | 0.349 | 0.352 |
| | Ozone | | | | |
| **$O_3$** | -0.125 | -0.356 | -0.304 | -0.305 | -0.336 |
| **$O_4$** | 0.249 | -0.075 | -0.088 | -0.088 | -0.075 |
| **$O_5$** | -0.125 | -0.269 | -0.281 | -0.280 | -0.270 |